



Master

2018

Open Access

This version of the publication is provided by the author(s) and made available in accordance with the copyright holder(s).

Aberrant white matter development in 22q11.2 Deletion Syndrome and association with risk factors of psychosis

Van Der Molen, Joëlle Ismay Rosanne

How to cite

VAN DER MOLEN, Joëlle Ismay Rosanne. Aberrant white matter development in 22q11.2 Deletion Syndrome and association with risk factors of psychosis. Master, 2018.

This publication URL: <https://archive-ouverte.unige.ch/unige:106309>



UNIVERSITÉ
DE GENÈVE

FACULTÉ DE PSYCHOLOGIE
ET DES SCIENCES DE L'ÉDUCATION



MASTER THESIS

Aberrant white matter development in 22q11.2 Deletion Syndrome and association with risk factors of psychosis

Author:

Joëlle VAN DER MOLEN

Supervisor:

Prof. Stephan ELIEZ

Jury:

Prof. Stephan ELIEZ

Dr. Tonia RIHS

Dr. Maude SCHNEIDER

*A thesis submitted to the Faculty of Psychology and Educational Sciences at the
University of Geneva in partial fulfilment of the requirements for a degree in the
Interdisciplinary Master of Neuroscience*

carried out in the

Developmental Imaging and Psychopathology laboratory

FACULTY OF PSYCHOLOGY AND EDUCATIONAL SCIENCES

Psychology section

University of Geneva

July 2018

Acknowledgements

First of all, I would like to sincerely thank my Master supervisor, Stephan Eliez, for providing me the exciting opportunity to carry out my Master project in the DIP lab. It has been an enriching two years, during which I have acquired valuable research experience and was given the chance to work on an extremely interesting research topic within a stimulating environment.

I would also like to thank the jury members, Tonia Rihs and Maude Schneider, for accepting to review and evaluate this work.

An immense thank you to Marica, my day-to-day supervisor who taught me an uncountable amount of things about research. Thank you for always providing me support and structure throughout my project; thank you also for your permanently cheerful mood and for your good advices. I am grateful for having had you as a mentor during my first research experiences.

Thank you to all members of the DIP lab for being such a great, cheerful team. It has been a pleasure to share great times in- and outside the lab with you people. Thanks also to the "neuroimaging team", who provided great support and advices on test runs.

Thank you to my master friends Emiliana and Maëlle for being such amazing people and for all the good laughs we had in- and outside the lab.

A special thank you to my family, for always being ready to help and for supporting me through great and tough times.

Finally, thank you, Timur, for always being there for me and for having taught me to enjoy life at all times; I am immensely grateful for that.

Abstract

Background: 22q11.2 Deletion Syndrome (22q11.2DS) is a neurogenetic disorder associated with widespread anomalies of white matter volume and microstructure. However, findings regarding the direction of microstructural alterations of white matter in this population are inconsistent. Moreover, although postnatal white matter maturation is known to follow complex non-linear patterns in healthy developing individuals, developmental trajectories of white matter have never been characterized in 22q11.2DS. Thus, the first aim of this study was to delineate the developmental trajectories of white matter microstructure in 22q11.2DS from childhood until adulthood, in order to improve our understanding of neuroanatomical development in this population.

22q11.2DS is also considered a model to study schizophrenia, given that approximately 30% of individuals with the deletion develop the illness by adulthood. Extensive research has recently led to the identification of several cognitive and psychiatric risk factors for psychosis in this population. However, neuroanatomical biomarkers of the disease have not yet been established. Given that schizophrenia is associated with widespread alterations of structural connectivity, the study of white matter development in patients with 22q11.2DS presenting risk factors of psychosis may help to identify neurodevelopmental markers of early stages of the disease. The identification of such biomarkers could not only provide powerful predictors of conversion to psychosis, but could also provide perspectives regarding early intervention targets. Thus, the second aim of this study was to characterize white matter development in association with two well-established risk factors for conversion to psychosis, namely cognitive decline and the ultra-high risk (UHR) status.

Method: To address these aims, a longitudinal design was adopted in order to capture the individual progression of brain structure over time. Diffusion tensor imaging (DTI) data was used to reconstruct 18 long-range white matter tracts using a global probabilistic tractography method. Four DTI metrics were extracted as averages for each tract: fractional anisotropy (FA), axial diffusivity (AD), radial diffusivity (RD) and mean diffusivity (MD). A preliminary characterization of white matter differences between individuals with 22q11.2DS and typical developing (TD) controls was obtained on a sample of 74 subjects (40 22q11.2DS; 34 TD controls) aged 8-25 years with two consecutive assessments (mean time interval = 3.395 ± 0.496 years). Repeated measures ANOVA and group comparisons of the annual percent change (APC) were performed for each DTI metric and white matter tract. We then extended the sample by including a total of 201 subjects (101 22q11.2DS; 100 TD controls) aged 5-35 with varying amounts of time points (mean time interval = 3.554 ± 0.867 years) and applied mixed models regression analyses to obtain a more fine-grained delineation of developmental trajectories of white matter microstructure. Finally, mixed models were also used to compare white matter development in subgroups of patients with 22q11.2DS categorized depending on the presence of risk factors of psychosis.

Results: Both in the preliminary study and main study comparing 22q11.2DS and TD controls, we found group differences in most white matter tracts, and alterations consistently followed a pattern of reduced AD, RD and MD combined with increased FA in patients with 22q11.2DS compared to TD controls. Group x time interaction effects were generally absent, as both groups showed identically shaped trajectories. These trajectories followed non-linear patterns for most DTI metrics and white matter tracts. Comparisons of APC between 22q11.2DS and TD controls yielded significant group differences in AD and MD for the right corticospinal tract (CST). In individuals with 22q11.2DS, an interaction effect was observed for FA in the splenium of the corpus callosum (forceps major, FMAJ) when comparing patients with a cognitive decline and patients without cognitive decline. The comparison of UHR and non-UHR patients again yielded an interaction effect in the FMAJ; an additional interaction effect was also observed for AD in the left angular bundle of the cingulum (CAB).

Conclusions: Although developmental changes were visible in 22q11.2DS and TD controls for most tracts and diffusion metrics, 22q11.2DS is associated with widespread alterations in most white matter tracts, suggesting extensive disruptions of long-range communication. Alterations were present from early on and persisted throughout development, pointing to a combination of both prenatal and postnatal pathological mechanisms. Moreover, findings indicate that individuals at high risk of psychosis are consistently characterized by deviant developmental trajectories in the splenium of the corpus callosum. As such, early developmental alterations in this tract may represent a valuable biomarker for the prediction of schizophrenia.

1	Introduction	1
1.1	22q11.2 Deletion Syndrome	2
1.1.1	Historical background of the syndrome	2
1.1.2	Genetic aspects and detection	3
1.1.3	Somatic phenotype	4
1.1.4	Cognitive phenotype	6
1.1.5	Psychiatric phenotype	7
1.1.6	22q11.2DS: a model to study psychosis	9
1.1.7	Risk factors of conversion to psychosis	10
1.2	White matter	12
1.2.1	Definition: white matter structure and function	13
1.2.2	Diffusion Tensor Imaging: a non-invasive tool to study white matter in vivo	14
1.2.3	White matter tracts	17
1.2.4	White matter development	18
1.3	White matter alterations in 22q11.2DS	20
1.3.1	Previous findings: widespread alterations of structural connectivity .	20
1.3.2	White matter alterations and psychotic symptoms	21
1.3.3	White matter alterations associated to risk factors of psychosis . . .	22
1.3.4	White matter in non-deleted patients with schizophrenia or at risk for psychosis	24
1.4	Methods for the analysis of DTI images	26
1.4.1	Whole-brain analysis techniques	26
1.4.2	Tractography	27
1.4.3	TBSS versus TRACULA	31
1.5	Longitudinal design	32
1.5.1	Longitudinal versus cross-sectional	32
1.5.2	Challenges of longitudinal studies	33
1.5.3	Prospective cohort studies for identifying biomarkers of psychosis . .	33
1.6	Aims and hypotheses	34
2	Materials and Methods	36
2.1	Materials	36
2.1.1	Preliminary study	37
2.1.2	Main study	38
2.2	MRI acquisitions	42

2.3	MRI image processing	42
2.4	Statistical analysis	43
2.4.1	Preliminary study	43
2.4.2	Main study	44
3	Results	45
3.1	Preliminary study	45
3.1.1	Repeated measures ANOVA	45
3.1.2	Annual percent change	50
3.2	Main study	51
3.2.1	Developmental trajectories of white matter tracts in 22q11.2DS versus TD controls	51
3.2.2	Relationship between white matter microstructure and cognition in 22q11.2DS	59
3.2.3	Relationship between white matter microstructure and UHR status in 22q11.2DS	60
4	Discussion	61
4.1	Preliminary study	61
4.2	Main study	62
4.2.1	Widespread white matter alterations in individuals with 22q11.2DS	62
4.2.2	Cognitive decline is associated with a lack of age-related changes in the corpus callosum	66
4.2.3	The UHR status is associated with deviant developmental trajectories of the corpus callosum and the cingulum	67
4.2.4	Limitations	69
5	Conclusion	73
A	Appendix	75
A.1	Supplementary material for the preliminary study	75
A.1.1	Annual percent change in 22q11.2DS and TD controls	75
A.1.2	Repeated measures ANOVA comparing 22q11.2DS and TD controls	78

CHAPTER 1

INTRODUCTION

22q11.2 Deletion Syndrome (22q11.2DS) is associated with specific cognitive, psychiatric and somatic characteristics. Since the emergence of neuroimaging techniques in the 1990s, a large body of evidence indicates that, on a neuroanatomical level, the syndrome is associated with extensive disruptions of white matter volume and microstructure. Yet, from a developmental perspective, white matter maturation is still largely unknown for this population.

Moreover, 22q11.2DS represents the third highest genetic risk for developing schizophrenia, a profoundly disabling disorder characterized by perturbations in cognition, perception and emotions (American Psychiatric Association, 2013). While schizophrenia is increasingly recognized as a neurodevelopmental disorder (Insel, 2010; Rapoport et al., 2012; Uhlhaas and Singer, 2010), the study of developmental pathways leading to the disorder is challenging, given that subjects are mostly identified and studied *after* the onset of the disease. In this context, 22q11.2DS provides a unique opportunity for the study of early stages preceding schizophrenia, given that this population can be identified at early ages and is associated with a high risk of developing the disorder. Previous research in 22q11.2DS has led to the identification of several cognitive and psychiatric risk factors that may help predicting schizophrenia (Gothelf et al., 2013; Kufert et al., 2016; Schneider et al., 2016; Van et al., 2016; Vorstman et al., 2015), but biomarkers¹ have thus far not been established. White matter development represents a particularly promising candidate biomarker, given that a large body of evidence points to an involvement of cerebral white matter in the pathophysiology of schizophrenia (Fornito et al., 2012; Heuvel and Fornito, 2014; Pettersson-Yeo et al., 2011). When following a neurodevelopmental perspective, is indeed likely that alterations visible in schizophrenia are the end-point of aberrant developmental processes occurring in years prior to the emergence of the disorder.

¹According to the Biomarkers Definitions Working Group. (2001), a biomarker can be defined as “a characteristic that is objectively measured and evaluated as an indicator of normal biological processes, pathogenic processes, or pharmacologic responses to a therapeutic intervention.”.

The identification of neurodevelopmental biomarkers associated with early stages of schizophrenia may not only provide a powerful mean for predicting the emergence of the disease, but may also help the development of early preventive intervention methods that would be able to forestall the emergence of the full-blown disorder.

Given the above considerations, the present work was organized around two main objectives. First, we sought to characterize white matter developmental trajectories in 22q11.2DS, in order to provide a more comprehensive understanding of the neuroanatomical profile associated with the syndrome. Then, a second objective involved the study of white matter maturation in patients with 22q11.2DS at high risk for schizophrenia.

In this introductory chapter, general characteristics of 22q11.2DS will first be outlined. Then, we will provide a detailed description of white matter structure, function and development, followed by a description of neuroimaging techniques adapted for the study of white matter in vivo. Next, previous findings pointing to white matter alterations in 22q11.2DS and associations with psychosis will be reviewed, followed by a description of state-of-the-art analysis methods used for group comparisons of white matter structure. Finally, we will conclude the chapter by defining the structure of a longitudinal study, describing the challenges associated with it and highlighting the importance of prospective longitudinal studies in the context of 22q11.2DS and the search for biomarkers of psychosis.

1.1 22q11.2 Deletion Syndrome

Chromosome 22q11.2DS can be defined as a common neurogenetic developmental disorder, occurring with a prevalence of around 1 in 2000-4000 live births (Oskarsdóttir et al., 2004; Shprintzen, 2005). In this section, the historical background of the syndrome will first be described. Then, we will outline the syndrome's genetic characteristics and methods used for its detection, followed by a characterization of the complex somatic, cognitive and psychiatric profile of individuals with the syndrome. Finally, we will discuss use of the 22q11.2 DS as a model to study psychosis, and describe several recently identified risk factors for conversion to psychosis in this population.

1.1.1 Historical background of the syndrome

Historically, the first accounts of the syndrome date back to the second half of the 20th century, when several authors independently described patients with similar symptomatic profiles (Cayler, 1969; Di George, 1965; Sedlackova, 1955; Strong, 1968). Symptoms included immune deficiency due to thymus dysfunctions, atypical facial features, congenital heart disease, hypernasal voice and mental retardation. Shortly after, Shprintzen et al. (1978) used the term "Velo-Cardio-Facial Syndrome" (VCFS) to describe a familial case of patients sharing these symptoms. Finally, in the early 1990s, developments in genome

sequencing technologies enabled the discovery of a common microdeletion on the long arm of chromosome 22 (locus 11.2) in most patients characterized by these symptomatic profiles (Driscoll et al., 1992; Scambler et al., 1991). Since then, the term "22q11.2 Deletion Syndrome" has been employed to describe this population and to unify the various previous denominations (such as DiGeorge syndrome, VCFS or Shprintzen syndrome).

1.1.2 Genetic aspects and detection

Currently, 22q11.2DS is defined as a genetic neurodevelopmental disorder resulting from the deletion of 30 to 60 genes on the long arm of chromosome 22, locus 11.2 (Squarcione et al., 2013). More specifically, in 90% of the cases, the deletion spans over 60 identified genes (3 Megabases); another 8% of patients have a more uncommon form of deletion that encompasses approximately 30 genes (1.5 Megabases); and the remaining 2% of patients have other diverse forms of deletions (Karayiorgou et al., 2010; Kobrynski and Sullivan, 2007). The two most common forms (3Mb and 1.5Mb) are represented in Figure 1.1.

The deletion most frequently results from a *de novo* mutation, thought to be caused by chromosomal base pairs misalignments during meiosis (Shaikh et al., 2007). The 22q11.2 locus is particularly vulnerable for misalignments due to the presence of several duplicated blocks of DNA, called low copy repeats (LCRs) (Kobrynski and Sullivan, 2007; Shaikh et al., 2007). In some rare cases, the deletion is inherited from an affected parent (Scambler, 2000), following an autosomal dominant transmission pattern (meaning that an affected parent has a 50% chance of passing the deletion to the children).

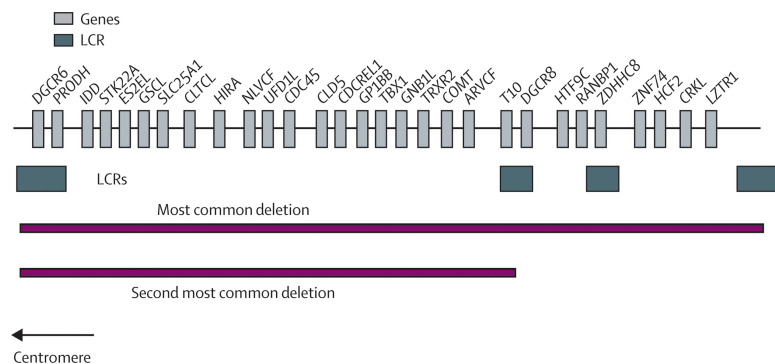


Figure 1.1: Representation of the first (3Mb) and second (1.5Mb) most common forms of deletion on the 22q11.2 locus. Deletions typically occur between low copy number repeats (LCRs), as these regions of duplicated DNA increase the probability of chromosomal misalignments (from Kobrynski and Sullivan, 2007).

Patients can be screened for 22q11.2DS using methods such as fluorescence in situ hybridization (FISH) or Quantitative Fluorescent Polymerase Chain Reaction (QF-PCR). While historically FISH has been the most widely used technique, it has the disadvantage of targeting only commonly deleted regions near the 22q11.2 locus, with the risk of missing atypical deletions (Bassett et al., 2011; McDonald-McGinn et al., 2015). By contrast, QF-PCR can reveal 22q11.2 deletions of any size, and is therefore a preferable technique for diagnosis (Bassett et al., 2011).

Currently, the prevalence of the syndrome is estimated between approximately 1 in 2000-4000 live births (Oskarsdóttir et al., 2004; Shprintzen, 2005) and around 1 in ev-

ery 1000 fetuses (McDonald-McGinn et al., 2015), making it one of the most common multiple anomaly syndromes (Shprintzen, 2008). These numbers are likely to rise, due to improvements in detection techniques, better health care and increases in the number of familial cases (McDonald-McGinn and Sullivan, 2011; McDonald-McGinn et al., 2015; Shprintzen, 2005). Indeed, as the syndrome follows an autosomal dominant transmission pattern, higher survival rates of affected parents (resulting from better health care) lead to an increased prevalence of the inherited form of the syndrome (McDonald-McGinn and Sullivan, 2011).

1.1.3 Somatic phenotype

Somatic characteristics of the syndrome can affect almost every part of the organism and are highly variable, as they range from severe, life-threatening alterations to mild atypical characteristics (McDonald-McGinn et al., 2015; Swillen and McDonald-McGinn, 2015). They most commonly involve cardiac anomalies, palatal deformations, immune system deficits, endocrine anomalies and facial malformations (McDonald-McGinn et al., 2015) (Figure 1.2).

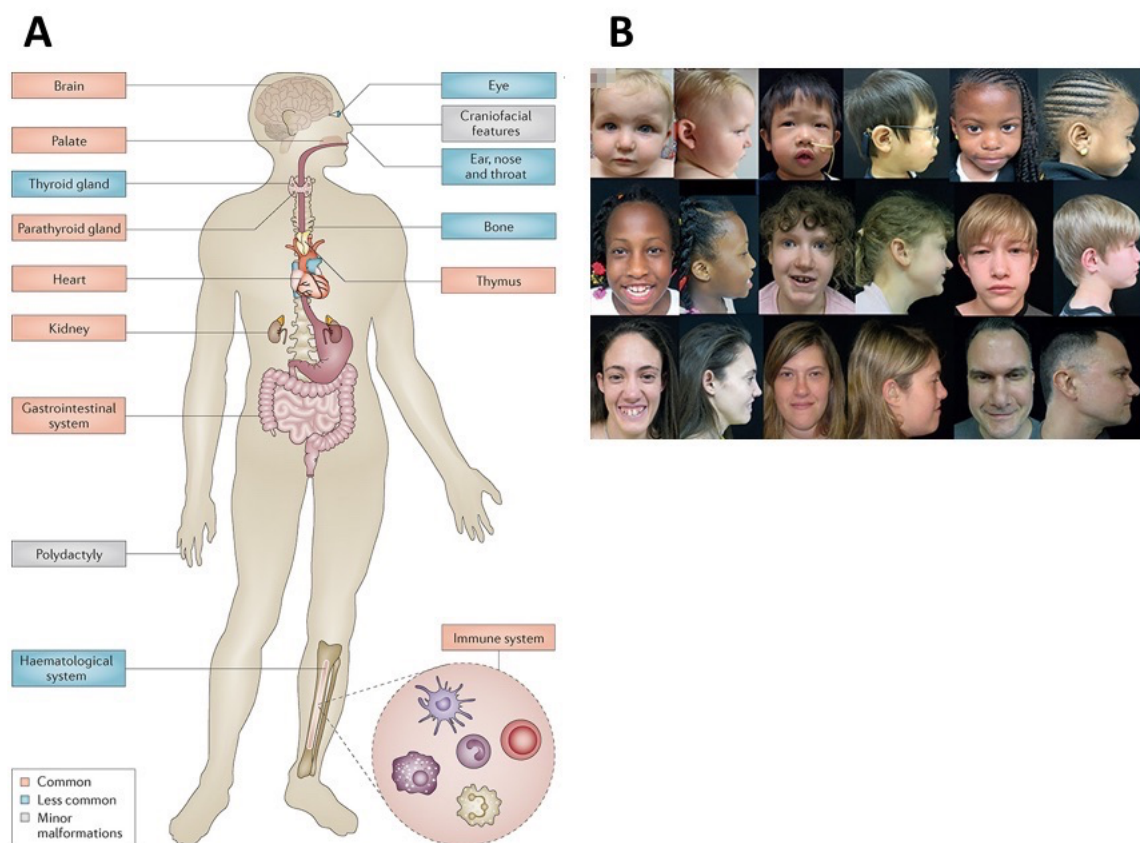


Figure 1.2: Most common somatic anomalies observed in individuals with 22q11.2DS (A) and typical facial features associated with the syndrome (B) (adapted from McDonald-McGinn et al., 2015).

More specifically, somatic manifestations of 22q11.2DS involve (McDonald-McGinn et al., 2015):

- **Cardiac anomalies:** congenital cardiac defects (CHD) form one of the earliest manifestations leading to diagnosis, as they become evident during the prenatal and neonatal stages. Most frequently, anomalies include conotruncal heart defects (i.e. malformations of the outflow tract) such as Fallot tetralogy, truncus arteriosus, interrupted aortic arch type B and ventricular septal defect. Pulmonary artery anomalies are also common and include hypoplasia (i.e., underdevelopment) and discontinuity. As CHDs are often life-threatening, they represent one of the most important early mortality causes in 22q11.2DS.
- **Palatal anomalies:** anomalies in velopharyngeal structures are also characteristic of 22q11.2DS. Around 65% of patients have relatively mild anomalies such as bifid uvula, velopharyngeal dysfunction, or occult submucosal cleft palate. In some cases (11%), patients have more severe palatal malformations such as overt cleft palate, or Pierre Robin sequence (i.e. smaller lower jaw, tongue placed further back, obstruction of the airways and often cleft palate). The above manifestations often induce feeding difficulties, nasal regurgitations, chronic sinus infections, hypernasal speech and articulation difficulties (McDonald-McGinn et al., 2015; Shprintzen, 2005).
- **Immunodeficiency:** it is estimated that 75% of patients with 22q11.2DS suffer from thymic hypoplasia and defective T cell production, leading to immunodeficiency. This implies manifestations such as chronic infections, poor immune responses, allergies, immunoglobulin A deficiencies and asthma.
- **Endocrine anomalies:** around 50-65% of patients have hypocalcaemia, resulting from hypoparathyroidism. Hypocalcaemia can manifest itself in the form of tetany, seizures, feeding difficulties, stridor and fatigue.
- **Facial features:** individuals with 22q11.2DS typically have subtle, albeit very characteristic facial features, namely hypertelorism (i.e., increased horizontal separation between the eyes), retrognathia (i.e., the lower jaw is placed further back than the upper jaw), a prominent nasal bridge and small ears.
- **Other physical anomalies:** other somatic manifestations include growth retardation, as well as ocular, gastro-intestinal and skeletal disorders.

1.1.4 Cognitive phenotype

The cognitive phenotype of patients with 22q11.2DS is very consistent and follows a specific developmental progression. In preschool children, a significant delay in language onset is commonly observed, as around 70% of children aged 24 months or older do not speak, or only use a few words or signs (Solot et al., 2000). At later stages, language disorders are also reported, although they are sometimes related to palatal anomalies (Solot et al., 2000). Individuals with 22q11.2DS also typically present visuospatial deficits, affecting both visual processing and visual memory (Bostelmann et al., 2016; Simon et al., 2005a). Regarding the latter, Bostelmann et al. (2016) demonstrated that visual memory of objects and faces is more severely affected than visuo-spatial memory. Impaired visual processing and memory probably partially account for deficits in emotion recognition and poor social cognition (McCabe et al., 2016), which are two other cognitive characteristics of the syndrome.

The cognitive profile is further characterized by impairments in executive functions (Campbell et al., 2010; Maeder et al., 2016), including working memory (Azuma et al., 2009; Woodin et al., 2001) and inhibition (McCabe et al., 2014; Shapiro et al., 2013).

More generally, cognitive functioning of individuals with 22q11.2DS follows a Gaussian distribution but is shifted to the left, with an average full-scale IQ (FSIQ) score of around 70 (Swillen and McDonald-McGinn, 2015). Specifically, around 55% of patients show a borderline to normal FSIQ (i.e., >70); around 45% have a mild to moderate intellectual disability (FSIQ from 55 to 70); and finally, a minority shows severe forms of intellectual disability. On a developmental level, a longitudinal collaborative multisite study (from the International Consortium on Brain and Behavior in 22q11.2 Deletion Syndrome (IBBC)) using data from 829 subjects aged 8-24 years found that FSIQ undergoes a gradual decline over time, with an average total decline of 7 percentile points (Vorstman et al., 2015). When considering subcomponents of IQ, it has been shown that Performance IQ (PIQ) is initially lower than Verbal IQ (VIQ) during childhood (Swillen, 2016; Tang et al., 2015); however, as the developmental trajectory of VIQ undergoes a stronger decline (average decline of 9 points) than PIQ (average decline of 5 points), this tendency is reversed by adulthood (Vorstman et al., 2015). Figure 1.3 represents the average cumulative decline in FSIQ, VIQ and PIQ from ages 8 to 24, as reported by Vorstman et al. (2015).

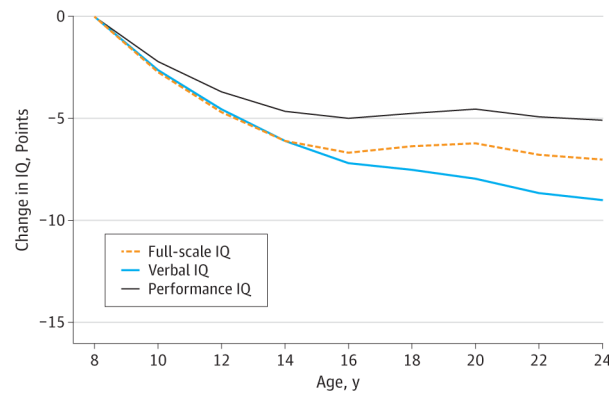


Figure 1.3: Cumulative decline in FSIQ, VIQ and PIQ observed in individuals with 22q11.2DS aged 8-24 years (from Vorstman et al., 2015).

1.1.5 Psychiatric phenotype

Data from the IBBC recently enabled the characterization of psychiatric morbidity in over 1400 subjects with 22q11.2DS, aged 6 to 68 years old (Schneider et al., 2014a). During childhood, Attention Deficit Hyperactivity Disorder (ADHD) was most frequently diagnosed, with a prevalence of around 37%. Anxiety disorders were present at all ages (prevalence ranging between 24-36%), albeit with an increased prevalence in children and adolescents. Autism Spectrum Disorders were also common across all ages, with a peak at adolescence (prevalence of around 26%). During adulthood however, schizophrenia spectrum disorders were by far the most prevalent psychiatric disorders, as they were diagnosed in 40% of adults older than 25 years. Of note, psychotic disorders were also present, albeit with a lower prevalence, during adolescence (10%) and early adulthood (23%), pointing to a relatively frequent early-onset form of psychotic disorders. The distribution of schizophrenia spectrum disorders across age ranges is shown in Figure 1.4. For a definition of psychotic disorders and schizophrenia, see Box 1.1.5.

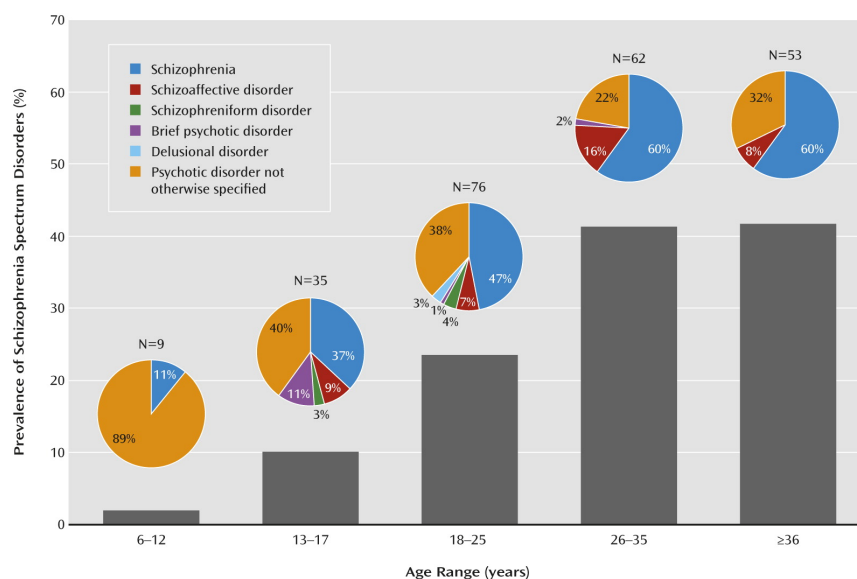


Figure 1.4: Prevalence of Schizophrenia Spectrum Disorders across different ages ranges in 22q11.2DS (from Schneider et al., 2014a).

Box 1.1.5. Psychosis, psychotic disorders and schizophrenia

Psychosis is defined as a group of functionally disabling symptoms characterized by a disconnection with reality and common to many psychiatric, neurologic, neurodevelopmental and medical conditions (Arciniegas, 2015). According to the DSM-5, *psychotic disorders* are more specifically defined by five types of abnormalities:

- **Delusions**, defined as fixed false beliefs that do not change, even in light of contradictory evidence.
- **Hallucinations**, defined as sensory perceptions occurring in the absence of any external stimulus. Together, hallucinations and delusions are commonly referred to as “positive” psychotic symptoms, in the sense that they describe an exacerbation of a normal process. Positive symptoms are considered as the central core of psychosis as they both reflect a disconnection with reality (Arciniegas, 2015).
- **Negative symptoms** (i.e., the reduction or absence of a normal process), such as reduced emotional expression, reduced drive for the initiation of goal-directed behaviors (avolition), social withdrawal (asociality), reduced speech production (alogia) and diminished ability to experience pleasure (anhedonia).
- **Disorganized thinking**, characterized by loose associations of thoughts and derailments of thoughts or even incomprehensible speech, which all should impair communication abilities.
- **Disorganized motor behavior**, reflected in any form of goal-directed behavior and ranging from simple clumsiness to unpredictable movements. Catatonia can also be observed, and is defined as a diminished reactivity to the environment.

Several types of psychotic disorders exist and are classified in the DSM-5 according to their severity, the mildest form being schizotypal (personality) disorder, followed by delusional

disorder, brief psychotic disorder, schizophreniform disorder, schizophrenia and schizoaffective disorder. Psychosis can also arise from substance/medication use, or from a medical condition.

With a lifetime prevalence of 0.3-0.7% in the general population (McGrath et al., 2008), *schizophrenia* is one of the most common forms of psychotic disorders and can be defined by perturbations of behavior, emotion and cognition (American Psychiatric Association, 2013). The onset of the disorder typically occurs between the late-teens and mid-30s (McGrath et al., 2008). According to the DSM-5, diagnosis of schizophrenia is established when two or more of the following symptoms are present: delusions, hallucinations, disorganized speech, grossly disorganized or catatonic behavior, and/or negative symptoms. These perturbations must be present for at least 6 months, including at least 1 month of active symptoms, and must significantly impair occupational and social functioning.

The etiology of schizophrenia - and more generally of psychosis - is largely unknown, and consequently current treatments are merely targeting some of the above-mentioned clinical symptoms and do not provide a permanent recovery. Hence, extensive research efforts have been dedicated to the identification of early biomarkers of schizophrenia, which could help both for the characterization of alteration mechanisms involved in the emergence of the disorder, but also for the early identification of subjects who will need therapeutic intervention. As will be discussed in the section below, 22q11.2DS may provide a unique opportunity for the research of the neurobiological substrate associated with psychosis, as the heterogeneity is considerably reduced in this population due to their shared genetic pathology.

1.1.6 22q11.2DS: a model to study psychosis

As mentioned earlier, one of the characteristic aspects of 22q11.2DS is the exceptionally high prevalence of psychotic disorders (40%). This makes 22q11.2DS the third highest genetic risk for the development of schizophrenia, after having a monozygotic twin with schizophrenia (50%) or two affected parents (42%) (McGuffin et al., 1995). Furthermore, the prevalence of schizophrenia in 22q11.2DS is significantly larger than the 1% prevalence observed in the general population (McGuffin et al., 1995). Thus, the behavioral phenotype of schizophrenia is observed with an increased frequency in individuals with the syndrome, which corresponds to the first criterion for election of 22q11.2DS as a model for schizophrenia. Figure 1.5 represents the main genetic risk factors for developing psychotic disorders.

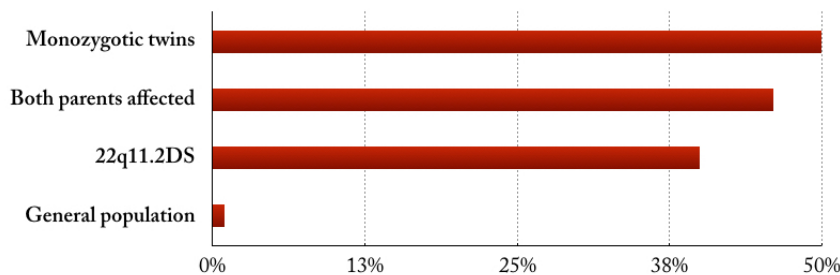


Figure 1.5: Genetic risk for schizophrenia (adapted from McGuffin et al., 1995).

However, for 22q11.2DS to be considered a model, a second necessary criterion is that, conversely, the schizophrenia population (i.e., patients who show the behavioral phenotype) also contains increased rates of the syndrome. This is indeed the case, as rates of 22q11.2DS range between 0.3-2% in the schizophrenia population (Arinami et al., 2001; Karayiorgou et al., 1995), contrasting with the 1:4000 prevalence of 22q11.2DS reported for the general population (Oskarsdóttir et al., 2004; Shprintzen, 2005).

Additional supportive evidence for the connection between 22q11.2DS and schizophrenia comes from genetic, behavioral and neurodevelopmental studies (Bassett and Chow, 1999). Indeed, genetic evidence from linkage studies points to a link between 22q11.2DS and schizophrenia (Blouin et al., 1998; Shaw et al., 1998), and multiple genes of the 22q11.2 locus have been related to increased risk for developing schizophrenia (Budell et al., 2008; Gothelf et al., 2005, 2008; Karayiorgou and Gogos, 2004; Karayiorgou et al., 2010). Furthermore, both disorders share a similar neurocognitive phenotype during the premorbid phase preceding schizophrenia, with delays in language onset, language difficulties, intellectual deficits, decreased affect, motor coordination deficits and social withdrawal. Finally, findings from studies focusing on brain alterations in 22q11.2DS and schizophrenia also largely converge, with common findings such as decreased grey matter and white matter volumes, ventricular enlargements, midline developmental abnormalities such as cavum septum pellucidum, and aberrant early neuronal migration (Bassett and Chow, 1999).

Together, these properties of 22q11.2DS justify the use of the syndrome as a model to study psychotic disorders. The existence of such a model offers unique research opportunities, since it brings about multiple valuable advantages: 1) 22q11.2DS represents

a genetically homogeneous population, allowing for a systematic investigation of the genetic roles in the onset of psychotic disorders; 2) the syndrome is generally detected early in life, which provides the opportunity to perform prospective follow-ups of patients before the onset of psychosis, potentially leading to key insights about the risk factors and mechanisms leading to psychosis; and finally 3) the high prevalence of schizophrenia in 22q11.2DS further makes this population ideal for studying mechanisms underlying psychotic disorders, and more specifically schizophrenia, once the disorder is established. These advantages cannot be found in other high risk populations (such as monozygotic twins, or affected parents for instance), as their prevalence is significantly lower, and their detection is typically later in life. Thus, 22q11.2DS represents an ideal framework for studying the developmental mechanisms leading to psychotic disorders.

1.1.7 Risk factors of conversion to psychosis

Since the formal establishment of 22q11.2DS as a model for schizophrenia around the late 1990s – early 2000s, extensive research has been carried out to better understand the developmental pathways leading to the emergence of psychotic disorders. As a result, several clinical and cognitive risk factors for conversion to psychosis in 22q11.2DS have been recently identified. Risk factors include preterm birth (Kufert et al., 2016; Van et al., 2016), the presence of anxiety disorders (Gothelf et al., 2013) and lower global functioning or IQ at baseline (Gothelf et al., 2013; Schneider et al., 2016; Vorstman et al., 2015), a decline in cognitive functioning in years prior to the onset of psychosis (Gothelf et al., 2013; Vorstman et al., 2015), and the presence of an ultra-high risk status (UHR) (Schneider et al., 2016). In this study, we will focus on two of these risk factors, namely cognitive decline and the UHR status. These factors are discussed in more detail below.

1. *Cognitive decline*

In the general population, a growing body of research shows that in the general population, a decline in cognitive functions precedes the onset of psychosis by several years (Meier et al., 2014; Rabinowitz et al., 2002; Reichenberg et al., 2005). As such, it is now considered as a fundamental component of psychotic disorders (Kahn and Keefe, 2013; Woodberry et al., 2008), and is a necessary diagnostic element for treatment initiation (Vorstman et al., 2015).

In 22q11.2DS, a prospective longitudinal cohort study using data from the IBBC in 22q11.2DS confirmed that early cognitive decline also represents a robust risk factor predicting the onset of psychotic disorders in this population (Vorstman et al., 2015). More specifically, they demonstrated that individuals with 22q11.2DS who develop schizophrenia had a steeper cognitive decline compared to subjects with 22q11.2DS who did not develop the disorder. This decline was visible in all three measures of IQ (i.e., FSIQ, PIQ and VIQ), but was steepest in VIQ. Note that the 22q11.2DS population *as a whole* is known to experience a steeper decline in verbal abilities compared to non-verbal abilities (Green et al., 2009; Swillen, 2016; Vorstman et al., 2015); thus, these data suggest that a deterioration of verbal functions is even stronger in patients who convert to psychosis.

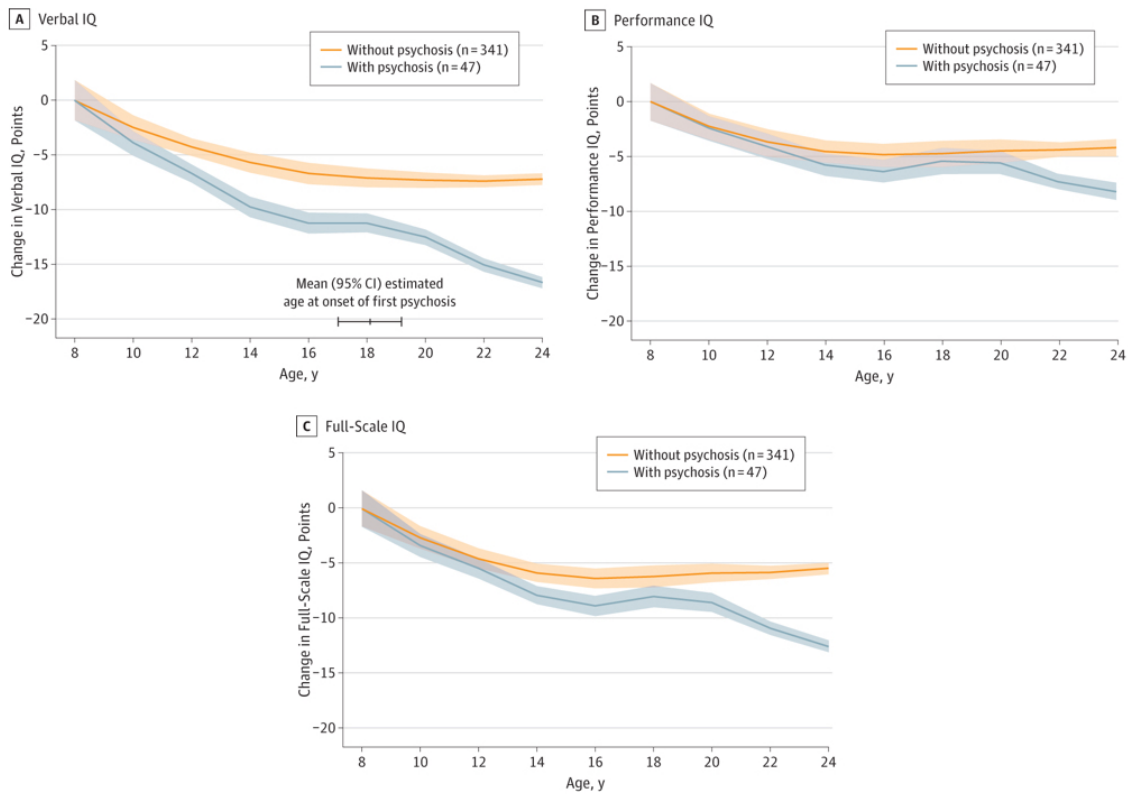


Figure 1.6: Cumulative plots of IQ decline in patients with 22q11.2DS who developed a psychosis compared to non-psychotic individuals with 22q11.2DS (adapted from Vorstman et al., 2015).

2. The UHR status

The UHR criteria were originally validated in the general population and have been developed to identify individuals with a high clinical risk for conversion to psychosis (Fusar-Poli et al., 2013). While different interview tools have been developed to assess the presence of UHR criteria, one of the most widely used in North America and Europe is the Structured Interview for Prodromal Syndromes (SIPS; Miller et al., 2002). According to the SIPS guidelines, an individual is considered at UHR when at least one of the following criteria are met:

1. **Attenuated Psychotic symptoms (APS)**, i.e. presence of subthreshold attenuated positive symptoms with an onset or a worsening in the past year, and a frequency of at least once per week in the past month. Such symptoms include unusual ideas, paranoia/suspiciousness, grandiosity, perceptual disturbance, or conceptual disorganization.
2. **Brief Limited Intermittent Psychotic Episode (BLIP)**, i.e. presence of transient psychotic symptoms with onset in the last three months. More specifically, these symptoms need to occur intermittently for at least several minutes per day and at least once a month; however, they should not last longer than one hour per day and should occur less frequently than 4 days per week over a period of one month.

Symptoms are typically forms of delusions, hallucinations, or disorganization, but are not seriously compromising the person's mental health.

3. **Genetic Risk and Deterioration Syndrome (GRD)**, i.e., either presence of a first-degree relative with a psychotic disorder, or presence of a schizotypal personality disorder combined with a significant decrease in functioning in the past month compared to one year ago.

In the general population, conversion rates to psychosis are significantly higher for UHR patients, with 9.6% of UHR patients converting after 6 months and 36-37% converting after 3 to 4 years (Fusar-Poli et al., 2012; Schultze-Lutter et al., 2015). In 22q11.2DS, a recent study by our group has shown that generally, approximately 24.7% of patients with 22q11.2DS meet the UHR criteria (Schneider et al., 2016). Moreover, the predictive value of the UHR criteria in the 22q11.2DS population was confirmed, with 27.5% of UHR patients converting to psychosis after approximately 3 years, versus only 4.5% conversion in non-UHR patients (Schneider et al., 2016).

1.2 White matter

In the field of schizophrenia, researchers increasingly converge to a neurodevelopmental view of the illness, where early developmental anomalies are responsible for generating the disruptions in cognition, perception and emotion expressed around late adolescence. Importantly, a large body of evidence indicates that patients with schizophrenia show widespread alterations of white matter structure (Canu et al., 2015; Fittsimmmons et al., 2013; Pettersson-Yeo et al., 2011; Wheeler and Voineskos, 2014), making it a valuable candidate biomarker for psychosis. However, studies of developmental trajectories of white matter are lacking in the field of schizophrenia, as this population is heterogeneous and difficult to identify before the illness onset. In this context, 22q11.2DS provides crucial research possibilities, since this syndrome is genetically homogeneous, is recognized as a model for psychosis and can be identified at early ages, which allows for extensive longitudinal prospective studies. As such, 22q11.2DS represents a unique opportunity to study white matter development and its role in the emergence of psychosis.

In this chapter, general aspects of white matter structure and function will first be discussed, followed by a description of recent advances in neuroimaging techniques enabling the study of human white matter in vivo, and ending by a description of findings on normal white matter development. In the next chapters, white matter alterations associated schizophrenia and 22q11.2DS will be discussed (1.3), and different methods used to analyze white matter structure will be outlined (1.4).

1.2.1 Definition: white matter structure and function

On a global level, the brain consists of three main components: grey matter, white matter, and cerebrospinal fluid (CSF). While the CSF is liquid and fills the ventricular spaces of the brain, grey and white matter are solid tissues, organized in a specific manner. Namely, grey matter, composed of neuronal cell bodies and the neuropil (i.e., a complex network of unmyelinated axons, dendrites and glial extensions), is mostly distributed along the surface of the brain. White matter, on the other hand, mainly consists of myelinated axons, and can be found in the deeper parts of the brain. Figure 1.7 contains a scheme of cortical white matter and grey matter organization.

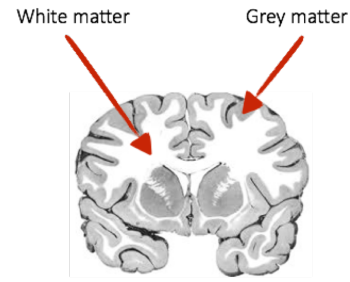


Figure 1.7: *Schematic illustration of brain tissues.*

In the central nervous system (CNS), axons are myelinated by extensions of oligodendrocytes, a type of glial cell that sends out its processes towards up to 50 axons. These processes wrap themselves multiple times around the axon, forming what is called a “myelin sheath”, an electrically insulating layer composed of lipids (70%) and proteins (30%) (Baumann and Pham-Dinh, 2001). Figure 1.8 is a schematic representation of myelin sheaths created by oligodendrocytes. The presence of this hydrophobic layer around axons has several functions (Nave, 2010): firstly, it accelerates the transmission of electric signals between neurons by up to 100 times, as depolarization occurs only at nodes of Ranvier, allowing a saltatory conduction of action potentials (APs); second, due to the saltatory conduction, the energy necessary for the reestablishment of resting potential after an AP is largely reduced; third, glial cells are known to communicate with neurons and to provide neurotrophic support, which is important for axonal integrity and survival.

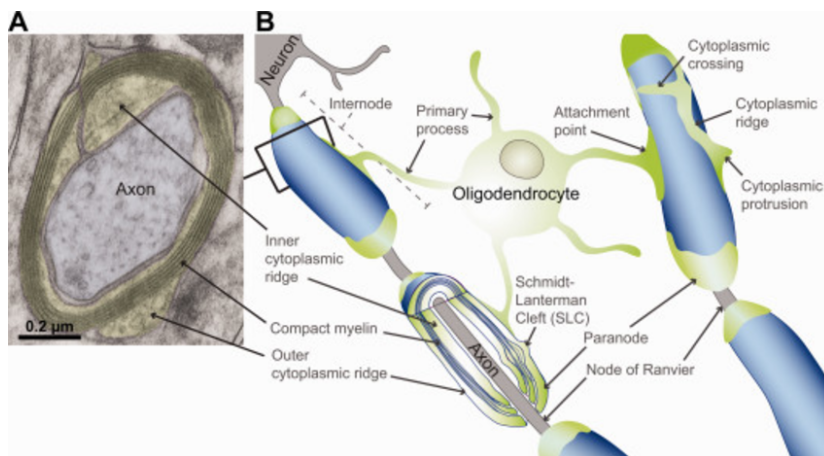


Figure 1.8: *Electron micrograph of a myelinated axon (A) and schematic representation of an oligodendrocyte wrapping its processes around axons in the CNS (B) (from Rinholm Johanne E et al., 2016).*

All together, these myelinated axons can be considered as the “wiring” of the brain, since they form thick bundles of insulated cables connecting areas to each other. As such, on a macroscopic level, their main function is to enable fast, long-range communication between distal areas.

Axons sharing similar destinations typically regroup into bundles, called “tracts” in the CNS. With the exception of some very large white matter tracts, such as the corpus callosum or the anterior commissure, the identification of white matter tracts is impossible on MRI images (i.e., T1-weighted images), and remains challenging in post-mortem brains (Mori et al., 2005).

Until the second half of the 20th century, our understanding of white matter tracts relied of a small number post-mortem dissection studies (Burdach, 1819; Dejerine and Dejerine-Klumpke, 1895; Talairach and Tournoux, 1988). However, these are based on small samples and have emphasized normative aspects of tracts organization, rather than inter-subject variability (de Schotten et al., 2011). Furthermore, they had the considerable limitation that white matter tracts could not be studied *in vivo*. The development of a specific type of Magnetic Resonance Imaging (MRI) called Diffusion Tensor Imaging (DTI), during the second half of the 20th century, allowed for tremendous advances in our understanding of white matter tracts organization in the brain. In what follows, we discuss this acquisition method in more detail.

1.2.2 Diffusion Tensor Imaging: a non-invasive tool to study white matter *in vivo*

In general, all MRI imaging techniques rely on the resonance properties of hydrogen protons, contained in water molecules. In conventional image acquisitions such as T1-weighted or T2-weighted imaging, magnetic fields and changing gradients are applied to the brain, allowing to excite protons and subsequently measure their relaxation time back to equilibrium. Each tissue is composed of a specific proton density, resulting in a specific relaxation time. Thus, this metric is then used to construct 3D images, in which different contrasts will reflect specific relaxation times. Note that the smallest unit of an MR image is called a “voxel” and typically corresponds to a 1x1x1mm cube (although the size can vary and be slightly larger, depending on the acquisition parameters). Accordingly, MR images thus commonly have a 1mm resolution.

Diffusion Tensor Imaging (DTI) is a different type of MRI imaging that measures the diffusion of water molecules inside the brain. In an isotropic, unrestricted environment such as a glass of water, molecules can diffuse freely in all directions. Correspondingly, the probability distribution of displacements of a molecule in such an environment can be represented by a spherical (i.e., isotropic Gaussian) distribution. By contrast, biological tissues, and in particular white matter, are anisotropic environments, meaning that the direction of diffusion is restricted towards specific directions. Indeed, the presence of hydrophobic cell membranes and myelin sheaths impedes the movement of water molecules, forcing them to move along the direction of the axon. As a result, the probability distribution becomes an anisotropic ellipsoid. In DTI, diffusion is measured in each voxel along a defined set of directions to reconstruct what is called a diffusion “tensor” (Basser et al.,

1994). This tensor is essentially a mathematical description of a 3D ellipsoid distribution. It is characterized by 6 parameters: 3 eigenvalues, describing the shape of the ellipsoid (i.e., eigenvalues indicate the length of the diffusion axes); and 3 eigenvectors, describing the diffusion orientation (i.e., eigenvectors indicate the orientation of the diffusion axes) (Mills and Tamnes, 2014; Mori et al., 2005). Figure 1.9 provides a representation of the ellipsoid in an isotropic and anisotropic situation.

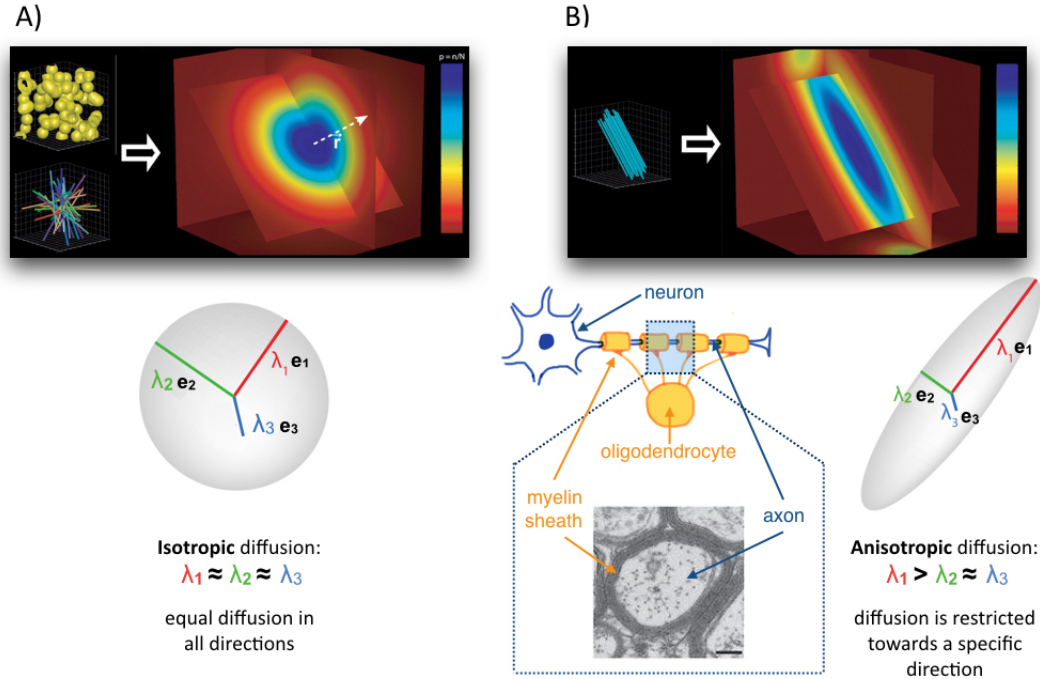


Figure 1.9: Figure A) illustrates an isotropic situation, where water molecules are unrestricted and can freely diffuse in all directions, producing a spheric probability distribution of diffusion. The corresponding tensor has three identical eigenvalues. Figure B) shows an anisotropic situation such as in a myelinated axon, where water diffusion is restricted towards a specific direction, corresponding to an ellipsoid probability distribution of diffusion. In this situation, the tensor's first eigenvalue (i.e., principal direction of diffusion) becomes larger than the two other eigenvalues. Adapted from Hagmann et al. (2006); electron microscopy picture taken from Yang et al. (2016).

The eigenvalues of the tensor are then used to compute four different scalar measures, each providing distinct information about the local microstructural properties of white matter (Figure 1.10):

1. **Fractional Anisotropy (FA)**, which takes values between 0-1 and indicates the fraction of diffusion that is anisotropic (i.e., directionally constrained). This measure is considered as a general measure of microstructural integrity;
2. **Axial Diffusivity (AD)**, corresponding to the main direction of diffusion and providing information about axonal integrity and tracts organization (Budde et al., 2009; Song et al., 2003);
3. **Radial diffusivity (RD)**, indicating the amount of diffusion perpendicular to the main direction and thought to inform about the degree of myelination (Song et al., 2002);

4. **Mean diffusivity (MD)**, representing the average magnitude of water diffusion in the tissue. It is typically considered as a summary measure.

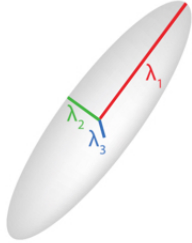
DTI measures	Relation to brain structure
 $\lambda_1 = \text{Axial diffusivity (AD)}$ $\frac{\lambda_2 + \lambda_3}{2} = \text{Radial Diffusivity (RD)}$ $\frac{\lambda_1 + \lambda_2 + \lambda_3}{3} = \text{Mean Diffusivity (MD)}$ $\sqrt{\frac{1}{2} \frac{(\lambda_1 - \lambda_2)^2 + (\lambda_1 - \lambda_3)^2 + (\lambda_2 - \lambda_3)^2}{(\lambda_1^2 + \lambda_2^2 + \lambda_3^2)}} = \text{Fractional Anisotropy (FA)}$	<p>Axonal integrity Tract organization Axonal diameter</p> <p>Myelination</p> <p>Summary measure</p> <p>General measure of microstructural integrity</p>

Figure 1.10: The three main directions of diffusion provided by the tensor can be used to compute four main measures of diffusion: Axial Diffusivity (AD), Radial Diffusivity (RD), Mean Diffusivity (MD) and Fractional Anisotropy (FA). Each measure provides distinct information about the local properties of white matter.

As illustrated in Figure 1.11, in a healthy, mature brain with coherently organized and myelinated white matter bundles, diffusion is typically characterized by high values of AD, resulting from densely packed, healthy axons; low values of RD reflecting the presence of thick myelin sheaths around the axons; intermediate values of MD as this measure comprises both high diffusion along the axon (AD) and low diffusion perpendicular to the axon (RD); and high values of FA pointing to a highly anisotropic environment. In the case of abnormal white matter microstructure, changes in diffusion metrics, particularly in RD and AD, are useful for pin-pointing the specific underlying pathological processes. Namely, increased levels of RD (i.e., increased diffusivity through the membrane of the axon) are thought to reflect a situation of demyelination (Song et al., 2003, 2002). Conversely, decreased levels of RD are indicative of excessive myelination. Decreased levels of AD (i.e., reduced diffusivity along the direction of the axon) have been suggested to reflect 3 possible events, which are axonal damage, reduced tracts organization or reduced axonal diameter (Budde et al., 2009; Harsan et al., 2006; Schwartz et al., 2005; Song et al., 2003).

Thus, the emergence of DTI has allowed for a non-invasive way to gain considerable knowledge about the microstructural properties of white matter in vivo. Note however, that DTI images provide information at a mm scale (similar to MR images). Therefore, they do not contain information at the axonal level (which is in the μm scale) (Mori et al., 2009), and DTI metrics should be considered as estimations of white matter microstructure.

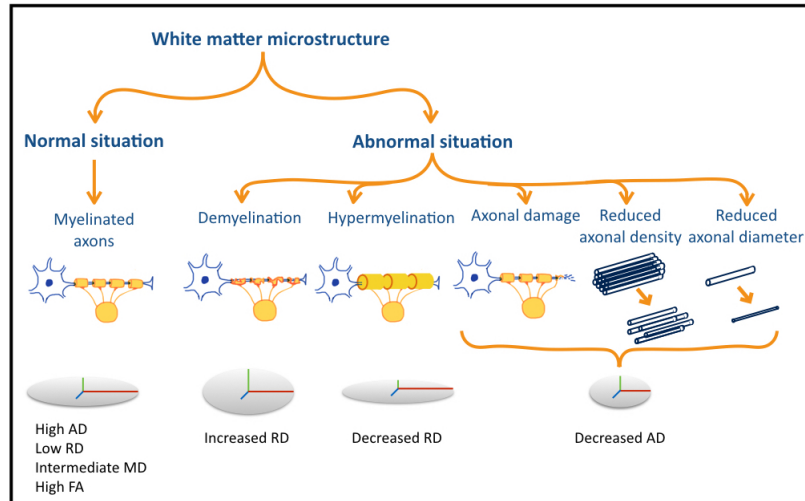


Figure 1.11: Normal versus abnormal brain wiring. White matter microstructure can be affected in multiple ways, each corresponding to changes in specific diffusion metrics.

1.2.3 White matter tracts

DTI-based tractography, defined as the computational reconstruction of white matter tracts in vivo (for more information, see section 2), has enabled the identification of the major long-range white matter tracts in the brain and the creation of several atlases (for a review, see Mori et al., 2009). Figure 1.12 illustrates the white matter tracts identified by Mori et al. (2005). These tracts can be divided into 3 different types, listed in Table 1.1:

Tract type	Tract name
Projection ²	Corticospinal Tract
	Corticopontine tract
	Corticobulbar tract
	Corticoreticular tract
	Thalamic radiations
Commissural	Corpus callosum
Association	Superior and inferior longitudinal fasciculus (SLF, ILF)
	Superior and inferior fronto-occipital fasciculus (SFO, IFO)
	Uncinate fasciculus (UNC)
	Cingulum (CG)
	Fornix (FX)
	Stria terminalis (ST)

Table 1.1: White matter tracts identified by Mori et al. (2005) in their atlas of white matter.

²Of note, projection fibers are both ascending and descending. They originate from a wide white matter sheet called the “corona radiata” at the level of the cortex. At the level of the basal ganglia, they make up distinct parts of a general white matter structure called the “internal capsule” (e.g., the anterior limb of the internal capsule comprises the anterior thalamic radiation; the genu contains the corticobulbar tract; and the posterior limb contains the corticospinal tract).

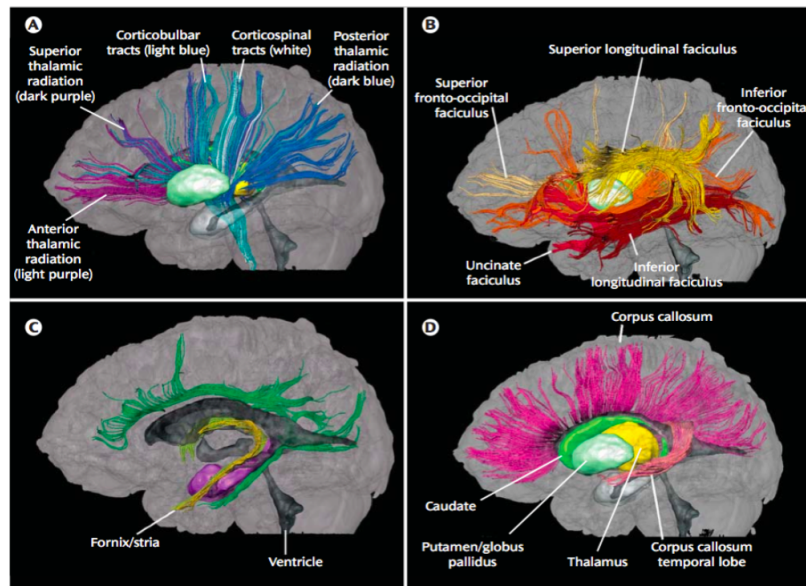


Figure 1.12: Left lateral views of major white matter tracts in the brain as identified in the white matter atlas from Mori et al. (2005). Panel A) displays projection tracts, panel B) illustrates association tracts, panel C) contains limbic fibers and panel D) displays commissural fibers (taken from Ottet, 2013).

These types of tracts are carrying out distinct functions: commissural tracts are responsible for interhemispheric communication (i.e., they connect the left and right hemispheres); projection tracts transfer afferent and efferent information between the peripheral nervous system and the brain; and association tracts ensure communication between different brain regions within the same hemisphere. Of note, the large majority of association tracts have a connection with the frontal lobe (with the exception of the fornix and the stria terminalis, which are exclusively connecting limbic regions).

Post-mortem dissection methods and animal studies using tracer techniques confirmed the reliability of tractography methods in identifying white matter tracts (Dyrby et al., 2007; Lawes et al., 2008).

1.2.4 White matter development

When studying a neurodevelopmental syndrome such as 22q11.2DS, and particularly when investigating biomarkers of psychosis, it is crucial to compare their neuroanatomical development with normative developmental trajectories, as these will help to pin-point early developmental deviations in patients and may contribute to the identification of prevention and treatment targets. In what follows, we will provide a description of white matter development as observed in typical developing individuals.

White matter development starts during the last weeks of gestation, with myelination of prosencephalic neurons (around week 20 for thalamic axons, week 35 for cortical axons). However, the largest part of white matter maturation occurs after birth, and is known to continue for several decades and to extend well into adulthood (Linderkamp et al., 2009). Given that white matter maturation mainly occurs during postnatal development, the

ability to study white matter structure in vivo using DTI imaging and tractography has provided crucial insights. Recent extensive longitudinal studies on healthy developing controls have revealed that white matter shows non-linear developmental trajectories extending all the way into adulthood (Lebel and Beaulieu, 2011; Lebel et al., 2012). More specifically, total cranial white matter volume follows a non-linear trajectory, with rapid increases during childhood, a peak at 37 years and progressive decreases later on (Lebel et al., 2012) (see Figure 1.13). When considering DTI metrics of major white matter tracts, findings indicate systematic non-linear FA increases in all tracts (Bendlin et al., 2010; Lebel et al., 2012). MD, on the other hand, follows an inverse non-linear trajectory (Lebel et al., 2012). Regarding AD, results are less consistent, as both developmental increases and decreases have been reported for this metric (Bava et al., 2010; Brouwer et al., 2012).

Importantly, findings consistently indicate that maturation processes of DTI metrics evolve with different rates depending on the tracts (Lebel et al., 2012; Mills and Tamnes, 2014). Indeed, maturation peaks and minima (for FA and MD, respectively) range from 18 years to over 40 years. Interestingly, it has been found that early maturing tracts (such as such as the fornix, the inferior longitudinal fasciculus and the corpus callosum) are more involved in basic processes, and late maturing tracts (mainly fronto-temporal connections such as the superior longitudinal fasciculus, the uncinate fasciculus and the cingulum bundle), on the other hand, are involved in more complex tasks such as language, emotions, memory and cognitive functions. Figure 1.13 shows the differential maturation rates of major white matter tracts.

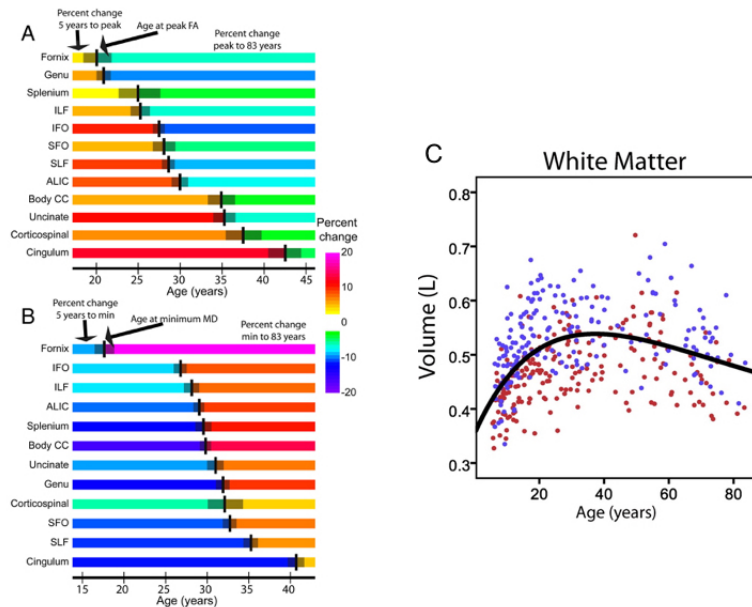


Figure 1.13: Panel A) shows the age at peak for fractional anisotropy (FA); panel B) indicates the age at minimum MD. Percent change 5 years prior to the peak/minimum and from there to 83 years is reflected through the colors of the bars. Panel C) shows the developmental trajectory of total white matter volume (adapted from Lebel et al., 2012).

1.3 White matter alterations in 22q11.2DS

1.3.1 Previous findings: widespread alterations of structural connectivity

A growing body of evidence suggests that 22q11.2DS is associated with widespread white matter alterations. Early volumetric studies have consistently reported white matter volume alterations in 22q11.2DS, with volume reductions in children (Eliez et al., 2000; Kates et al., 2001) and adolescents (Baker et al., 2011), and a combination of reductions and increases of white matter volume in adults (da Silva Alves et al., 2011; Van Amelsvoort et al., 2001). Of interest, white matter volume alterations appeared to be greater in magnitude than grey matter volume alterations (Eliez et al., 2000; Kates et al., 2001; Van Amelsvoort et al., 2001), pointing to a more severe pathology of white matter structure in this syndrome. To date, only one study focused on the longitudinal development of white matter volume in 22q11.2DS, and confirmed that white matter volume reductions persist from late adolescence to adulthood (Gothelf et al., 2007).

More recently, Diffusion Tensor Imaging (DTI) has provided insights into the microstructural properties of white matter in vivo. Whole-brain voxel-based DTI studies indicate that 22q11.2DS is associated with widespread white matter microstructure alterations. These affect most long-range white matter tracts, including the superior longitudinal fasciculus (SLF), the inferior longitudinal fasciculus (ILF), the inferior fronto-occipital fasciculus (IFOF), the cingulum bundle, the uncinate fasciculus (UNC), the arcuate fasciculus, the corpus callosum, the internal capsule (anterior and posterior limbs) and the corona radiata (reviewed in Scariati et al., 2016).

However, results regarding the nature of alterations in diffusion metrics are subject to considerable variations. Very inconsistent findings have been reported on FA, where a number of studies found increases (Bakker et al., 2016; Barnea-Goraly et al., 2003; da Silva Alves et al., 2011; Jalbrzikowski et al., 2014; Kates et al., 2015; Olszewski et al., 2017; Perlstein et al., 2014; Simon et al., 2005b, 2008; Sundram et al., 2010; Tylee et al., 2017), as well as decreases (Barnea-Goraly et al., 2003; da Silva Alves et al., 2011; Deng et al., 2015; Jalbrzikowski et al., 2014; Kates et al., 2015; Kikinis et al., 2012, 2013; Perlstein et al., 2014; Radoeva et al., 2012; Roalf et al., 2017; Simon et al., 2005b; Sundram et al., 2010; Villalon-Reina et al., 2013) in patients with 22q11.2DS. More consistent results are reported concerning RD and AD, which both mostly show decreases (Jalbrzikowski et al., 2014; Kates et al., 2015; Kikinis et al., 2012, 2017, 2013; Olszewski et al., 2017; Perlstein et al., 2014; Radoeva et al., 2012; Roalf et al., 2017; Simon et al., 2008; Tylee et al., 2017; Villalon-Reina et al., 2013).

As pointed out by a previous review of structural connectivity by our group (Scariati et al., 2016), the overall heterogeneity of results regarding DTI metrics is likely due to several methodological differences - namely, the very variable age ranges for the selected samples, the relatively small sample sizes of some studies, the presence/absence of correction for potential confounding effects (such as gender, age, IQ), the algorithm and templates chosen for registration, and the software used for DTI image analysis. Another

potential factor contributing to the inconsistency of DTI findings is the MRI image quality, which can substantially vary depending on the magnet (1.5.T or 3T) used for the image acquisition. Finally, it is also likely that the heterogeneity of previous findings is, at least in part, due to the complex nature of white matter microstructural maturation (see section 1.2.4). Indeed, due to this complexity, group comparisons might yield different results depending on the period of development that is being considered. This is even more likely given that some preliminary evidence from DTI studies on 22q11.2DS suggests the existence of alterations in age-related changes in this population. More specifically, findings indicated that, while the total white matter volume progressively increased with age for 22q11.2DS individuals in a similar way to controls (Ottet et al., 2013), DTI and tractography metrics failed to show the age-related changes normally observed in typical developing subjects (Deng et al., 2015; Jalbrzikowski et al., 2014; Ottet et al., 2013; Padula et al., 2015).

Taken together, these preliminary findings suggest the existence of potentially abnormal developmental trajectories of white matter microstructure in 22q11.2DS. However, these results are all based on cross-sectional studies, and need to be confirmed using longitudinal study designs, as these provide the opportunity to capture the complexity of developmental trajectories of white matter microstructure.

1.3.2 White matter alterations and psychotic symptoms

Besides general alterations inherent to 22q11.2DS, DTI studies also report associations between white matter alterations and psychotic symptoms in the syndrome (da Silva Alves et al., 2011; Gothelf et al., 2011; Jalbrzikowski et al., 2014; Kates et al., 2015; Kikinis et al., 2017; Ottet et al., 2013; Padula et al., 2017; Perlstein et al., 2014; Scariati et al., 2016; Tylee et al., 2017; Van Amelsvoort et al., 2004). To date, these studies have mostly performed correlational analyses between positive symptoms scales and DTI metrics. The most consistent finding is a negative association between the severity of prodromal positive symptoms and DTI metrics (FA, AD and RD) and, overall, these white matter integrity disruptions affected long-range and midline white matter tracts, such as the IFOF, the anterior and posterior limbs of the internal capsule, the corona radiata, the uncinate fasciculus, the ILF, the cingulum bundle and the body of the corpus callosum (Scariati et al., 2016). Thus, a growing body of evidence suggests that white matter alterations are existent in prodromal stages of psychosis. Nevertheless, some studies also report an absence of association between white matter metrics and the intensity of positive symptoms (Padula et al., 2015). A longitudinal characterization of white matter development in prodromal stages of psychosis may help to clarify the role of white matter structure at early stages of the disease. Moreover, the use of established risk factors, rather than prodromic symptoms scales, may further improve the delineation of neuroanatomical correlates associated with early stages of psychosis. In what follows, we will describe these risk factors in more details.

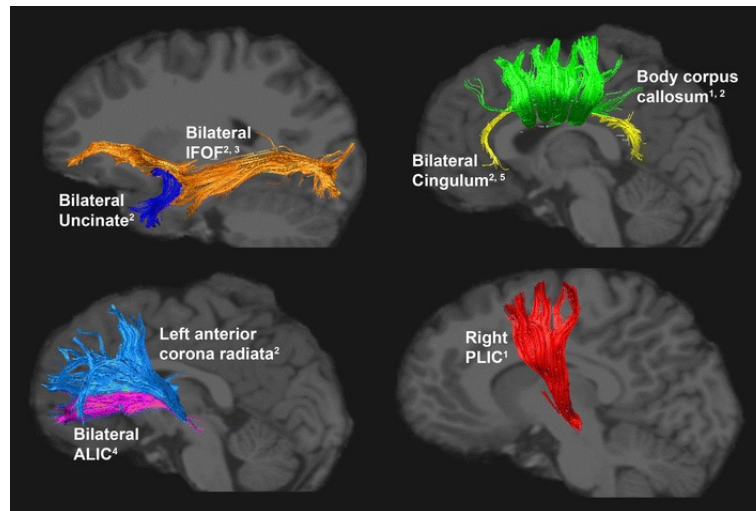


Figure 1.14: White matter tracts showing alterations associated with psychotic symptoms in 22q11DS. Note that the ILF is not displayed here, but also shows an association between disruptions of white matter integrity and psychotic symptoms (from Scariati et al., 2016).

Legends: IFOF = inferior fronto-occipital fasciculus; ALIC = anterior limb of the internal capsule; PLIC = posterior limb of the internal capsule.

1.3.3 White matter alterations associated to risk factors of psychosis

Studying the relationship between white matter pathology and recently established risk factors for conversion to psychosis (see section 1.1.7) could potentially lead to a better identification of biomarkers preceding the emergence of the disease. Indeed, as mentioned in a previous study done by our group (Padula et al., 2018), the use of reliable risk factors allows to delineate a more homogenous group of patients in terms of their symptomatic characteristics. In addition, findings are not biased by the usual confounds related to medication in populations with full-blown psychosis. Therefore, characterizing neurodevelopmental patterns in patients who display these risk factors is a promising strategy for identifying the underlying brain alterations preceding the emergence of psychosis.

1. Cognitive decline and white matter alterations

A single previous study has investigated the association between cognitive decline and white matter integrity in 22q11.2DS (Nuninga et al., 2017). In this study, IQ was measured twice, once prior to scan and once at the time of scan. Results indicated significant white matter disruptions in individuals who experienced a cognitive decline prior to MRI scan, compared to subjects without cognitive decline. Specifically, cognitive decline was associated with increased FA in several white matter tracts, including the SLF, the cingulum, the internal capsule and the superior fronto-occipital fasciculus.

However, to date, the parallel evolution of white matter microstructure and cognitive function has not yet been investigated. Longitudinal studies with multiple neuroanatomical and cognitive assessments are needed to determine whether prodromal cognitive decline is associated with deviant white matter maturational trajectories.

2. UHR status and white matter alterations

To date, white matter microstructure has not been characterized in UHR and non-UHR patients with 22q11.2DS. However, three previous studies have divided patients depending on the severity of positive symptoms (where a subject was considered “at high risk of psychosis” when presenting a score higher than 3 in one of the 5 positive symptoms scales) (Kikinis et al., 2017; Padula et al., 2017; Roalf et al., 2017). This categorization yielded significant group differences in multiple white matter tracts, including the corpus callosum (Kikinis et al., 2017), the cingulum (Padula et al., 2017; Roalf et al., 2017), the corona radiata (Kikinis et al., 2017), the internal capsule (Kikinis et al., 2017), the inferior longitudinal fasciculus (Padula et al., 2017), the superior longitudinal fasciculus (Kikinis et al., 2017) and the uncinate fasciculus (Roalf et al., 2017). Thus, existent findings suggest that high levels of psychotic symptoms are associated with disruptions in all tract types (i.e., projection, commissural and association tracts). Of note, alterations affected different DTI metrics depending on the study, making it difficult to discern a specific disruptive pattern. Nevertheless, a tendency of reduced levels of AD and FA was most consistent across all three studies.

Moreover, as mentioned earlier, multiple DTI studies have performed correlations between DTI metrics and the severity of positive symptoms, and results (summarized in a review by Scariati et al., 2016) consistently suggested an involvement of fronto-temporal and limbic tracts, which is in line with studies who studied white matter in subgroups of patients.

Thus, a growing body of evidence points to the existence of white matter disruptions in patients with 22q11.2DS experiencing prodromal psychotic symptoms. Although encouraging, existent findings would need to be confirmed using robust, well-established risk factors for psychosis such as UHR. Indeed, while raw positive symptoms scales are informative about the current state of the patient, they do not account for the frequency or duration of symptoms, which is specifically assessed by the UHR diagnosis. Furthermore, current findings are exclusively based on cross-sectional study designs. A longitudinal characterization of white matter development in patients at UHR may provide valuable insights regarding the early developmental anomalies preceding psychosis.

1.3.4 White matter in non-deleted patients with schizophrenia or at risk for psychosis

In schizophrenia research, a long-standing hypothesis proposes that the illness results from a general disconnection between cortical areas. Note that the term “dysconnectivity” refers to alterations of cortical connections and considers both the “hypo-“ (i.e., reduced connectivity) and “hyperconnectivity” (i.e., excessive connectivity) situations. The proposal was originally made by Wernicke (1906), and later formalized by Friston and Frith (1995) using neuroimaging evidence. Recent reviews of structural connectivity findings largely support this hypothesis. Indeed, although findings are somewhat heterogeneous, a growing bulk of evidence indicates that schizophrenia is associated with widespread white matter alterations, mostly affecting frontal connections (Canu et al., 2015; Fitzsimmons et al., 2013; Pettersson-Yeo et al., 2011; Wheeler and Voineskos, 2014). More specifically, the large majority of results suggests reductions in connectivity manifested by reduced levels of FA. Canu et al. (2015) reviewed the structural connectivity anomalies visible at different stages of the disease and described an increasingly widespread pattern of alterations towards more severe illness stages: patients at UHR most frequently showed decreased FA in long association tracts; patients with first episode psychosis showed reductions in similar regions and additionally had more severe abnormalities in anterior white matter regions (such as the genu of the corpus callosum, the anterior limb of the internal capsule, the anterior cingulum and frontal white matter); finally, patients with chronic schizophrenia presented FA reductions in all the above mentioned tracts, with an additional spreading to other regions of the corpus callosum, thalamic radiations and temporal white matter. Together, these results suggest that schizophrenia is associated with abnormal neurodevelopmental mechanisms, leading to progressive alterations in white matter integrity. A theoretical model has been proposed by Insel (2010) to characterize the relationship between aberrant neuroanatomical development (including myelination) and the emergence of a psychotic disorder (see Figure 1.15). Recently, a DTI study using one of the largest samples of patients with schizophrenia confirmed the presence of widespread FA reductions affecting more than 40% of cerebral white matter volume (Klauser et al., 2017). When considering white matter tracts, they found that the corpus callosum, cingulum and thalamic radiations showed the most severe alterations.

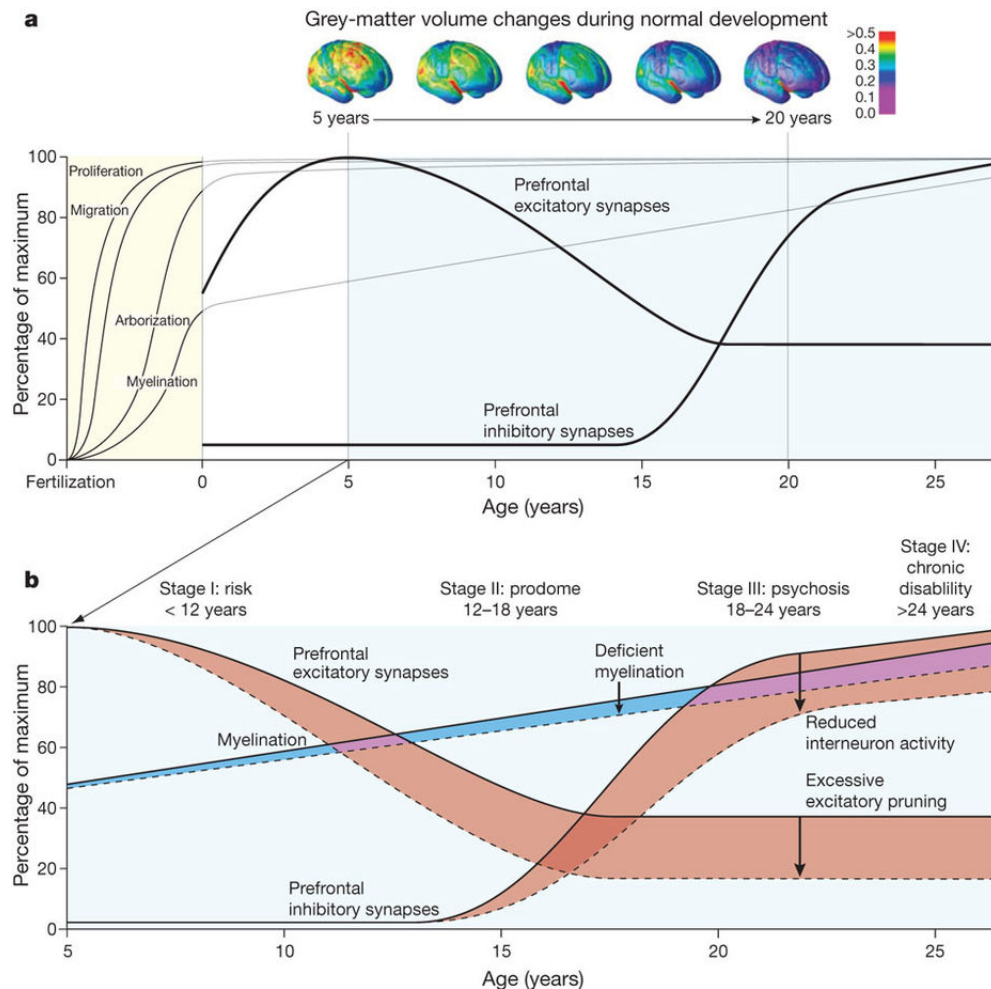


Figure 1.15: Normal cortical development is shown in figure a). The prenatal phase is characterized by proliferation and migration of neurons. Circuit formation (arborization) and myelination also begin in the prenatal period, but continue until adulthood. The combination of axonal pruning and myelination deposition leads to progressive reductions of grey matter during postnatal development. Figure b) shows a theoretical model of events leading to the emergence of schizophrenia. In this neurodevelopmental model, the combined effect of aberrant axonal pruning and myelination is thought to cause altered excitatory-inhibitory balance and disrupted connectivity, respectively. This, in turn, induces the emergence of psychosis (from Insel, 2010).

1.4 Methods for the analysis of DTI images

1.4.1 Whole-brain analysis techniques

Many DTI studies investigating white matter group differences between controls and clinical samples used approaches such as voxel-based morphometry (VBM), introduced in the late 1990s (Wright et al., 1995) and elaborated in 2000 (Ashburner and Friston, 2000). Briefly, this technique performs a voxel-wise comparison (of grey, white matter, FA values) between groups, allowing to find focal group differences in brain anatomy. To achieve this, images are spatially normalized (i.e., aligned to a common template), segmented into grey and white matter and smoothed to normalize values and compensate for inexact spatial normalization. Statistical voxelwise analysis is then applied on all brain images in order to detect group differences (Ashburner and Friston, 2000, 2001). VBM methods have the considerable advantage to enable very exploratory analyses, as they can identify focal group differences directly based on the data, without the need of a priori knowledge about the way in which the brain is affected by a given disease. Additionally, they are fully automated, making them considerably less time consuming and more objective than manual analysis techniques. However, it has been shown that registration misalignments can occur in case of significant morphological differences due to factors such as disease, which in turn considerably biases results from group comparisons (Bookstein, 2001; Davatzikos, 2004). This is particularly problematic when applying such methods on FA maps of white matter, as misalignments could imply that one is not necessarily comparing the same anatomical regions of white matter tracts for all subjects. Moreover, the amount of smoothing is known to considerably affect the results (Jones et al., 2005); yet, this criterion is arbitrarily chosen as there is no standardized way to determine the best smoothing amount.

Tracts Based Spatial Statistics

Tract Based Spatial Statistics (TBSS) has been developed with the goal to overcome these limitations of conventional voxel-based methods. Essentially, it proposes an alternative procedure leading to better alignment of subjects' white matter tracts, without the need for smoothing (Smith et al., 2006). The algorithm achieves this through three steps, starting with 1) a careful non-linear registration of all subjects to the most typical subject of the sample, followed by 2) a registration to the Montreal Neurological Institute (MNI) template, and finally 3) the creation of an FA skeleton, which can be defined as an alignment-invariant representation of tract centers across subjects. The study-specific skeleton is then filled with the highest neighboring FA values from each subjects' image. Once this has been achieved for all subjects, voxelwise group comparisons can be made on the FA skeletons. Figure 1.16 illustrates the main steps involved in TBSS.

This method is particularly relevant for clinical populations with gross morphological brain alterations such as 22q11.2DS. Indeed, by avoiding standard registration algorithms and identifying tract centers using the skeleton, TBSS is less affected by misalignment issues due to morphological differences, and can ensure tracts correspondence across all subjects. Therefore, TBSS provides a better interpretability (because of the improved

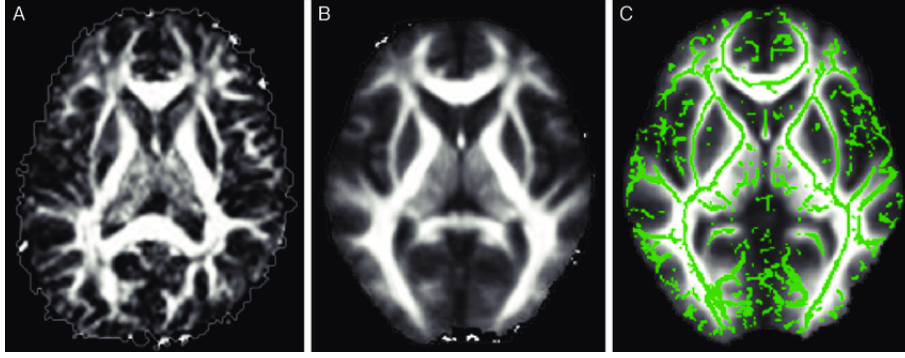


Figure 1.16: *Main steps involved in TBSS: first, a non-linear registration of subjects' FA images (A); second, the normalisation to a template space (B); and third, the creation of an FA skeleton representing the tract centers (C) (from Andica et al., 2017).*

alignment) and an increased sensitivity to white matter changes.

However, TBSS also has several significant limitations. Firstly, the creation of the skeleton involves keeping only the highest FA values across subjects. Even though this step has the advantage of providing a better alignment of the subjects' white matter pathways, the drawback is a non-negligible loss of information regarding regions with lower FA values (Hecke et al., 2010). Second, evidence suggests that TBSS is affected by the subject used as a target for registration (Keihaninejad et al., 2012), which might compromise its application in clinical samples. Third, the method shows a limited anatomical specificity, meaning that different tracts cannot always be sufficiently well distinguished when using the skeleton (Bach et al., 2014). Finally, the fourth and most important limitation in the context of a longitudinal study is that TBSS does not come with a unified adaptation for longitudinal data. This is problematic, because when measuring changes between repeated assessments of the same individual, it becomes essential to ensure spatial correspondence of white matter tracts across all time points. Without any guarantee of tract correspondence across time, TBSS might thus not be an optimal method for longitudinal studies.

1.4.2 Tractography

Diffusion information extracted from DTI images can alternatively be used to retrace pathways of white matter tracts throughout the brain. This procedure, called “tractography”, can be defined as the computational reconstruction of white matter tracts in vivo. This technique uses the anisotropy and diffusion orientation to deduce the underlying network of structural connections. This information is generally extracted from color-coded orientation maps. Figure 1.17 depicts the raw FA map, the color map extracted from DTI images and an example of tracts reconstruction performed by a tractography algorithm.

Tractography methods can be broadly categorized in two different ways (see also Figure 1.18):

1. **Tractography algorithms can be either deterministic or probabilistic.** In deterministic tractography, the algorithm starts by placing a seed point and reconstructs the tract by following the main direction of diffusion. It terminates when it encounters certain stop criteria, such as diffusion values lower than a defined thresh-

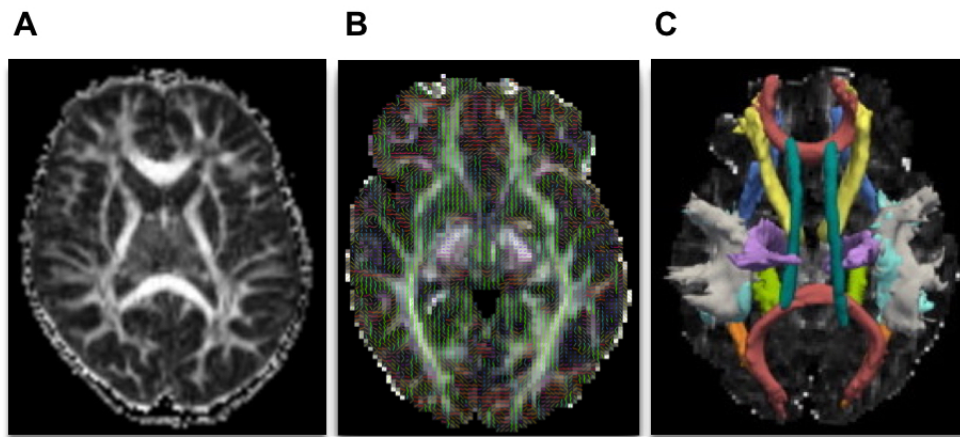


Figure 1.17: (A) Raw FA image resulting from a DTI acquisition, (B) color-coded orientation map based on the main direction of diffusion, and (C) an example of tracts reconstruction as performed by TRACULA (for details regarding this method, see below).

old, or a turn that exceeds a certain angle. In probabilistic tractography, tract orientation probability distributions are estimated at each voxel to determine the likelihood of a tract following a certain direction given by the diffusion information (Behrens et al., 2003). In other words, this method provides information regarding the uncertainty (i.e., probability distribution) of the estimated direction. Probabilistic methods are known to handle crossing pathways in a more reliable way (Behrens et al., 2007). Outputs from both algorithms are different: deterministic tractography algorithms will produce one streamline per seed voxel; probabilistic algorithms will output a probability distribution, meaning a sum of all streamline samples from all seed voxels.

2. **Tractography algorithms can be local or global.** A local method estimates a pathway sequentially, using the local orientation of diffusion to determine each next step. Global algorithms, on the other hand, fit the entire pathway at once, by simultaneously using diffusion orientation information from all voxels located on the pathway. Local tractography methods are best suited for exploratory analyses, where the goal is to identify all possible connections of a specific brain region. However, when the goal is to study white matter structure of known white matter tracts, global tractography is better suited. Clinical studies often relate to the latter goal, as the aim is mostly to characterize alterations in specific, well-established tracts, rather than describing all connections expanding from a given brain region.

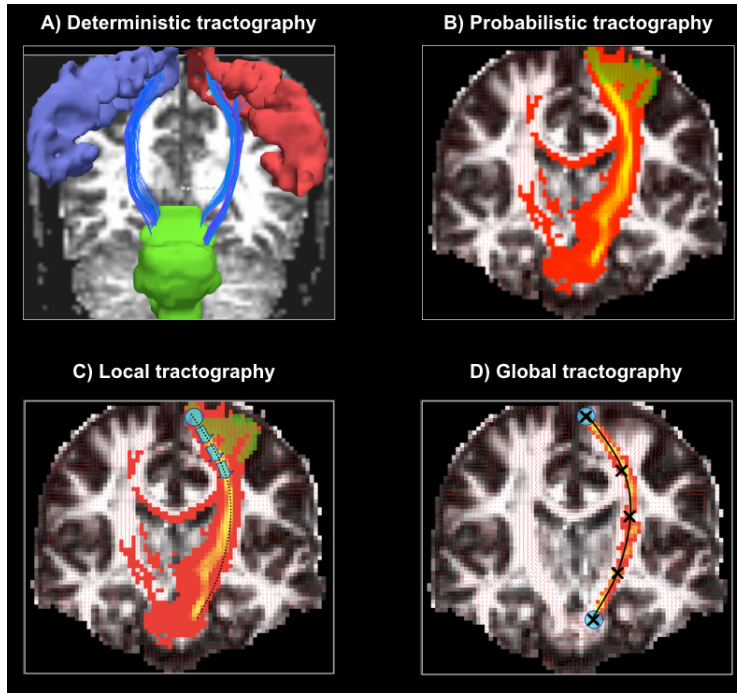


Figure 1.18: Examples of the four main categorizations of tractography methods. In deterministic tractography (A), each placed seed point leads to the reconstruction of a streamline, following the main direction of diffusion. In probabilistic tractography (B), tract orientation probability is estimated at each voxel, resulting in a probability distribution of streamlines. In local tractography (C), a pathway is estimated in a sequential way, where the local diffusion information determines each next step. Finally, in global tractography (D), the entire pathway is estimated at once, using diffusion orientation at all voxels located along the pathway (taken from TRACULA workshop ii).

TRacts Constrained by UnderLying Anatomy

TRacts Constrained by UnderLying Anatomy (TRACULA), developed by Yendiki et al. (2011) as part of Freesurfer’s framework (<https://surfer.nmr.mgh.harvard.edu/>) can be defined as an automated method for the reconstruction of 18 predefined major white matter pathways using a global probabilistic approach (see Figure 1.19 and Table 1.2). As such, it estimates the probability distribution of white matter pathways using diffusion information from voxels located all along the tract length. It should be noted that, rather than using tensor information, TRACULA uses the “ball-and-stick” model of diffusion, an alternative modelling of diffusion information that allows for more than one anisotropy orientation within a single voxel (Behrens et al., 2007).

TRACULA’s novelty, however, lies in the fact that it uses prior anatomical knowledge regarding the brain regions traversed by a given tract, to guide tract reconstruction. To achieve this, a set of training subjects in which all 18 tracts have been manually drawn is used to learn the probability of each pathway to cross (or pass next to) a given anatomical segmentation label. This anatomical knowledge is then used to initialize and constrain the algorithm’s decisions on the actual data, informing it about the brain regions a given pathway is more likely to traverse. Thus, the assumption is merely that tracts traverse the same anatomical regions, not that tracts necessarily have the exact same shape across subjects. The advantage of this procedure is that TRACULA does not require a perfect alignment between training subjects and study subjects in order to efficiently reconstruct

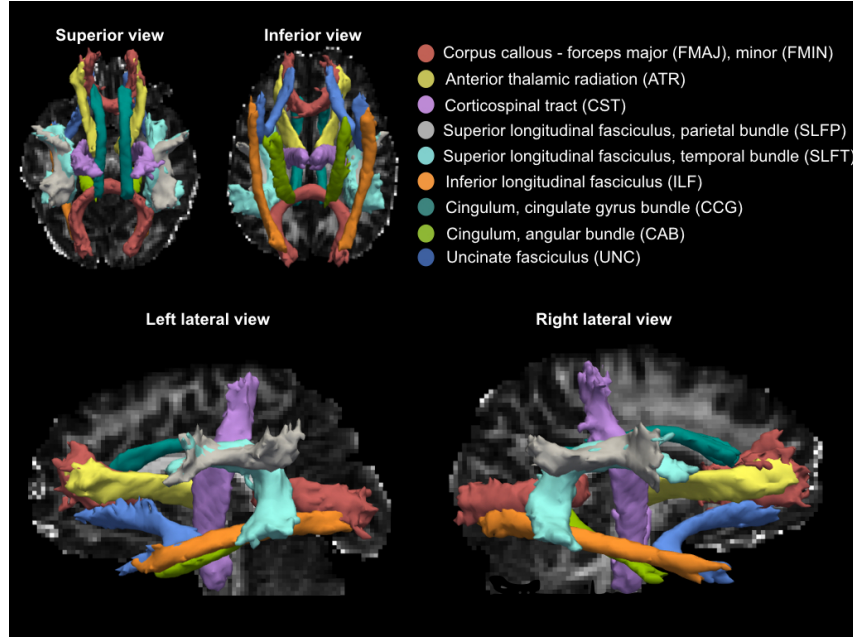


Figure 1.19: Illustration of the 18 white matter tracts reconstructed by TRACULA.

Tract type	Tract name
Projection	Corticospinal Tract (CST)
	Anterior Thalamic Radiation (ATR)
Commissural	Corpus callosum, forceps major (FMAJ)
	Corpus callosum, forceps minor (FMIN)
Association	Cingulum, cingulate gyrus (supracallosal) bundle (CCG)
	Cingulum, angular bundle (CAB)
	Superior longitudinal fasciculus, parietal bundle (SLFP)
	Superior longitudinal fasciculus, temporal bundle (SLFT)
	Inferior longitudinal fasciculus (ILF)
	Uncinate fasciculus (UNC)

Table 1.2: White matter tracts reconstructed by TRACULA.

tracts. This is particularly relevant for clinical samples, where tracts are likely to be somewhat altered in shape and location.

Once the tracts distributions have been estimated, TRACULA computes tensor information for the corresponding regions, and extracts commonly used diffusion parameters (FA, AD, RD, MD) averaged over the whole tract, and also as point-by-point values along the tract.

Importantly, TRACULA also has a well-defined pipeline for the analysis of longitudinal data (Yendiki et al., 2016). In this adaptation, the algorithm estimates the probability distribution of white matter tracts given all available time points jointly. It should also be noted that, for each individual, tracts are reconstructed on a within-subject template created based on all the subject's time points. The reconstruction of pathways within the subject's native space ensures that the same parts of white matter tracts are compared between time points. For details regarding the methodology of the longitudinal pipeline,

please refer to section 2.

TRACULA also has a number of limitations. Firstly, due to its conceptual foundations, the algorithm can only be used to assess the predefined white matter tracts. As such, it is blind to potential white matter alterations located in other fibers, such as short range associational tracts. Moreover, the method is time-consuming, mainly due to the computation of the ball-and-stick model of diffusion. In the longitudinal pipeline, processing is further prolonged by the preliminary creation of a within-subject template. Finally, it should be mentioned that the within-subject registration of all time points is made using a robust rigid registration. This procedure does not rise any concerns in cases where intracranial volume (and therefore, tract shapes) do not extensively change during the studied developmental period; however, if the latter scenario were true, non-linear methods would provide a better alternative (Yendiki et al., 2016).

1.4.3 TBSS versus TRACULA

Based on the above descriptions, TBSS and TRACULA share a common characteristic in that they have both been developed to overcome the risk of tract misalignments across subjects and are thus suited for clinical samples with gross morphological alterations. However, they considerably differ on several fundamental aspects (Table 1.3). Indeed, while TBSS uses a whole-brain approach to derive tract centers, TRACULA uses a tractography approach to reconstruct a set of predefined tracts based on prior anatomical knowledge. Hence, TBSS searches for group differences among the highest FA values (i.e., tract centers), whereas TRACULA assesses the entire range of diffusion values located within the tracts of interest. Additionally, since TBSS is a voxel-based method it will perform voxelwise comparisons; TRACULA on the other hand will provide averaged diffusion values over the entire tract and per position along the tract. TBSS is thus better suited for exploratory analyses of white matter integrity, where one has no knowledge about potential alterations caused by a given disease and the goal is to obtain a preliminary, whole-brain description of these possible abnormalities. On the other hand, TRACULA is better suited for a more detailed investigation of white matter structure in known major white matter tracts, once knowledge about alterations associated with a disease has already been acquired to some extent. Thus, the conceptual differences between TBSS and TRACULA imply considerably different strategies to study white matter integrity, and make each method adapted for distinct goals. In the context of 22q11.2DS, white matter alterations have already been identified by multiple previous studies (see introduction, section 1.3), some of which using TBSS (Bakker et al., 2016; Jalbrzikowski et al., 2014; Kikinis et al., 2012, 2017, 2013; Roalf et al., 2017). A more detailed characterization of white matter integrity in well-defined, systematically reconstructed tracts using an algorithm such as TRACULA would thus be a preferable next step in white matter studies on 22q11.2DS.

Finally, as mentioned earlier, TRACULA comes with an adapted longitudinal pipeline capable of handling multiple time points per subject and ensuring the point-to-point tract correspondence across assessments. Not only is this feature absent in TBSS, but it has also been demonstrated that small decisions in the preprocessing pipeline have significant

influences in its ability to detect longitudinal changes (Madhyastha et al., 2014). Thus, TRACULA is much more suitable for longitudinal studies.

	TRACULA	TBSS
Approach	ROI-based	Whole-brain
Sensitivity to diffusion measures	Captures the entire range of diffusion values within the tract	Captures the highest diffusion values in vicinity of tracts centers
Longitudinal adaptation	Adapted longitudinal pipeline	No longitudinal pipeline

Table 1.3: *Main differences between TBSS and TRACULA.*

1.5 Longitudinal design

1.5.1 Longitudinal versus cross-sectional

Several cross-sectional DTI studies have analyzed white matter integrity in 22q11.2DS using large age ranges (Bakker et al., 2016; Barnea-Goraly et al., 2003; da Silva Alves et al., 2011; Jalbrzikowski et al., 2014; Kates et al., 2015; Olszewski et al., 2017; Perlstein et al., 2014; Sundram et al., 2010), in an effort to characterize developmental changes of white matter integrity. However, as demonstrated by Steen et al. (2007) with the example of total brain volume analysis, cross-sectional designs require significantly more participants to detect group differences in brain structure. Indeed, they showed that a sample of 146 subjects was needed to detect a 5% difference in whole-brain volume in a cross-sectional design, whereas a sample of only 10 subjects was sufficient to detect similar changes in a longitudinal design. The drastic reduction of statistical power in cross-sectional designs is due to the natural variability in brain sizes (Steen et al., 2007), which will be reflected in other neuroanatomical measures. Part of this anatomical variation is likely irrelevant for the group differences that are being tested (Mills and Tamnes, 2014), but will however necessarily influence the results. Longitudinal designs are not affected by this issue, as they do not only measure inter-individual variability, but also intra-individual changes of brain structure over time. This allows to detect more subtle changes and will therefore naturally increase statistical power and sensitivity to group differences. Thus, longitudinal designs represent a powerful tool to capture age-related changes.

Moreover, Kraemer et al. (2000) demonstrated that when cross-sectional designs are used to make inferences about developmental processes, this can sometimes produce seriously misleading results. Indeed, most commonly (and particularly in psychiatric studies investigating disease progression), developmental measures follow non-parallel trajectories, meaning that subjects show variability in their changes over time. However, correlations between non-linear developmental measures may yield drastically different values depending on the age ranges included in the tested sample (for instance, when the measures of interest start to show correlations only after a certain age), which may provide a biased representation of the actual underlying anomalies. Thus, although cross-sectional studies

have the advantage of being less costly and less time-consuming, longitudinal designs are significantly better suited for studies that aim at characterizing the relationship between several developmental processes, such as white matter maturation and the emergence of psychotic disorders.

1.5.2 Challenges of longitudinal studies

Longitudinal studies also present a number of challenges (Caruana et al., 2015). First, data collection for type of study design is highly time consuming, and extensive periods of time are needed until patterns can start to emerge from the data. Second, longitudinal studies are costly, due to their extended periods of data collection and the considerable amount of workforce needed to complete this task. Third, longitudinal designs also require adapted statistical analysis techniques. Indeed, as Fitzmaurice et al. (2008) pointed out, repeated measurements have an inherently correlated nature, which needs to be carefully modelled and should not be overlooked. Furthermore, outcome measures (such as white matter integrity measures) often follow non-linear developmental trajectories, which should be modelled accordingly. Finally, when following subjects over time, missing data issues are likely to arise, since the full assessment of all variables of interest at each time point is not always guaranteed due to circumstantial reasons, and drop-out is possible as well. These aspects, among others, entail the need for a more complex handling of statistical modelling methods. Details regarding the method chosen for this study are provided in section 2.

1.5.3 Prospective cohort studies for identifying biomarkers of psychosis

Longitudinal designs can be further separated into different subtypes. Among others, some frequently used designs are retrospective cohort studies and prospective cohort studies (Song and Chung, 2010). Retrospective studies “look backwards”, meaning that subjects are selected based on a current outcome of interest and past history is assessed to reconstruct exposure to risk factors. On the other hand, prospective cohort studies “look forward”: subjects are initially enrolled based on a specific feature of interest (for instance, a genetic abnormality), and are followed in time to investigate the impact of certain risk factors on a given outcome (for instance, psychosis). Therefore, prospective cohort studies represent a particularly adapted type of design when searching for biomarkers informative of early stages of disease progression in the 22q11.2DS population. Indeed, individuals with 22q11.2DS can be readily identified at any age through genetic detection techniques such as PCR or FISH, making it possible to study them from early on and throughout their development. This provides a unique opportunity for the identification of potential deviant developmental trajectories associated with the emergence of psychotic disorders, which occurs for about 40% of the 22q11.2DS population.

1.6 Aims and hypotheses

Based on findings reported in the introduction, this project had three main aims:

1. **Characterize the developmental trajectories of major white matter tracts' microstructure in patients with 22q11.2DS compared to controls.**

To the best of our knowledge, developmental trajectories of white matter tracts in 22q11.2DS have never been characterized using a longitudinal design. However, given the complex patterns of white matter development seen in typically developing subjects and the inconsistency of DTI results previously reported in individuals with the syndrome (see section 1.3), it becomes essential to characterize the developmental trajectories of white matter microstructure in 22q11.2DS. It is likely that the heterogeneity of previous findings is, at least in part, due to the complex, non-linear nature of white matter microstructural maturation, and that group comparisons might yield different results depending on the period of development that is being considered. A comparison of white matter development in 22q11.2DS and TD controls has the potential to clarify the nature of white matter alterations associated with the syndrome.

Hence, a first aim of this study was to delineate the maturational trajectories of the main long-range white matter tracts in 22q11.2DS and TD controls in a robust way, by assessing subjects multiple times throughout their childhood, adolescence and up to their adulthood. Based on previous findings reported in cross-sectional studies, we expected to find widespread alterations in all DTI metrics for individuals with 22q11.2DS, with probable non-linear developmental tendencies in most tracts and DTI metrics. Moreover, as grey matter development is known to follow differential trajectories in 22q11.2DS compared to controls (Schaer et al., 2009), we hypothesized that white matter maturation may also show distinct developmental curves, reflecting altered maturation rates for patients with the deletion compared to TD controls.

To obtain a preliminary estimation of potential alterations associated with 22q11.2DS, we first performed an exploratory analysis on a subgroup of patients and TD controls with two equally spaced time points. This type of balanced design allowed the use of simple statistical methods (see section 2) and provided first insights the alterations present in individuals with the syndrome. Next, we extended our sample to include the full available cohort, which comprised subjects with variable numbers of time points in order to obtain a more fine-grained characterization of developmental trajectories in 22q11.2DS and TD controls. More complex statistical analysis techniques were used to address the increased complexity of this type of data.

2. Investigate the developmental trajectories of major white matter tracts' microstructure in patients with 22q11.2DS experiencing a cognitive decline compared to patients without cognitive decline.

Preliminary evidence suggests that a cognitive decline is associated with alterations of white matter microstructure in 22q11.2DS (Nuninga et al., 2017). However, the impact of this risk factor on white matter developmental trajectories has yet not been measured. Thus, our second aim was to characterize the maturational trajectory of major white matter tracts in patients who showed a cognitive decline over time, versus patients who maintained or improved their cognitive functioning. We expected to observe focal deviations of microstructural maturation in several white matter tracts for patients who experienced a cognitive decline. Specifically, in light of previous findings from Nuninga et al. (2017), we hypothesized that cognitive decline would be associated with altered developmental trajectories of diffusion measures in association tracts (such as the superior longitudinal fasciculus and the cingulum bundle) and projection tracts (such as the internal capsule).

3. Investigate the developmental trajectories of major white matter tracts' microstructure in patients with 22q11.2DS fulfilling the UHR diagnosis compared to patients without UHR.

In the general population, several studies have reported white matter microstructure alterations in individuals with UHR (Canu et al., 2015; Carletti et al., 2012; Karlsgodt et al., 2009; Peters et al., 2008). In 22q11.2DS, evidence from multiple white matter studies suggests a particular involvement of long-range fronto-temporal and limbic tracts in patients experiencing high levels of positive symptoms (reviewed in Scariati et al., 2016). In addition, three previous studies dividing patients depending on the severity of positive symptoms significant group differences in commissural, projection and association tracts, including limbic and fronto-temporal tracts (Kikinis et al., 2017; Padula et al., 2017; Roalf et al., 2017). However, to date, no studies in 22q11.2DS have categorized subjects using the well-established UHR diagnosis, nor have investigated the relationship between the presence of this risk factor and white matter maturation. Consequently, our third aim was to determine whether patients at UHR showed distinct white matter developmental trajectories compared to non-UHR patients. Based on previous findings, we hypothesized that patients with 22q11.2DS meeting the criteria for a UHR status would show deviant structural developmental trajectories, with specifically more pronounced alterations of white matter microstructure in long-range fronto-temporal, commissural and limbic tracts.

Thus, overall, the present study aims at providing a reliable characterization of white matter maturational trajectories in 22q11.2DS in order to develop a better understanding of the alterations associated with the deletion. In addition, a second focus consisted in the identification of potential developmental biomarkers at the level of white matter, as these may provide valuable predictions in the conversion to psychosis.

CHAPTER 2

MATERIALS AND METHODS

In this section, subjects' selection will first be detailed for the comparison of 22q11.2DS and TD controls, both for the preliminary study including only subjects with two consecutive time points, as for the main study including the full available cohort. Psychiatric and cognitive assessment methods will then be outlined, along with a description of the participants' selection for the analysis of white matter development in relation to risk factors of psychosis. Finally, the MRI image acquisition and processing steps will be described, and the different statistical methods used for the preliminary study, the main study and the analysis of risk factors will be explained.

2.1 Materials

Individuals with 22q11.2DS and TD subjects were recruited in the context of the ongoing "Swiss longitudinal study" started in 2002 (Maeder et al., 2016; Schaer et al., 2009). This prospective cohort study comprises around 170 individuals with 22q11.2DS and 170 TD controls. All subjects have been recruited through word of mouth and advertisements at 22q11.2DS associations. Written informed consent was given by the patients or their parents (when the participant was younger than 18 years), and the protocols of the study were validated by the cantonal ethic commission of research. Diagnosis of 22q11.2DS was established using quantitative fluorescent polymerase chain reaction (QF-PCR). Patients and TD controls were followed longitudinally with assessments made approximately every three years. At each visit, participants were submitted to a clinical and cognitive evaluation and underwent an extensive MRI scanning protocol, including T1-weighted imaging, resting-state functional MRI (fMRI), task-based fMRI (when participants were old enough) and diffusion tensor imaging. Of note, the latter acquisition started in 2008, thus some years after the initial creation of the longitudinal cohort. Currently, a majority of participants have one time point, and a maximum of five time points have been collected for 19 subjects (12 patients and 7 controls).

2.1.1 Preliminary study

Participants

For the preliminary study comparing individuals with 22q11.2DS and controls, we included subjects for which two consecutive time points were available. The resulting sample was composed of 74 subjects (40 22q11.2DS (17 male); 34 TD controls (14 male)), with ages ranging from 8 to 25 years old. As all subjects had exactly two time points, this resulted in a total of 148 scans. The average time interval between time points was 3.395 years (SD = 0.496 years). Figure 2.1 shows the distribution of subjects across the entire age range. There were no significant group differences in gender ($p = 0.908$) or age at first time point ($p = 0.646$).

For a flowchart describing the subjects' selection for each of the analyses included in this study, see Figure 2.2.

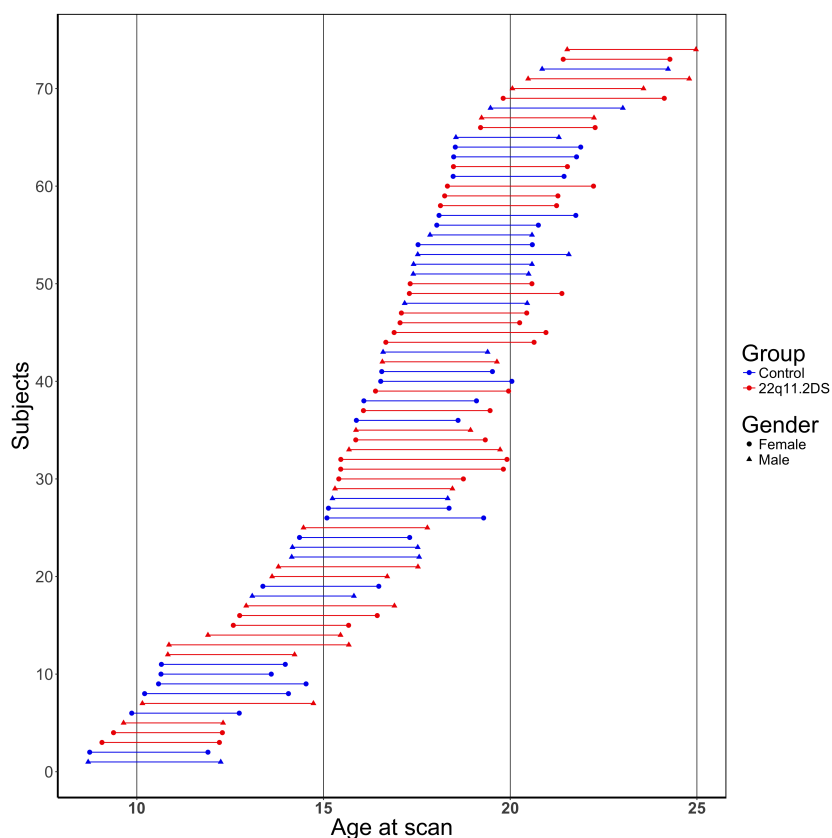


Figure 2.1: Age distribution of the 74 subjects included in the preliminary study. Each scan is represented by a point; scans from each subject are connected by a line.

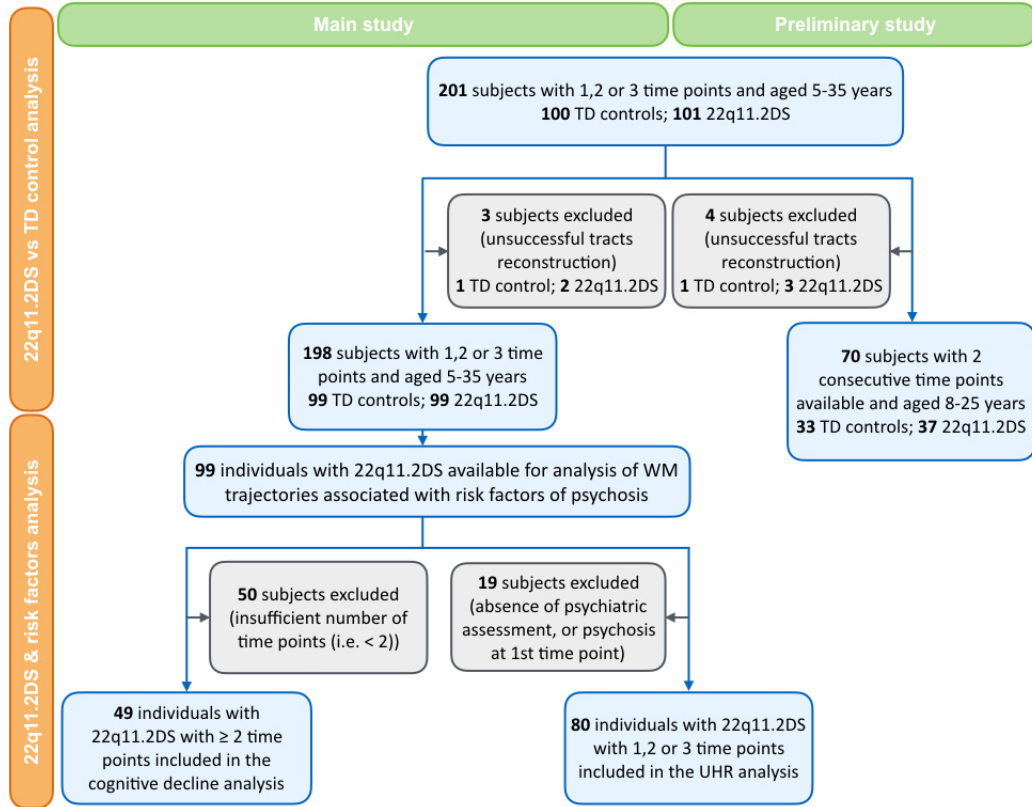


Figure 2.2: Data from the 201 subjects (101 22q11.2DS; 100 TD controls) corresponded to a total of 302 scans (120 with a single scan, 61 with 2 scans, and 20 with 3 scans), all made between ages 5-35. After exclusion of 4 subjects due to unsuccessful tracts reconstruction, the sample for the preliminary study comparing white matter development in 22q11.2DS vs TD controls with 2 consecutive time points resulted in a sample of 70 subjects (37 22q11.2DS; 33 TD controls). The sample for the comparison of white matter development in 22q11.2DS vs TD controls including all available scans comprised a total of 198 subjects (99 22q11.2DS; 99 TD controls), after exclusion of 3 subjects due to unsuccessful tracts reconstruction. The analysis of risk factors in the 22q11.2DS population comprised 49 subjects for the analysis of cognitive decline (20 decline; 29 no decline) and 80 subjects for the UHR analysis (17 UHR; 63 non-UHR).

2.1.2 Main study

Participants

For the extended study comprising all available time points of TD controls and 22q11.2DS, the sample consisted of 201 subjects (101 22q11.2DS (55 males); 100 TD controls (48 males)) aged from 5-35 years old. One hundred and twenty subjects had a single time point (52 22q11.2DS; 68 TD controls), 61 subjects had two time points (33 22q11.2DS; 28 TD controls), and 20 subjects had three time points (16 22q11.2DS; 4 TD controls), resulting in a total number of 302 scans. For subjects with follow-up(s), the average time interval between time points was 3.554 years (SD = 0.867 years). The distribution of subjects across the entire age span is shown in Figure 2.3. Groups did not differ in gender ($p = 0.723$) or age at first time point ($p = 0.421$), but did show significant differences in mean FSIQ at first time point ($p < 0.001$). Demographic information of TD controls and patients with 22q11.2DS is described in Table 2.1.

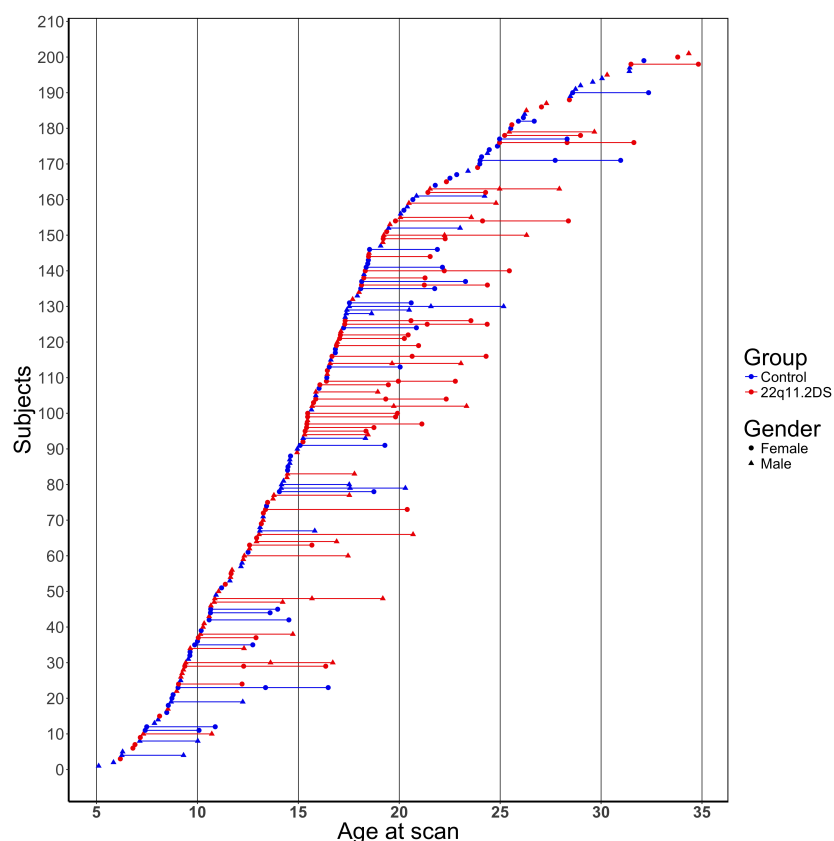


Figure 2.3: Age distribution of the 201 subjects included in the main study.

	22q11.2DS	TD controls	Total	p-value
Number of subjects included in study	101	100	201	
Subjects with 1 time point	52	68	120	
Subjects with 2 time points	33	28	61	
Subjects with 3 time points	16	4	20	
Total number of visits	166	136	302	
Proportion of males/females	51/50	48/52	99/102	0.724
Mean age at first tp (SD)	15.952 (6.037)	16.684 (6.797)		0.421
mean FSIQ at first tp (SD)	70.71 (11.489)	111.58 (14.436)		<0.001
Number of subjects with psychiatric diagnosis at first visit	65			
Attention deficit disorder	26			
Anxiety disorder	50			
Mood disorder	17			
Psychotic disorder	6			
Schizophrenia	2			
More than one psychiatric disorder	44			
Number of subjects medicated at first visit	31			
Methylphenidate	13			
Antidepressants	8			
Antipsychotics	6			
Anticonvulsants	6			
Anxiolytics	4			
More than one type of medication	6			

Table 2.1: Demographic information of subjects included in the main study.

Cognitive assessment

IQ measurements were acquired for all 22q11.2DS individuals using age-adapted versions of the Wechsler intelligence scale (i.e. the Wechsler Intelligence Scale for Children, version III or IV, or the Wechsler Adult Intelligence Scale, version III or IV) (Wechsler, 1991, 1997, 2004, 2008). A subset of 49 patients with two or three time points was selected for the assessment of cognitive development within the 22q11.2DS population ($n = 33$ subjects with 2 time points; $n = 16$ subjects with 3 time points). To determine the presence of a cognitive decline, the annual rate of change was calculated for each subject by subtracting the IQ at the last time point from the IQ at the first time point, and dividing this by the time interval between time points (in years). Accordingly, patients with a negative rate of change ($n = 20$) were considered to show a cognitive decline (*decline* group), and patients with a null or positive rate of change ($n = 29$) were considered to show no cognitive decline (*no decline* group). The distribution of decline and no decline subjects is illustrated in Figure 2.4.

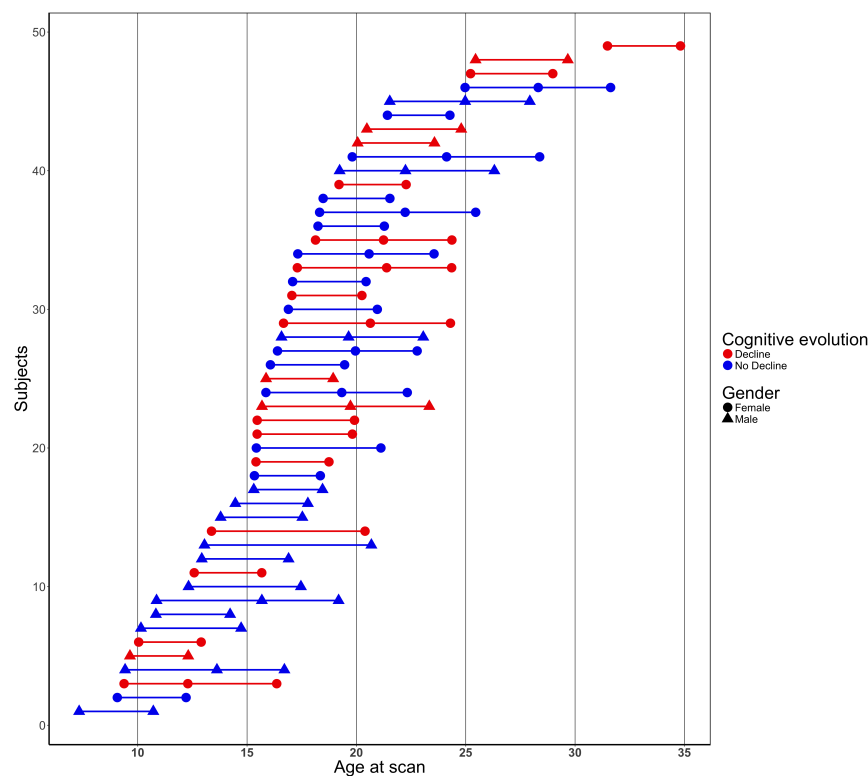


Figure 2.4: Age distribution of the 49 subjects included in the cognitive decline analysis.

Psychiatric assessment

Assessment of psychiatric disorders was performed using the Diagnostic Interview for Children and Adolescents Revised (DICA-R; Reich, 2000), the psychosis component from the Kiddie-Schedule for Affective Disorders and Schizophrenia Present and Lifetime version (K-SADS-PL; Kaufman et al., 1997), and the Structured Clinical Interview for DSM-IV Axis I Disorders (SCID-I; First, 1996) for adult patients (starting from 18 years). Sixty-five individuals with 22q11.2DS fulfilled the criteria for a psychiatric diagnosis at their

first time point. Thirty-one individuals with 22q11.2DS were medicated at their first time point (Table 2.1).

UHR criteria (i.e., APS, BLIP and GRD, see section 1.1.7 for definitions) were evaluated at each time point in individuals with 22q11.2DS starting from 10 years old, using the Structured Interview of Prodromal Symptoms (SIPS; Miller et al., 2002). Patients diagnosed with a full-blown psychosis at their first time point ($n = 7$) were excluded from the analysis, as the aim of the study was to investigate the developmental pathways prior to the emergence of the disease. Thus, a sample of 80 individuals with 22q11.2DS was available for the characterization of their psychiatric developmental profile ($n = 39$ with one time point, $n = 30$ with two time points, $n = 11$ with three time points). Developmental trajectories were categorized as follows: patients where considered “at high risk for psychosis” when they met the UHR criteria for at least one of their time points ($n = 17$) (*UHR* group); conversely, patients who never fulfilled the UHR criteria were considered “at low risk for psychosis” ($n = 63$) (*non-UHR* group). Two subjects converted to psychosis at later time points; among those, one was UHR at earlier assessments and one was non-UHR. There were no significant group differences for age and gender between UHR and non-UHR patients. The distribution of UHR and non-UHR subjects is illustrated in Figure 2.5.

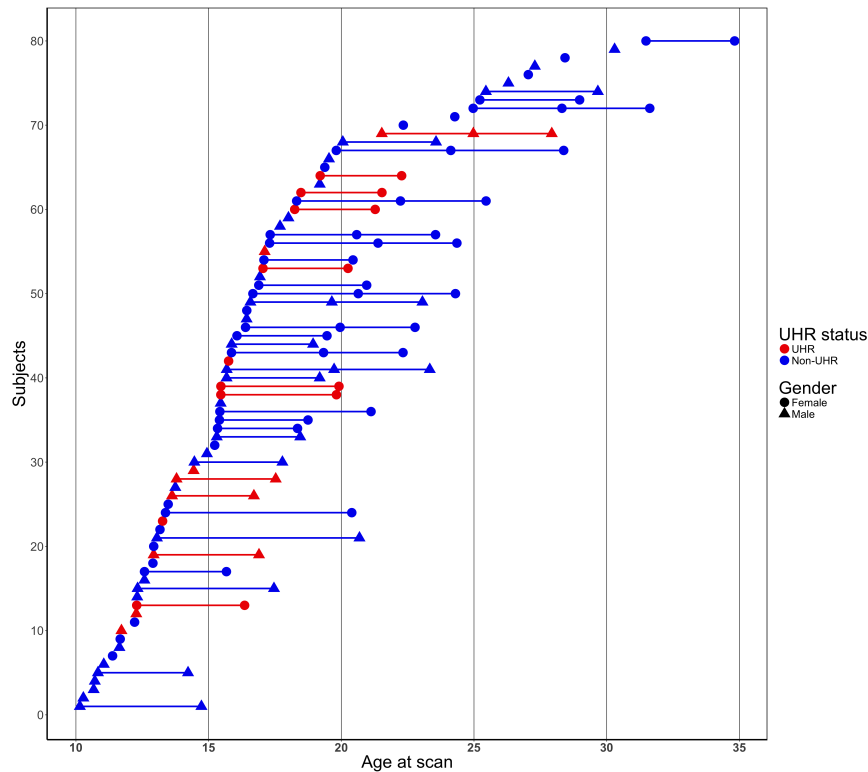


Figure 2.5: Age distribution of the 80 subjects included in the UHR analysis.

2.2 MRI acquisitions

Structural T1-weighted and Diffusion Tensor Imaging (DTI) images were acquired at the Center for Biomedical Imaging (CIBM) in Geneva, using either a Siemens Trio (191 scans) or a Siemens Prisma (111 scans) 3 Tesla MRI scanner. The T1-weighted sequence was acquired with a 3D volumetric pulse, TR = 2500 ms, TE = 3 ms, flip angle = 8° , acquisition matrix = 256 x 256, field of view = 23.5 cm, slice thickness = 3.2 mm, 192 slices. DTI images parameters were as follows: number of directions = 30, b = 1000s/mm², TR = 8800 ms, TE = 84 ms, flip angle = 90° , acquisition matrix = 128 x 128, field of view = 25.6 cm, GRAPPA acceleration = 2, 64 axial slices, slice thickness = 2 mm. The head coil differed between the two scanners (12 channels for the Siemens Trio and 20 channels for the Siemens Prisma).

2.3 MRI image processing

First, T1-weighted structural scans were visually checked for motion artefacts and processed using the default cross-sectional pipeline of *Freesurfer* (version 5.1. and 6.0), to obtain skull-stripped and intensity-normalized images. Then, the cross-sectionally processed scans were fed into the longitudinal stream of *Freesurfer*, version 6.0 (Reuter et al., 2012). Briefly, this adapted processing method uses all available scans of a given individual to create an unbiased within-subject template containing the common information of all time points (Reuter and Fischl, 2011). The template is then processed using the usual cross-sectional pipeline to obtain initial segmentation and surfaces. Finally, this information is used as an initial guess for the processing of each time point. This method has the advantage of significantly increasing reliability and statistical power, thereby improving the estimation of within-subject age-related changes (Reuter et al., 2012).

After visual inspection of DTI images for motion artefacts, we used the longitudinal pipeline of the TRacts Constrained by UnderLying Anatomy (TRACULA) tool (Yendiki et al., 2016) from *Freesurfer* (version 6.0) to reconstruct 18 major white matter paths in each subjects' time points (for details regarding this method, see section 1.4.2). In short, the longitudinal framework of TRACULA is an automated global probabilistic tractography algorithm that estimates the probability distribution of white matter tracts given all available time points. The probability distribution of each pathway is computed partly using the “ball-and-stick” model of diffusion, and partly using prior anatomical knowledge from a training data set, in which all 18 tracts have been manually drawn. For each subject, TRACULA joins information from the within-subject template, the anatomical segmentations from all structural scans and all DTI scans available for this subject to compute the probability distribution of the 18 white matter pathways (Figure 2.6). The reconstruction of white matter pathways within the native space of the subject ensures that the same white matter parts are compared between time points. This has been demonstrated to improve test-retest reliability and increase sensitivity to longitudinal changes in white matter tracts (Yendiki et al., 2016), making it a particularly adapted tool for longitudinal studies of white matter development. Once the tracts distributions have

been estimated, TRACULA computes a tensor fit and extracts commonly used diffusion parameters (FA, AD, RD, MD) averaged over the entire tract.

For the preliminary study on subjects with 2 consecutive time points, 4 subjects (3 22q11.2DS, 1 TD control) were excluded from the analysis due to unsuccessful tracts reconstruction, resulting in a sample of 70 subjects (37 22q11.2DS; 33 TD controls) for the preliminary analysis. For the main study, tracts reconstruction was unsuccessful in three subjects (2 22q11.2DS, 1 TD control), resulting in a sample of 198 subjects for the main analysis (99 22q11.2DS; 99 TD controls).

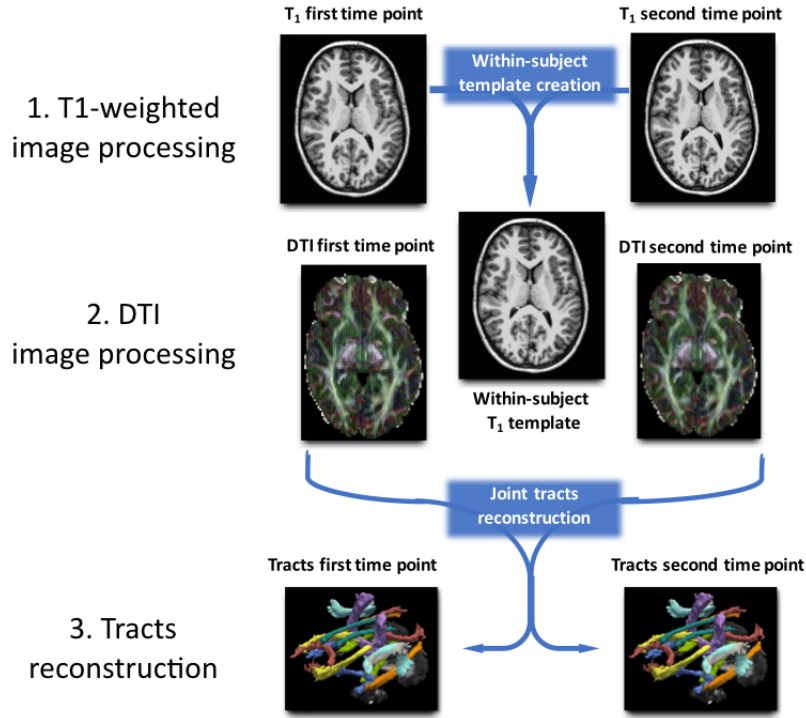


Figure 2.6: Simplified representation of the main steps involved in the longitudinal processing pipeline of TRACULA.

2.4 Statistical analysis

2.4.1 Preliminary study

The preliminary study was conducted using a balanced study design, as all subjects had two approximately equally spaced time points. As such, relatively simple statistical methods could be used to analyze age-related changes (Locascio and Atri, 2011). Specifically, we used two different approaches: firstly, used repeated measures analysis of variance (ANOVA) to model the effect of time (within-subject factor) and diagnosis (between-subjects factor). Gender and age were included as covariates. Second, to determine whether developmental changes followed distinct progression rates, the annual percent change with respect to the first time point was computed for each tract and each diffusion measure using the following formula: $((\text{diffusion metric at T2} - \text{diffusion metric at T1}) * 100) / (\text{age at T2} - \text{age at T1})$. Group differences rates of

changes were then tested using non-parametrical Mann-Whitney tests, as data did not follow normal distributions. Results were corrected for multiple comparisons using the false discovery rate (FDR) method (Benjamini and Hochberg, 1995). Analyses were performed using R, version 3.3.3 (<http://www.r-project.org/>).

2.4.2 Main study

For the analysis of developmental trajectories of white matter tracts in 22q11.2DS and TD controls, as well as for the analyses of subgroups of patients with 22q11.2DS presenting risk factors of psychosis, more complex analysis methods were necessary. Hence, developmental trajectories of white matter tracts were investigated in 22q11.2DS patients and in typical developing controls using mixed models regression analyses (Mutlu et al., 2013; Shaw et al., 2006; Thompson et al., 2011), as this approach can handle data with varying number of time points and a variable time interval between assessments. This type of method has been applied in previous studies by our group with a similar longitudinal design (Maeder et al., 2016; Schneider et al., 2014b). Using an algorithm developed by our group and described elsewhere (Mutlu et al., 2013), random-intercept models were fitted to the data using matlab R2014b (MathWorks). Within-subject variables were modelled as random effects, and population variables (diagnosis and age and their interaction) were implemented as fixed effects. Different models (constant, linear or quadratic) were fitted on each developmental trajectory using the nlmeFit function. The Bayesian Information Criterion (BIC) was then used to select the best fitting model, as this is considered one of the most efficient model selection methods in the context of mixed models (Peng and Lu, 2012). Group differences were assessed using a log-likelihood approach. All models included gender and type of scanner as covariates. All results were corrected for multiple comparisons using the FDR method (Benjamini and Hochberg, 1995). A model was fitted for each diffusion measure x tract combination, resulting in a total of 72 models.

CHAPTER 3

RESULTS

3.1 Preliminary study

Results of the preliminary study using a sample of exclusively two time points per subject are presented below. All reported results were corrected for multiple comparisons using the FDR method.

3.1.1 Repeated measures ANOVA

Results of the repeated measures ANOVA are reported for each diffusion measure. Overall, MD was most severely affected, with diagnosis and time effects for most tracts. AD and RD were also showing diagnosis and time effects in multiple tracts. FA values were relatively similar in both groups for most tracts, and only a subgroup of tracts showed changes over time. Interaction effects were absent, with the exception of AD. Significant results are detailed below; for corresponding graphs, see Appendix A.

Mean Diffusivity

MD yielded significant effects of diagnosis in almost all tracts, that is, in the corpus callosum (forceps major (FMAJ) and forceps minor (FMIN)) and bilaterally in the anterior thalamic radiation (ATR), the cingulum (angular bundle (CAB), and cingulate gyrus bundle (CCG)), the inferior longitudinal fasciculus (ILF), the superior longitudinal fasciculus (parietal (SLFP) and temporal (SLFT) bundles) and in the uncinate fasciculus (UNC). Regarding the direction of alterations, MD was systematically reduced in all of the mentioned tracts. A time effect was observed in the bilateral ATR, right CST, left CAB, left ILF, left SLFT and left UNC. We did not observe any interaction effects for MD. Results are reported in Table 3.1, and tracts with significant group or time effects are displayed in Figure 3.1.

Tract type	Hem.	Tract	p-value		
			Main effect diagnosis	Main effect time	Interaction effect
Projection	left	ATR	≤ 0.001	0.009	0.155
	right	ATR	≤ 0.001	0.018	0.390
	left	CST	0.070	0.420	0.155
	right	CST	0.849	0.009	0.083
Commissural		FMAJ	≤ 0.001	0.420	0.323
		FMIN	≤ 0.001	0.110	0.323
Association	left	CAB	0.004	0.049	0.855
	right	CAB	0.046	0.944	0.110
	left	CCG	0.004	0.815	0.323
	right	CCG	0.004	0.760	0.155
	left	ILF	≤ 0.001	0.009	0.323
	right	ILF	≤ 0.001	0.237	0.968
	left	SLFP	0.003	0.237	0.323
	right	SLFP	0.014	0.760	0.297
	left	SLFT	≤ 0.001	0.009	0.183
	right	SLFT	≤ 0.001	0.320	0.323
	left	UNC	0.002	0.042	0.323
	right	UNC	≤ 0.001	0.176	0.968

Table 3.1: Mean Diffusivity - repeated measures ANOVA. Results are provided for each white matter tract. All results were corrected for multiple comparisons. P-values showed in bold indicate a significant effect for the corresponding tract.

Legends: lh = left hemisphere; rh = right hemisphere; fmajor = forceps major; fminor = forceps minor; ATR = anterior thalamic radiation; CAB = cingulum, angular bundle; CCG = cingulum, cingulate bundle; CST = corticospinal tract; ILF = inferior longitudinal fasciculus; SLFP = superior longitudinal fasciculus, parietal bundle; SLFT = superior longitudinal fasciculus, temporal bundle; UNC = uncinate fasciculus.

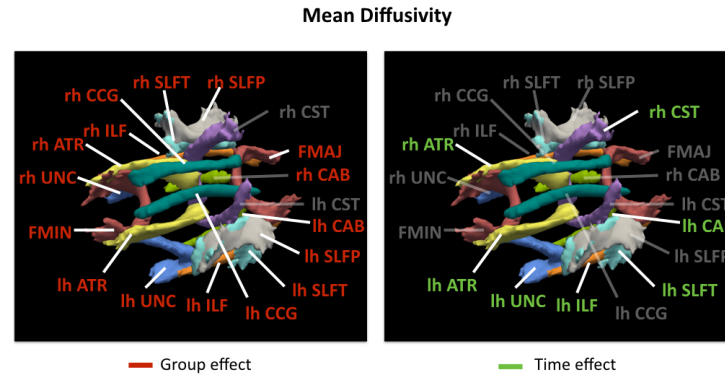


Figure 3.1: Tracts showing significant group (red) or time (green) effects in Mean Diffusivity. Displayed results were corrected for multiple comparisons using the FDR method.

Axial Diffusivity

For AD, a significant effect of diagnosis was observed in the corpus callosum (FMIN), left CAB, bilateral ILF, bilateral SLFP, bilateral SLFT and bilateral UNC; with a pattern of decreased AD values in patients. A time effect was evident in the corpus callosum (FMIN), left CAB and right CST. A significant diagnosis x time interaction effect was observed in the right CST. Results are indicated in Table 3.2, and tracts with significant group or time effects are displayed in Figure 3.2.

Tract type	Hem.	Tract	p-value		
			Main effect diagnosis	Main effect time	Interaction effect
Projection	left	ATR	0.402	0.123	0.223
	right	ATR	0.275	0.123	0.438
	left	CST	0.321	0.126	0.223
	right	CST	0.945	0.006	0.039
Commissural		FMAJ	0.125	0.765	0.833
		FMIN	0.024	≤0.001	0.576
Association	left	CAB	0.045	0.027	0.833
	right	CAB	0.342	0.433	0.223
	left	CCG	0.794	0.973	0.879
	right	CCG	0.711	0.552	0.223
	left	ILF	0.003	0.728	0.968
	right	ILF	≤0.001	0.539	0.833
	left	SLFP	0.010	0.552	0.778
	right	SLFP	0.008	0.138	0.576
	left	SLFT	≤0.001	0.091	0.247
	right	SLFT	≤0.001	0.710	0.720
	left	UNC	0.002	0.123	0.833
	right	UNC	≤0.001	0.138	0.778

Table 3.2: Axial Diffusivity - repeated measures ANOVA. Results are provided for each white matter tract. All results were corrected for multiple comparisons. P-values showed in bold indicate a significant effect for the corresponding tract.

Legends: lh = left hemisphere; rh = right hemisphere; fmajor = forceps major; fminor = forceps minor; ATR = anterior thalamic radiation; CAB = cingulum, angular bundle; CCG = cingulum, cingulate bundle; CST = corticospinal tract; ILF = inferior longitudinal fasciculus; SLFP = superior longitudinal fasciculus, parietal bundle; SLFT = superior longitudinal fasciculus, temporal bundle; UNC = uncinate fasciculus

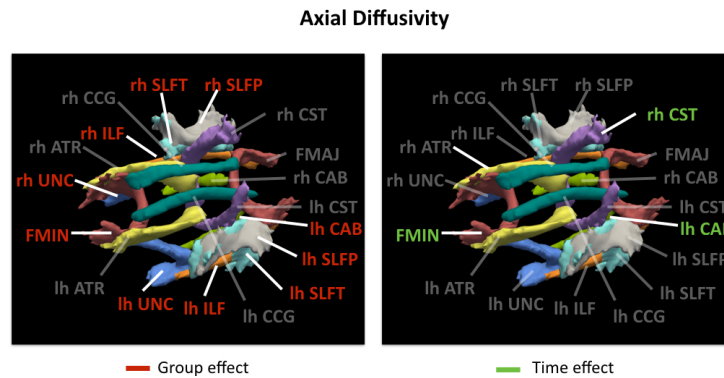


Figure 3.2: Tracts showing significant group (red) or time (green) effects in Axial Diffusivity. Displayed results were corrected for multiple comparisons using the FDR method.

Radial Diffusivity

We found a significant effect of diagnosis, with reductions of RD in the corpus callosum (FMAJ, FMIN), bilateral ATR, left CAB, bilateral CCG, left ILF, left SLFP and bilateral SLFT. Time had a significant effect in the bilateral ATR, left CAB, left ILF, left SLFT and right CST. There were no significant interaction effects. Results are provided in Table 3.3, and tracts with significant group or time effects are displayed in Figure 3.3.

			p-value		
Tract type	Hem.	Tract	Main effect diagnosis	Main effect time	Interaction effect
Projection	left	ATR	≤ 0.001	0.002	0.199
	right	ATR	≤ 0.001	0.017	0.548
	left	CST	0.234	0.741	0.199
	right	CST	0.778	0.022	0.108
Commissural		FMAJ	0.008	0.376	0.199
		FMIN	0.008	0.753	0.492
Association	left	CAB	0.036	≤ 0.001	0.544
	right	CAB	0.071	0.465	0.108
	left	CCG	0.008	0.741	0.210
	right	CCG	0.003	0.430	0.199
	left	ILF	≤ 0.001	≤ 0.001	0.217
	right	ILF	0.058	0.234	0.795
	left	SLFP	0.036	0.187	0.199
	right	SLFP	0.160	0.741	0.199
	left	SLFT	0.008	0.004	0.199
	right	SLFT	0.012	0.234	0.199
	left	UNC	0.050	0.068	0.199
	right	UNC	0.058	0.273	0.795

Table 3.3: Radial Diffusivity - repeated measures ANOVA. Results are provided for each white matter tract. All results were corrected for multiple comparisons. P-values showed in bold indicate a significant effect for the corresponding tract.

Legends: lh = left hemisphere; rh = right hemisphere; fmajor = forceps major; fminor = forceps minor; ATR = anterior thalamic radiation; CAB = cingulum, angular bundle; CCG = cingulum, cingulate bundle; CST = corticospinal tract; ILF = inferior longitudinal fasciculus; SLFP = superior longitudinal fasciculus, parietal bundle; SLFT = superior longitudinal fasciculus, temporal bundle; UNC = uncinate fasciculus.

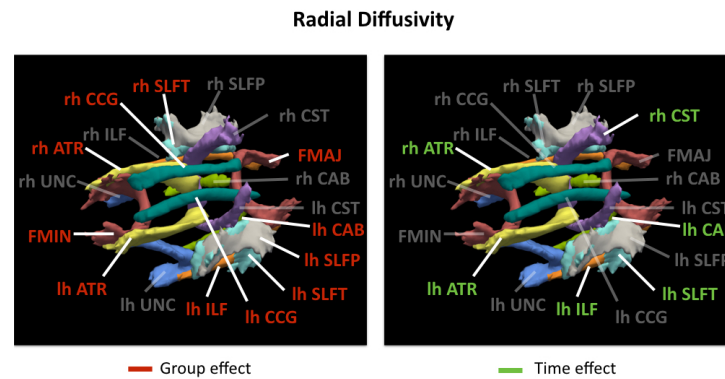


Figure 3.3: Tracts showing significant group (red) or time (green) effects in Radial Diffusivity. Displayed results were corrected for multiple comparisons using the FDR method.

Fractional Anisotropy

Repeated measures ANOVA yielded a significant effect of diagnosis for FA in the bilateral ATR, with increased levels of FA for patients with 22q11.2DS. A significant effect of time was visible for the bilateral ATR, left CAB, left ILF and bilateral SLFT. No significant diagnosis x time interaction effects were observed in any of the white matter tracts. Results are reported in Table 3.4, and tracts with significant group or time effects are displayed in Figure 3.4.

Tract type	Hem.	Tract	p-value		
			Main effect diagnosis	Main effect time	Interaction effect
Projection	left	ATR	≤ 0.001	≤ 0.001	0.348
	right	ATR	0.027	0.026	0.682
	left	CST	0.820	0.620	0.109
	right	CST	0.820	0.245	0.075
Commissural		FMAJ	0.136	0.579	0.075
		FMIN	0.093	0.620	0.682
Association	left	CAB	0.869	≤ 0.001	0.125
	right	CAB	0.434	0.073	0.075
	left	CCG	0.070	0.786	0.075
	right	CCG	0.070	0.216	0.125
	left	ILF	0.070	≤ 0.001	0.348
	right	ILF	0.434	0.520	0.938
	left	SLFP	0.442	0.094	0.075
	right	SLFP	0.922	0.081	0.075
	left	SLFT	0.442	0.002	0.075
	right	SLFT	0.820	0.031	0.075
	left	UNC	0.745	0.094	0.076
	right	UNC	0.922	0.416	0.938

Table 3.4: Fractional Anisotropy - repeated measures ANOVA. Results are provided for each white matter tract. All results were corrected for multiple comparisons. P-values showed in bold indicate a significant effect for the corresponding tract.

Legends: lh = left hemisphere; rh = right hemisphere; fmajor = forceps major; fminor = forceps minor; ATR = anterior thalamic radiation; CAB = cingulum, angular bundle; CCG = cingulum, cingulate bundle; CST = corticospinal tract; ILF = inferior longitudinal fasciculus; SLFP = superior longitudinal fasciculus, parietal bundle; SLFT = superior longitudinal fasciculus, temporal bundle; UNC = uncinate fasciculus.

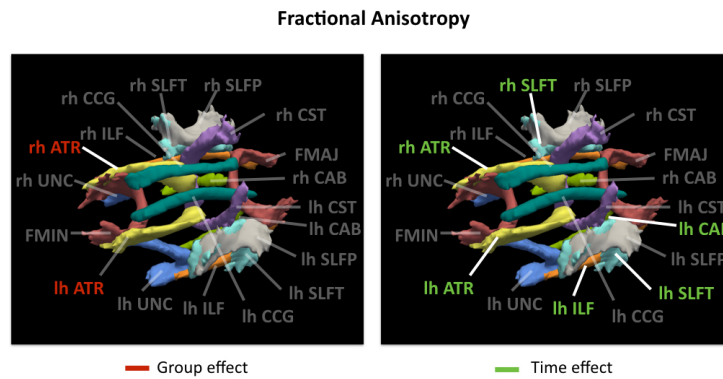


Figure 3.4: Tracts showing significant group (red) or time (green) effects in Fractional Anisotropy. Displayed results were corrected for multiple comparisons using the FDR method.

3.1.2 Annual percent change

After correcting for multiple comparisons, annual percent change (APC) was significantly different in AD and MD for the right CST, with an APC of -0.9% in patients with 22q11.2DS versus -0.2% in TD controls in AD, and an APC of -1.5% in patients with 22q11.2DS versus -0.3% In TD controls (Table 3.5; for detailed tables of results and graphs, see appendix). Other diffusion metrics did not reveal any significant group differences.

Tract type	Hem.	Tract	p-value			
			MD	AD	RD	FA
Projection	left	ATR	0.124	0.184	0.17	0.215
	right	ATR	0.327	0.542	0.287	0.433
	left	CST	0.124	0.187	0.112	0.151
	right	CST	0.037	0.011	0.069	0.081
Commissural		FMAJ	0.356	0.916	0.243	0.151
		FMIN	0.356	0.475	0.287	0.426
Association	left	CAB	0.356	0.807	0.261	0.151
	right	CAB	0.124	0.187	0.123	0.125
	left	CCG	0.327	0.807	0.243	0.125
	right	CCG	0.124	0.187	0.184	0.199
	left	ILF	0.327	0.763	0.261	0.464
	right	ILF	0.882	0.834	0.991	0.953
	left	SLFP	0.327	0.627	0.243	0.167
	right	SLFP	0.221	0.686	0.17	0.111
	left	SLFT	0.124	0.227	0.17	0.151
	right	SLFT	0.224	0.661	0.17	0.081
	left	UNC	0.472	0.763	0.264	0.151
	right	UNC	0.888	0.791	0.98	0.953

Table 3.5: Group comparisons of mean annual percentage change in MD, AD, RD and FA for each white matter tract. Significant group differences are indicated in bold. All displayed p-values were corrected for multiple comparisons.

Legends: lh = left hemisphere; rh = right hemisphere; fmajor = forceps major; fminor = forceps minor; ATR = anterior thalamic radiation; CAB = cingulum, angular bundle; CCG = cingulum, cingulate bundle; CST = corticospinal tract; ILF = inferior longitudinal fasciculus; SLFP = superior longitudinal fasciculus, parietal bundle; SLFT = superior longitudinal fasciculus, temporal bundle; UNC = uncinate fasciculus.

3.2 Main study

We first report analyses assessing group differences between 22q11.2DS subjects and TD controls; then, we describe results regarding the relationship between white matter microstructural maturation and two major risk factors for psychosis, that is cognitive decline and UHR status, in the 22q11.2DS population.

3.2.1 Developmental trajectories of white matter tracts in 22q11.2DS versus TD controls

After correcting for multiple comparisons, significant group differences were found in all diffusion measures and for most white matter tracts, the CST being the only unaffected bundle. Overall, white matter alterations were very consistent, with 22q11.2DS patients showing increases in FA, and reductions in RD, AD and MD when compared to TD controls. Of note, the shape of white matter developmental trajectories did not differ between the two populations for any of the tracts or DTI metrics, thus confirming the absence of interaction effects reported in the preliminary analysis. Results detailing tracts alterations, effect of diagnosis and developmental tendencies are reported for each diffusion measure.

Mean Diffusivity

Group differences were massively present in the MD measure, as patients with 22q11.2DS had significant reductions in MD for the FMAJ, FMIN, bilateral ATR, UNC, ILF, SLFP, SLFT, CCG and for the left CAB (Figure 3.5). Apart from the left CAB, who had a $p \leq 0.01$, all mentioned tracts showed highly significant group effects, with $p \leq 0.001$ (Table 3.6). No age x diagnosis interaction effects were found.

Developmental trajectories were non-linear for both groups in many tracts (FMAJ, left ATR, CCG, ILF, SLFP, SLFT, right UNC), with progressive decreases of MD visible even during adulthood. In some cases (i.e., for the FMIN, left CAB, left UNC, right ATR), the trajectory was linear, but was still following a similar pattern of progressive decrease.

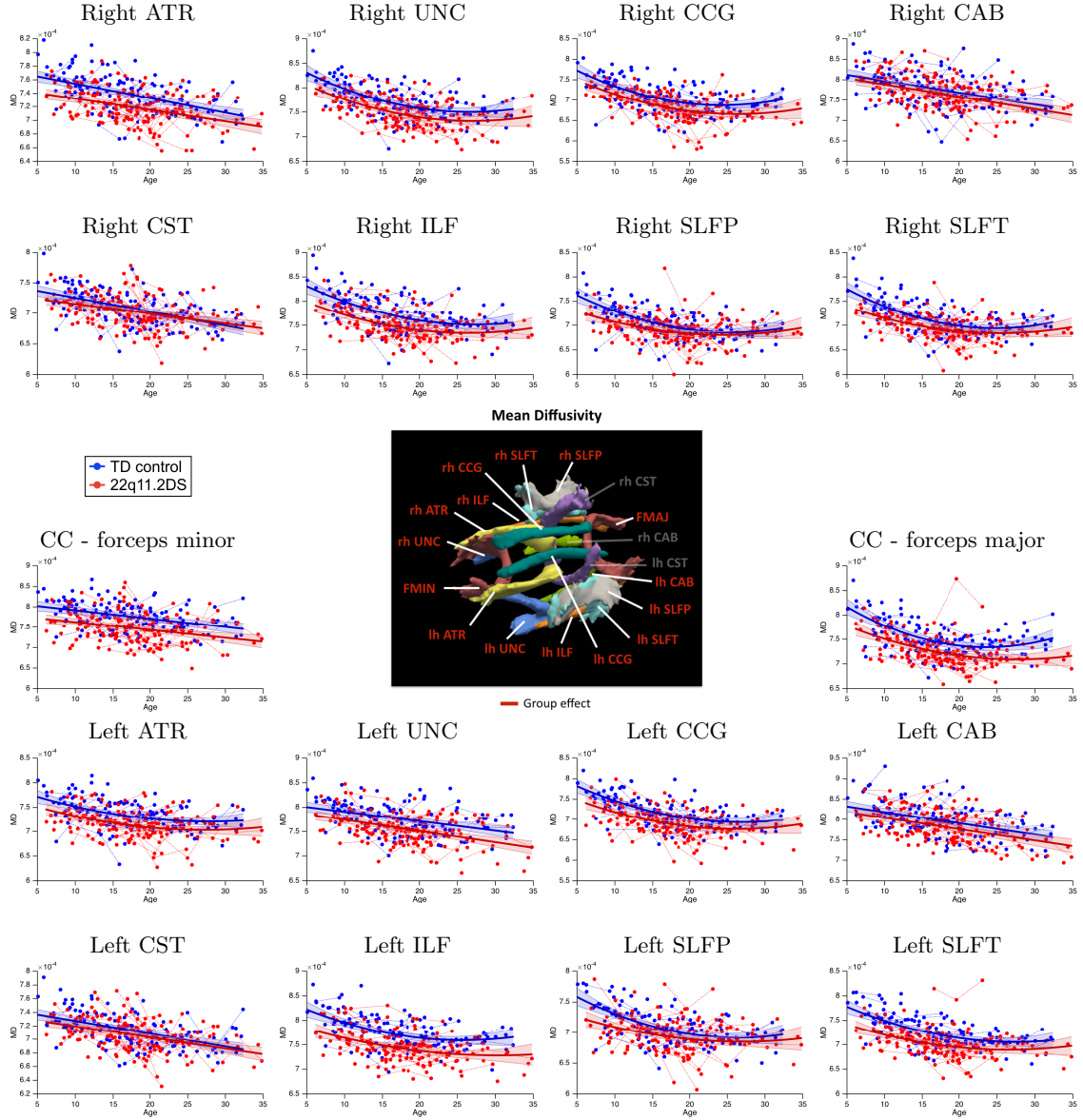


Figure 3.5: Mean Diffusivity (MD). Developmental trajectories of individuals with 22q11.2DS (red) and TD controls (blue) are represented for the 18 white matter tracts reconstructed by TRACULA. Age is represented on the x axis, MD is indicated on the y axis. Tracts with significant group differences are highlighted in red in the central figure.

Legends: lh = left hemisphere; rh = right hemisphere; fmajor = forceps major; fminor = forceps minor; ATR = anterior thalamic radiation; CAB = cingulum, angular bundle; CCG = cingulum, cingulate bundle; CST = corticospinal tract; ILF = inferior longitudinal fasciculus; SLFP = superior longitudinal fasciculus, parietal bundle; SLFT = superior longitudinal fasciculus, temporal bundle; UNC = uncinate fasciculus.

Tract type	Hem.	Tract	Model	p-value	
				Group effect	Interaction effect
Projection	left	ATR	Quadratic	≤ 0.001	0.999
	right	ATR	Linear	≤ 0.001	0.623
	left	CST	Linear	0.052	0.88
	right	CST	Linear	0.076	0.591
Commissural		FMAJ	Quadratic	≤ 0.001	0.623
		FMIN	Linear	≤ 0.001	0.981
Association	left	CAB	Linear	0.009	0.999
	right	CAB	Linear	0.146	0.981
	left	CCG	Quadratic	≤ 0.001	0.88
	right	CCG	Quadratic	≤ 0.001	0.981
	left	ILF	Quadratic	≤ 0.001	0.933
	right	ILF	Quadratic	≤ 0.001	0.88
	left	SLFP	Quadratic	≤ 0.001	0.591
	right	SLFP	Quadratic	≤ 0.001	0.591
	left	SLFT	Quadratic	≤ 0.001	0.623
	right	SLFT	Quadratic	≤ 0.001	0.591
	left	UNC	Linear	≤ 0.001	0.88
	right	UNC	Quadratic	≤ 0.001	0.981

Table 3.6: *Mean Diffusivity. For each white matter tract, the fitted model and p-values for group and interaction effects are indicated. Displayed results have been corrected for multiple comparisons using the FDR method.*

Legends: lh = left hemisphere; rh = right hemisphere; fmajor = forceps major; fminor = forceps minor; ATR = anterior thalamic radiation; CAB = cingulum, angular bundle; CCG = cingulum, cingulate bundle; CST = corticospinal tract; ILF = inferior longitudinal fasciculus; SLFP = superior longitudinal fasciculus, parietal bundle; SLFT = superior longitudinal fasciculus, temporal bundle; UNC = uncinate fasciculus.

Axial Diffusivity

Compared to the other diffusion metrics, AD showed fewer significant group differences. Nonetheless, AD values were significantly reduced for patients bilaterally in the UNC, ILF, SLFT, right SLFP and left CAB (Figure 3.6). Most of these tracts had a group effect with a $p \leq 0.001$, except the right SLFP (≤ 0.01) (Table 3.7).

All tracts showed a linear trajectory for both groups, with a progressive decrease of AD over time for most significant tracts. Among tracts with significant group differences, the right SLFP was the only pathway displaying a constant trajectory.

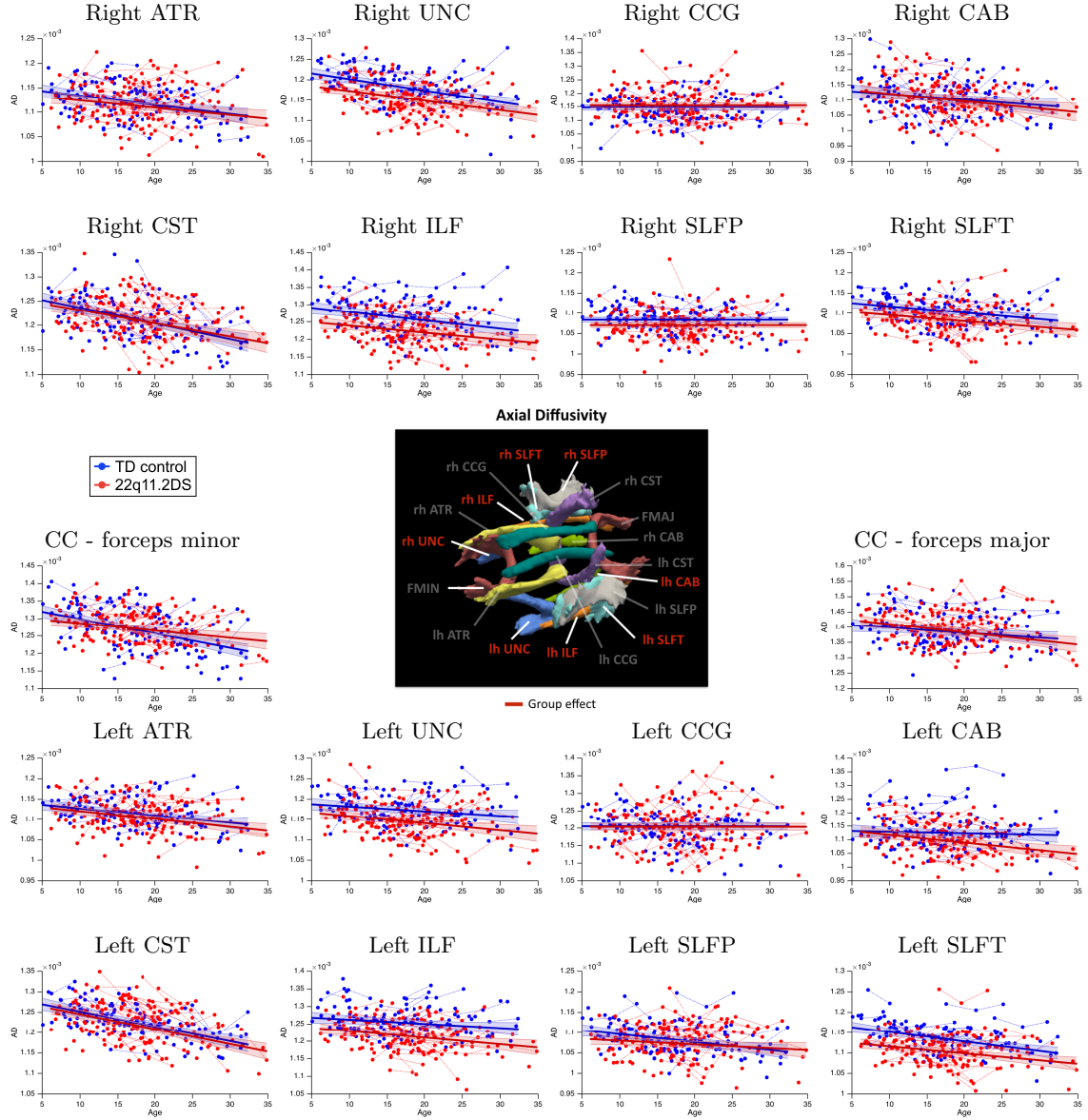


Figure 3.6: Axial Diffusivity (AD). Developmental trajectories of individuals with 22q11.2DS (red) and TD controls (blue) are represented for the 18 white matter tracts reconstructed by TRACULA. Age is represented on the x axis, AD is indicated on the y axis. Tracts with significant group differences are highlighted in red in the central figure.

Legends: lh = left hemisphere; rh = right hemisphere; fmajor = forceps major; fminor = forceps minor; ATR = anterior thalamic radiation; CAB = cingulum, angular bundle; CCG = cingulum, cingulate bundle; CST = corticospinal tract; ILF = inferior longitudinal fasciculus; SLFP = superior longitudinal fasciculus, parietal bundle; SLFT = superior longitudinal fasciculus, temporal bundle; UNC = uncinate fasciculus.

Tract type	Hem.	Tract	Model	p-value	
				Group effect	Interaction effect
Projection	left	ATR	Linear	0.352	0.898
	right	ATR	Linear	0.411	0.762
	left	CST	Linear	0.558	0.958
	right	CST	Linear	0.837	0.762
Commissural		FMAJ	Linear	0.558	0.635
		FMIN	Linear	0.103	0.074
Association	left	CAB	Linear	≤ 0.001	0.14
	right	CAB	Linear	0.837	0.762
	left	CCG	Constant	0.86	
	right	CCG	Constant	0.411	
	left	ILF	Linear	≤ 0.001	0.711
	right	ILF	Linear	≤ 0.001	0.774
	left	SLFP	Linear	0.15	0.457
	right	SLFP	Constant	0.007	
	left	SLFT	Linear	≤ 0.001	0.635
	right	SLFT	Linear	≤ 0.001	0.898
	left	UNC	Linear	≤ 0.001	0.711
	right	UNC	Linear	≤ 0.001	0.762

Table 3.7: *Axial Diffusivity. For each white matter tract, the fitted model and p-values for group and interaction effects are indicated. Displayed results have been corrected for multiple comparisons using the FDR method.*

Legends: lh = left hemisphere; rh = right hemisphere; fmajor = forceps major; fminor = forceps minor; ATR = anterior thalamic radiation; CAB = cingulum, angular bundle; CCG = cingulum, cingulate bundle; CST = corticospinal tract; ILF = inferior longitudinal fasciculus; SLFP = superior longitudinal fasciculus, parietal bundle; SLFT = superior longitudinal fasciculus, temporal bundle; UNC = uncinate fasciculus.

Radial Diffusivity

We found significant group differences in RD, with reductions of this measure in individuals with 22q11.2DS in the FMAJ, FMIN, and bilaterally in the ATR, UNC, ILF, CCG, SLFP and SLFT (Figure 3.7). Most tracts showing significant group differences had a $p \leq 0.001$, with the exception of the left and right UNC, as well as the right ILF, who had a $p \leq 0.01$ (Table 3.8). No significant group x age interaction effects were found for any of the white matter tracts. Overall, both for TD controls and patients with 22q11.2DS, most white matter tracts showed a non-linear developmental trajectory (FMAJ, ATR, CCG, ILF, SLFP, SLFT, UNC), with regular decreases in RD until adulthood. The FMIN was the only tract with a constant trajectory. Curve shapes were identical for both groups in all tracts.

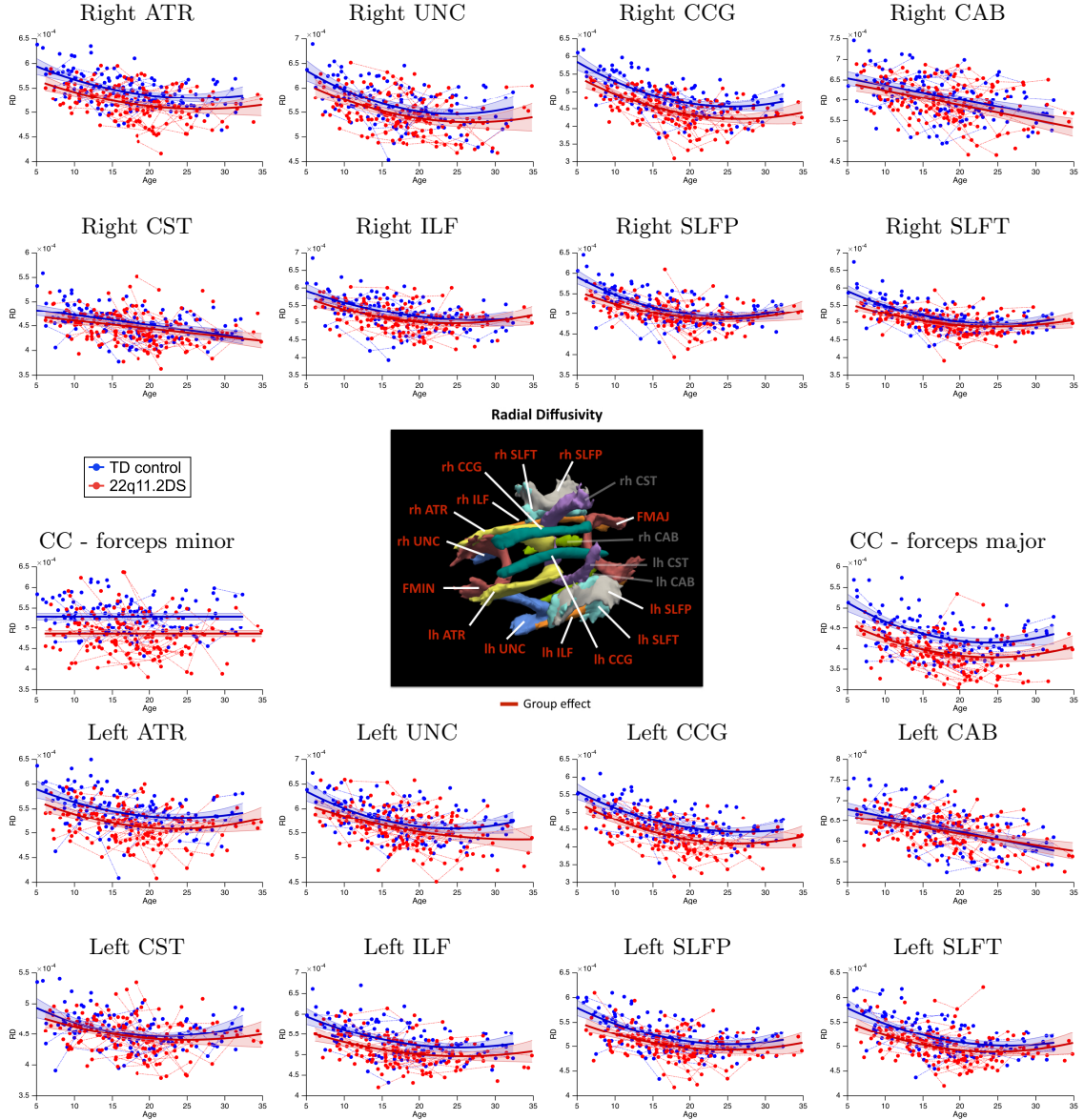


Figure 3.7: Radial Diffusivity (RD). Developmental trajectories of individuals with 22q11.2DS (red) and TD controls (blue) are represented for the 18 white matter tracts reconstructed by TRACULA. Age is represented on the x axis, RD is indicated on the y axis. Tracts with significant group differences are highlighted in red in the central figure.

Legends: lh = left hemisphere; rh = right hemisphere; fmajor = forceps major; fminor = forceps minor; ATR = anterior thalamic radiation; CAB = cingulum, angular bundle; CCG = cingulum, cingulate bundle; CST = corticospinal tract; ILF = inferior longitudinal fasciculus; SLFP = superior longitudinal fasciculus, parietal bundle; SLFT = superior longitudinal fasciculus, temporal bundle; UNC = uncinate fasciculus.

Tract type	Hem.	Tract	Model	p-value	
				Group effect	Interaction effect
Projection	left	ATR	Quadratic	≤ 0.001	0.975
	right	ATR	Quadratic	≤ 0.001	0.975
	left	CST	Quadratic	0.178	0.963
	right	CST	Linear	0.074	0.963
Commissural		FMAJ	Quadratic	≤ 0.001	0.963
		FMIN	Constant	≤ 0.001	
Association	left	CAB	Linear	0.193	0.963
	right	CAB	Linear	0.098	0.975
	left	CCG	Quadratic	≤ 0.001	0.975
	right	CCG	Quadratic	≤ 0.001	0.975
	left	ILF	Quadratic	≤ 0.001	0.963
	right	ILF	Quadratic	0.008	0.963
	left	SLFP	Quadratic	≤ 0.001	0.963
	right	SLFP	Quadratic	≤ 0.001	0.728
	left	SLFT	Quadratic	≤ 0.001	0.963
	right	SLFT	Quadratic	≤ 0.001	0.728
	left	UNC	Quadratic	0.006	0.963
	right	UNC	Quadratic	0.005	0.963

Table 3.8: *Radial Diffusivity.* For each white matter tract, the fitted model and p-values for group and interaction effects are indicated. Displayed results have been corrected for multiple comparisons using the FDR method.

Legends: lh = left hemisphere; rh = right hemisphere; fmajor = forceps major; fminor = forceps minor; ATR = anterior thalamic radiation; CAB = cingulum, angular bundle; CCG = cingulum, cingulate bundle; CST = corticospinal tract; ILF = inferior longitudinal fasciculus; SLFP = superior longitudinal fasciculus, parietal bundle; SLFT = superior longitudinal fasciculus, temporal bundle; UNC = uncinate fasciculus.

Fractional Anisotropy

Individuals with 22q11.2DS had significantly higher FA values for a number of white matter tracts, including the FMAJ, FMIN, and bilaterally in the ATR, CCG and SLFP (Figure 3.8). All mentioned tracts had p values ≤ 0.001 , with the exception of the right SLFP who had a p value ≤ 0.05 (Table 3.9). We found no significant group x age interaction effects.

Trajectories were either linear or quadratic: the FMIN and left ATR displayed constant curves, whereas the FMAJ, right ATR, bilateral CCG, and bilateral SLFP had quadratic curves, with increases until adulthood and peaks reached around 20-30 years old. For tracts showing significant group differences, 22q11.2DS patients and controls always had similar trajectory shapes, with however a systematically higher intercept for the 22q11.2DS group.

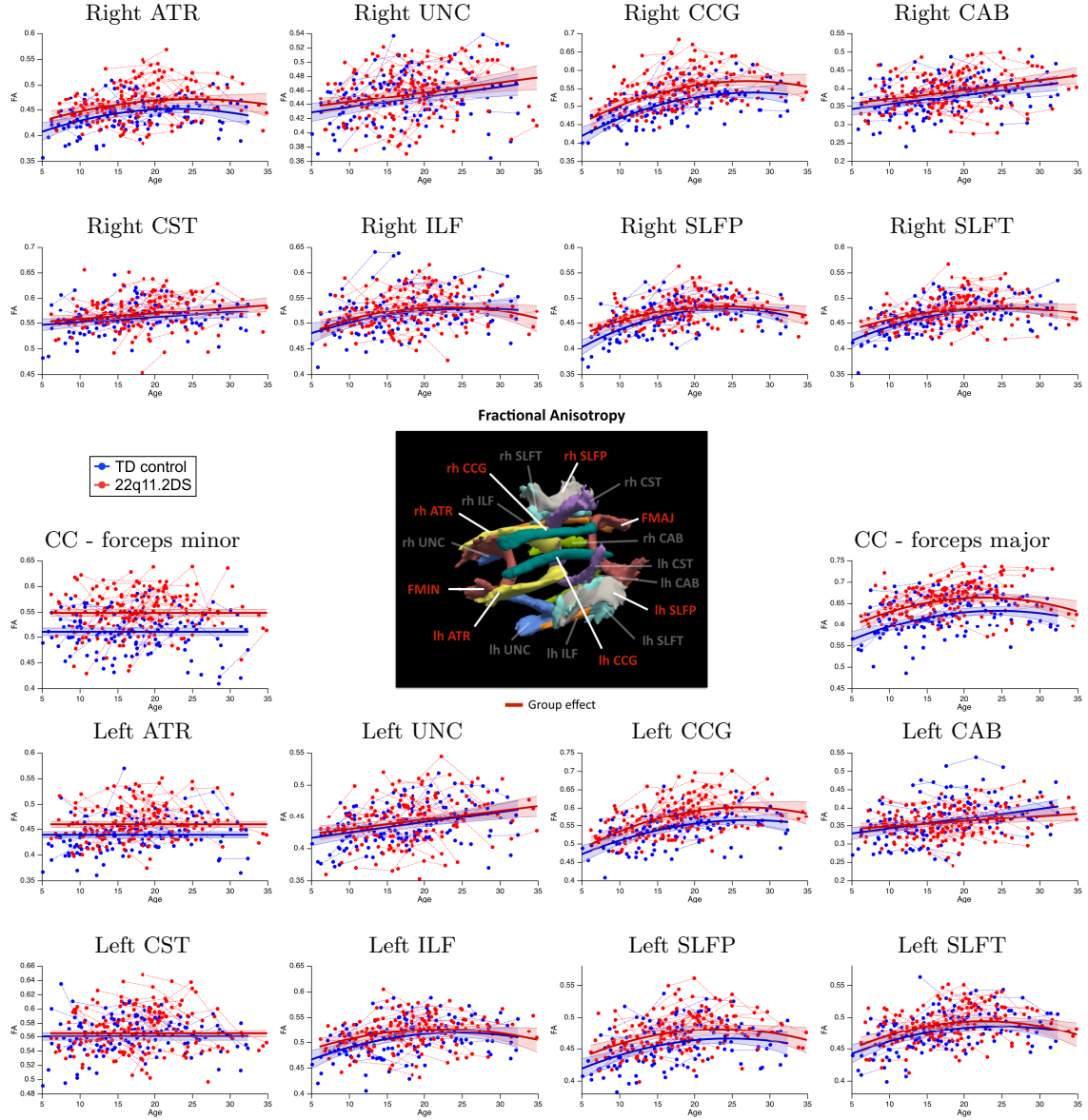


Figure 3.8: Fractional Anisotropy (FA). Developmental trajectories of individuals with 22q11.2DS (red) and TD controls (blue) are represented for the 18 white matter tracts reconstructed by TRACULA. Age is represented on the x axis, FA is indicated on the y axis. Tracts with significant group differences are highlighted in red in the central figure.

Legends: lh = left hemisphere; rh = right hemisphere; fmajor = forceps major; fminor = forceps minor; ATR = anterior thalamic radiation; CAB = cingulum, angular bundle; CCG = cingulum, cingulate bundle; CST = corticospinal tract; ILF = inferior longitudinal fasciculus; SLFP = superior longitudinal fasciculus, parietal bundle; SLFT = superior longitudinal fasciculus, temporal bundle; UNC = uncinate fasciculus.

Tract type	Hem.	Tract	Model	p-value	
				Group effect	Interaction effect
Projection	left	ATR	Constant	≤ 0.001	
	right	ATR	Quadratic	≤ 0.001	0.966
	left	CST	Constant	0.289	
	right	CST	Linear	0.258	0.966
Commissural		FMAJ	Quadratic	≤ 0.001	0.966
		FMIN	Constant	≤ 0.001	
Association	left	CAB	Linear	0.258	0.428
	right	CAB	Linear	0.122	0.966
	left	CCG	Quadratic	≤ 0.001	0.966
	right	CCG	Quadratic	≤ 0.001	0.966
	left	ILF	Quadratic	0.09	0.966
	right	ILF	Quadratic	0.605	0.966
	left	SLFP	Quadratic	≤ 0.001	0.966
	right	SLFP	Quadratic	0.023	0.962
	left	SLFT	Quadratic	0.108	0.966
	right	SLFT	Quadratic	0.108	0.734
	left	UNC	Linear	0.605	0.966
	right	UNC	Linear	0.351	0.966

Table 3.9: *Fractional Anisotropy. For each white matter tract, the fitted model and p-values for group and interaction effects are indicated. Displayed results have been corrected for multiple comparisons using the FDR method.*

Legends: lh = left hemisphere; rh = right hemisphere; fmajor = forceps major; fminor = forceps minor; ATR = anterior thalamic radiation; CAB = cingulum, angular bundle; CCG = cingulum, cingulate bundle; CST = corticospinal tract; ILF = inferior longitudinal fasciculus; SLFP = superior longitudinal fasciculus, parietal bundle; SLFT = superior longitudinal fasciculus, temporal bundle; UNC = uncinate fasciculus.

3.2.2 Relationship between white matter microstructure and cognition in 22q11.2DS

When subjects with 22q11.2DS were categorized depending on the presence or absence of cognitive decline, a significant interaction effect was found for FA in the FMAJ. Developmental trajectories for patients with a cognitive decline and without decline are visible in Figure 3.9. Patients showing a decline were characterized by a flattened developmental trajectory compared to patients with no cognitive worsening. The reported results were corrected using FDR.

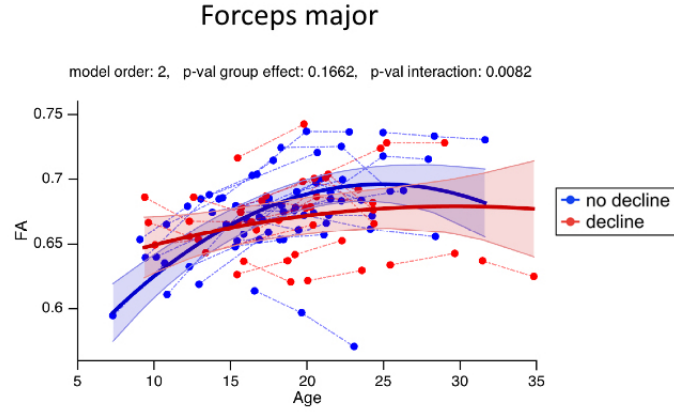


Figure 3.9: *Developmental trajectories of FA in the splenium of the corpus callosum (forceps major), for patients with a cognitive decline versus without cognitive decline. A quadratic model fit (i.e., model order = 2) was chosen based on the BIC selection criterion.*

3.2.3 Relationship between white matter microstructure and UHR status in 22q11.2DS

When individuals with 22q11.2DS were divided according to their UHR status, a significant interaction effect was observed for FA in the FMAJ, where UHR patients failed to show normative non-linear increases peaking around 20 years, and instead demonstrated a constant increase of FA throughout development (Figure 3.10). In addition, a significant interaction effect was also found for AD in the left CAB. In this tract, UHR patients had low values of AD at early ages and showed progressive increases in this metric. Conversely, non-UHR patients were characterized by initially higher AD, followed by a gradual decrease over time.

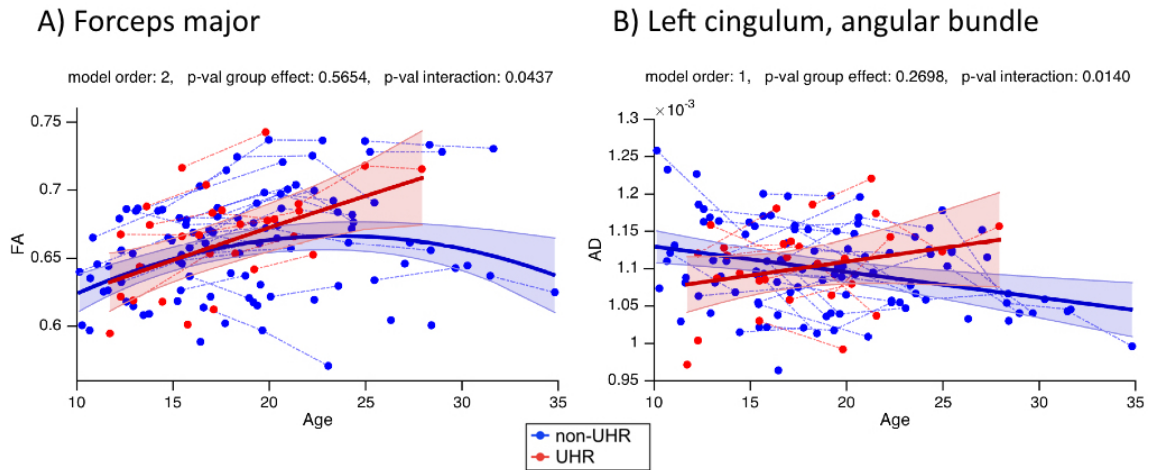


Figure 3.10: *Developmental trajectories of FA in the splenium of the corpus callosum (forceps major, FMAJ) and AD of the left angular bundle of the cingulum (CAB) in patients with 22q11.2DS fulfilling the UHR criteria for at least one of their assessments, compared to patients with 22q11.2DS who never fulfilled the UHR criteria. Based on the BIC selection criterion, a quadratic model fit (model order = 2) was chosen for FMAJ, and a linear model fit (model order = 1) was chosen for the left CAB.*

CHAPTER 4

DISCUSSION

4.1 Preliminary study

The aim of the preliminary study was to obtain an initial estimation of connectivity alterations present in 22q11.2DS throughout their development. To this end, we utilized a balanced design with an equal amount of assessments per subject (in this case, 2 time points) and similar time intervals, as this allowed the use of relatively straight forward statistical methods for the analysis of longitudinal data such as repeated measures ANOVA, or tests on group differences in the annual percent change. Using the former method, we found significant alterations in all diffusion metrics and for multiple white matter tracts in 22q11.2DS, with systematic increases of FA and reductions of RD, AD and MD. Briefly, increased FA values indicate abnormal increases in the directionality of diffusion; reductions of RD suggest increases in myelination; reductions of AD point to axonal damage or reduced tracts organization; and finally reductions in MD are possibly reflecting a decreased magnitude of diffusion (for a detailed discussion, see section 4.2). Moreover, developmental changes were evident, as DTI metrics significantly changed over time (i.e., from the first time point to the second) for some white matter tracts. Finally, an interaction between diagnosis and time was almost never observed, indicating that group differences remained constant over time. This finding was further confirmed by the second analysis, as group comparisons of the annual percent change revealed similar progression rates of diffusion measures in most tracts. Thus, preliminary observations suggest that: 1) 22q11.2DS is associated with widespread microstructural alterations of white matter tracts, 2) developmental changes are similar in patients and TD controls.

However, these findings should be considered with caution, due to several limitations. Firstly, the statistical analysis methods applied in this study merely capture linear developmental changes (Krueger and Tian, 2004), which might be suboptimal given that white matter maturation is known to follow non-linear trajectories (Lebel et al., 2012). Second, time is modelled in a simplified way. Indeed, repeated measures ANOVA can only treat time as a categorical factor (i.e., number of time points), and a summary measure such

as the annual percent change only reflects an overall estimation of change. When this is applied on subjects with very large ages ranges at each assessment, this involves the inclusion of a considerable amount of variance in the measures of interest (especially since white matter undergoes significant changes throughout development; e.g. Lebel et al. (2012)), which might affect the results of group comparisons. Finally, a third limitation of these approaches is that they are suitable only for balanced designs with a small number of equally spaced time points, and cannot handle missing data. Consequently, a limited sample size could be used for these analyses, which may have reduced statistical power.

Thus, the aim of our next study was to characterize the developmental trajectories of white matter tracts over a large age span, including the entire available cohort of subjects from our ongoing longitudinal project. Mixed models regression analyses were used, as this type of method can model nonlinear relationships across time and handle data with missing time points.

4.2 Main study

To the best of our knowledge, this is the first and largest DTI study to have used longitudinal data and an automated probabilistic tractography approach to: 1) characterize the developmental trajectories of white matter in 22q11.2DS individuals compared to TD controls, 2) study the developmental trajectories of white matter microstructure in individuals with 22q11.2DS with and without a cognitive decline, and 3) investigate the relationship between developmental patterns of white matter microstructure and UHR status in 22q11.2DS. Findings resulting from these three analyses will be discussed in the following sections.

4.2.1 Widespread white matter alterations in individuals with 22q11.2DS

In this section, a detailed discussion will first be provided regarding the direction of alterations observed in 22q11.2DS for each of the four DTI metrics. This will be followed by a discussion regarding the shape of the developmental trajectories observed for each of the DTI metrics for 22q11.2DS and TD controls. Finally, potential causal mechanisms underlying the observed alterations will be discussed.

In line with our initial hypothesis, our first observation was that compared to TD controls, individuals with 22q11.2DS showed alterations in all four DTI metrics and for most white matter tracts. Consistent with results of our preliminary study, the direction of alterations was very consistent, as all tracts showed increased FA, combined with reduced RD, AD and MD for the 22q11.2DS population.

More specifically, reductions of MD were visible in almost all tracts, as the corpus callosum (FMAJ, FMIN), the ATR, the UNC, the ILF, the superior longitudinal fasciculus (SLFP, SLFT) and the cingulum (CCG, CAB) were affected in patients with 22q11.2DS. Although only few studies have analyzed this diffusion metric, these mostly

reported similar reductions in MD (Kikinis et al., 2017; Roalf et al., 2017; Simon et al., 2008; Villalon-Reina et al., 2013). Regarding the interpretation of this diffusion measure, MD is indicative of the average magnitude of water diffusion in the tissue and can be considered as a summary measure. Accordingly, our results suggest that white matter tracts of patients with 22q11.2DS are characterized by smaller magnitudes of diffusivity, indicating that water diffusion is more restricted towards a specific direction. This finding is rather counter-intuitive, since alterations of white matter integrity are more typically linked to increases in diffusivity (i.e., water molecules are less restricted due to the disruption of axonal or myelin components). Other diffusion metrics can however provide a better understanding of the pathological processes underlying this observation. Findings related to these metrics will be detailed below.

Consistent with most previous cross-sectional studies in 22q11.2DS, we found reduced values of AD in multiple association tracts (Bakker et al., 2016; Jalbrzikowski et al., 2014; Kates et al., 2015; Kikinis et al., 2017, 2013; Perlstein et al., 2014; Radoeva et al., 2012; Roalf et al., 2017; Simon et al., 2008; Villalon-Reina et al., 2013), including the UNC, ILF, SLFT, SLFP and CAB. Fewer reports (Bakker et al., 2016; Jalbrzikowski et al., 2014; Kikinis et al., 2017; Radoeva et al., 2012; Roalf et al., 2017; Villalon-Reina et al., 2013) indicate the presence of AD anomalies in commissural or projection tracts, which were not confirmed in this study. Our results thus contribute to a growing body of evidence indicating that AD reductions in patients with 22q11.2DS are specifically localized in association tracts. Studies conducted in mouse models suggest that AD reductions are driven by axonal disruption, reduced tract organization or a reduction in the diameter of axonal tracts (Budde et al., 2009; Harsan et al., 2006; Schwartz et al., 2005; Song et al., 2003). Interestingly, a previous cross-sectional tractography study by our group including patients with a relatively similar age range (7-25 years old) found a 10% reduction in the number of reconstructed streamlines in 22q11.2DS compared to controls (Ottet et al., 2013). Together with our results of reduced AD, this finding supports the idea of axonal disruptions or a reduction in tracts organization, where fibers are composed of less numerous, or more loosely packed axons.

RD showed more widespread reductions and affected a large majority of white matter tracts, including the corpus callosum (FMAJ, FMIN), the ATR, the UNC, the ILF, the CCG, the SLFP, and the SLFT. Reductions of RD have also been largely reported by previous studies in 22q11.2DS (Bakker et al., 2016; Jalbrzikowski et al., 2014; Kates et al., 2015; Kikinis et al., 2017; Olszewski et al., 2017; Perlstein et al., 2014; Simon et al., 2008; Tylee et al., 2017; Villalon-Reina et al., 2013), although few also found increases (Deng et al., 2015; Roalf et al., 2017; Villalon-Reina et al., 2013). It has been demonstrated that RD changes are due to modifications in the myelination of axons (Song et al., 2003, 2002); as such, reductions of RD are thus indicative of excessive myelination of axonal tracts. Indeed, the presence of thicker myelin sheaths considerably restrains the perpendicular diffusion water molecules, leading to smaller values of RD.

Regarding FA, we found significant increases in patients with 22q11.2DS, in tracts including the corpus callosum (FMAJ, FMIN), the ATR, the CCG and in the SLFP. This is in line with several previous white matter studies in 22q11.2DS (Bakker et al., 2016; Barnea-Goraly et al., 2003; da Silva Alves et al., 2011; Jalbrzikowski et al., 2014; Kates et al., 2015; Olszewski et al., 2017; Perlstein et al., 2014; Sundram et al., 2010). However, as reviewed in Scariati et al. (2016), reductions of FA have also been frequently reported in 22q11.2DS, making the results regarding this measure considerably heterogeneous. Although most frequently, FA is argued to represent a general measure of white matter integrity (where increased levels suggest healthier, more coherently packed and myelinated bundles), it has also been suggested that increased levels of FA could reflect abnormal decreases in axonal branching, which would in turn lead to a reduction of the amount of fiber crossings (Arlinghaus et al., 2011; Hoeft et al., 2007). Other proposals regarding the cellular nature of increased FA include flattened bundles allowing for increased white matter density (Bode et al., 2011), or fewer arched fibers (Cheng et al., 2011). Importantly however, a recent study on adolescents (ranging from 15 to 21 years) with 22q11.2DS has observed that increases in FA were driven by reductions in RD which, as mentioned, reflect excessive levels of myelination (Perlstein et al., 2014). These results were later confirmed on the same sample, at ages 18-25 (Olszewski et al., 2017). Interestingly, murine models of white matter pathology indicate that FA and RD metrics are interdependent (Harsan et al., 2006). Indeed, white matter bundles become more anisotropic when myelination is increased (i.e., RD is reduced). Our results support these findings, as we found systematic combinations of increased FA and reduced RD in many white matter tracts and throughout their full developmental trajectory. Thus, although higher FA has traditionally been linked to higher white matter integrity, in 22q11.2DS, its combination with decreased RD suggests that high FA might rather be an indicator of abnormal developmental gains in diffusion directionality, driven by excessive myelination processes.

When considering the shape of the developmental trajectories, findings confirmed our hypothesis proposing that most tracts and DTI metrics should follow non-linear patterns of development. Indeed, we found non-linear curves for most tracts in FA, RD and MD, both in TD controls and in patients. While FA showed progressive increases until reaching its peak, RD and MD followed inverse trajectories with progressive decreases until reaching a minimum. AD was the only measure to show almost exclusively linear trajectories. For FA and MD, our results regarding the developmental trajectories and the age ranges of maturation peaks match results reported in previous longitudinal studies performed on healthy TD subjects (Lebel and Beaulieu, 2011; Lebel et al., 2012). For RD and AD, although developmental trajectories have not been characterized in TD controls and findings are somewhat heterogeneous, most evidence points to progressive reductions in RD and relatively subtle decreases (or even no changes) in AD (Kumar et al., 2012; Schmithorst and Yuan, 2010), which is also consistent with our findings.

Still regarding the shape of the trajectories, we also initially hypothesized that 22q11.2DS would be associated with different developmental curves compared to TD controls, which would reflect alterations in the timing of maturation. This observation has indeed been made for grey matter maturation in the syndrome (Schaer et al., 2009). However, this hypothesis could not be confirmed, as developmental trajectories did not differ in shape between TD controls and patients with 22q11.2DS in our study. This is in contrast with previous cross sectional studies showing significant age x group interactions (Deng et al., 2015; Jalbrzikowski et al., 2014) and a lack of normal increase in whole-brain FA and in the total number of streamlines for patients with 22q11.2DS (Ottet et al., 2013; Padula et al., 2015). Note, however, that these studies were all based on cross-sectional data with smaller samples and narrower age ranges than the current study, making it difficult to determine the exact nature of developmental trajectories in each group. By contrast, the current study used a large sample and statistical methods specifically constructed to capture developmental trajectories. Results of this more detailed characterization of white matter development thus suggest the existence of parallel maturational processes in 22q11.2DS individuals and TD controls, albeit with a persistent pathological “gap” in patients with 22q11.2DS that does not appear to be compensated over time. Finally, the presence of identical trajectory shapes for white matter microstructure also contrasts with the typical age x group interaction effects found for grey matter maturation in this population (e.g. multiple studies report accelerated cortical thinning in 22q11.2DS during the transition from childhood to adulthood) (Schaer et al., 2009). This suggests that white matter and grey matter development are regulated by distinct developmental mechanisms.

Although the exact causal mechanism leading to white matter microstructural disruptions is unknown, the differences in group intercepts and persistent alterations in AD, in particular, point to the existence of early prenatal developmental abnormalities. Indeed, evidence from animal models (Meechan et al., 2009) and post-mortem neuropathological studies (Kiehl et al., 2009) indicates that 22q11.2DS involves aberrant prenatal neuronal migration, resulting in abnormal positioning of axonal tracts through mediation of axonal guidance cues (López-Bendito et al., 2006). Given that AD is thought to reflect tracts organization, it is possible that reductions in this metric are caused by disrupted axonal organization, which occurred during early stages of cortical development.

However, the maturation process of white matter structure also involves myelination, which mainly occurs after birth and extends into the third decade of life (Lebel et al., 2012; Linderkamp et al., 2009). Thus, the persistent white matter alterations observed throughout the entire developmental trajectories of 22q11.2DS individuals cannot exclusively be the consequence of prenatal mechanisms, but are also necessarily caused by abnormal developmental processes occurring during postnatal development.

Preliminary evidence for a genetic mechanism underlying disrupted postnatal white matter development has been recently provided (Perlstein et al., 2014). Indeed, the authors found associations between white matter microstructural alterations and the Nogo-66 receptor gene (also called or Reticulon 4 receptor, i.e., RTN4R) polymorphism. This gene is known to be involved in the inhibition of axonal outgrowth through the interaction of

axon terminals and myelin (Fournier et al., 2001). In 22q11.2DS, the altered expression of this gene (due to the presence of a single allele) could affect myelination and/or axonal sprouting processes (Perlstein et al., 2014), resulting in alterations of local diffusion properties. Thus, an interesting future line of work could focus on the potential role of the RTN4R gene in alterations of white matter developmental trajectories.

The second aim of the main study was to characterize white matter developmental trajectories in individuals with 22q11.2DS based on the presence of two risk factors, cognitive decline and the UHR status. In what follows, we first discuss findings relative to cognitive decline, and subsequently for the UHR status.

4.2.2 Cognitive decline is associated with a lack of age-related changes in the corpus callosum

When patients were divided depending on their individual cognitive evolution, a significant interaction effect was observed for FA in the corpus callosum (FMAJ). More specifically, patients with constant or improving cognitive function were characterized by a pronounced non-linear trajectory with evident increases in FA until adulthood, which resembles the shape of normative developmental trajectories. By contrast, patients experiencing a cognitive decline showed a flattened developmental trajectory, with higher initial FA values around the age of 10 and very subtle increases later on, such that this group has reduced values of FA starting from around 14 years old (see Figure 3.9). Thus, our findings suggest that cognitive decline is associated with a co-occurrent impairment of maturational processes in the FMAJ.

It is important to note that our findings did not confirm our initial hypothesis proposing that cognitive decline would be associated with alterations in association and projection tracts, which was based on results from the only previous study investigating the relationship between cognitive decline and white matter microstructure (Nuninga et al., 2017). The authors indeed found that a cognitive decline prior to scan is associated with increased FA in the SLF, the cingulum, the internal capsule and the superior frontal-occipital fasciculus, but did not detect any differences in the corpus callosum. Although surprising, this difference might be explained by several methodological differences. First, while previous findings are based on a sample with a narrow age range (mean age = 17.8; SD = 3.2), our study includes patients from 7-35 years. Second, results from Nuninga et al. (2017) are based on cross-sectional diffusion data, whereas our analysis characterized the longitudinal trajectory of white matter across multiple assessments. Finally, group differences were assessed using a voxel-based approach in Nuninga et al. (2017), but our study used probabilistic tractography. Thus, when using the recommended longitudinal design adapted for the delineation of multiple developmental processes (e.g., cognitive and neuroanatomical development) (Kraemer et al., 2000), findings suggest that individuals experiencing a cognitive decline have alterations in commissural tracts.

Generally, the corpus callosum is responsible for interhemispheric communication, as it connects the left and right hemispheres. Its caudal part, called the splenium or forceps major, more specifically connects the temporal, parietal and occipital lobes (Aboitiz et al.,

1992; Hofer and Frahm, 2006). Interestingly, increased size of the corpus callosum has been associated with higher cognitive scores in non-psychotic individuals with 22q11.2DS (Shashi et al., 2012), which points to the existence of compensatory mechanisms in patients showing better cognitive functioning. This is in line with our findings, as the non-linear developmental increases in FA observed in patients with a favorable cognitive evolution in our study suggests the presence of microstructural reorganizations (which may induce changes in tract size) throughout development. Our longitudinal findings further refined this developmental picture by indicating that conversely, patients experiencing a cognitive degradation show a lack of age-related changes in the splenium of the corpus callosum. Thus, these results confirm our hypothesis suggesting that cognitive decline is associated with deviant developmental trajectories of white matter microstructure. As such, white matter alterations in the splenium of the corpus callosum might provide a useful anatomical marker for conversion to psychosis and may potentially reflect early neurobiological alterations underlying the emergence of the illness.

4.2.3 The UHR status is associated with deviant developmental trajectories of the corpus callosum and the cingulum

When classifying subjects based on the UHR criteria (i.e., when comparing patients with 22q11.2DS who fulfilled the UHR criteria for at least one of their assessments, versus those who never qualified as UHR), results again yielded a significant interaction effect for FA in the FMAJ. An additional interaction effect was also observed for AD in the left CAB. More specifically, FA in the FMAJ followed a similar trajectory in UHR and non-UHR patients until late adolescence; after this stage however, they became increasingly divergent (Figure 3.10). Indeed, in non-UHR individuals, the trajectory followed a pattern similar to normative development of FA for this tract, as levels of FA reached a peak around 20 years and then gradually decreased. By contrast, UHR individuals showed abnormal age-related changes, as FA followed a constant increase into adulthood for this group.

Regarding the left CAB, AD showed slowly declining values in non-UHR subjects, whereas UHR patients initially showed lower values of AD but followed gradual increases, resulting in higher AD values starting from late adolescence (Figure 3.10). Thus, our results suggest that individuals qualifying for the UHR diagnosis at least once during their development are characterized by altered maturational trajectories of commissural and limbic connections.

Our findings are in partial alignment with other DTI studies investigating the relationship between prodromal psychotic symptoms and white matter in patients with 22q11.2DS. Indeed, while significant group differences were found in the splenium of the corpus callosum (Kikinis et al., 2017) and the cingulum (Padula et al., 2017; Roalf et al., 2017), studies also reported group differences in multiple fronto-temporal tracts which were not significant in the current study. Moreover, alterations were not observed in the same DTI metrics as our study. Thus, our results partially confirm our initial hypothesis, which was based on existing literature in 22q11.2DS. Indeed, we could confirm structural alterations in limbic and commissural tracts for patients at UHR, but fronto-temporal tracts were not

associated with any alterations in our study.

However, two major differences between the design of the above-mentioned studies and ours could explain the difference in results. First, these studies were cross-sectional, whereas we used a longitudinal design to delineate white matter integrity. While cross-sectional designs may still provide valuable information regarding the nature of group differences, results should be interpreted with some caution, as correlations may significantly vary depending on the age ranges included in the tested sample and may thus not necessarily truthfully reflect the underlying neurodevelopmental process (Kraemer et al., 2000). Second, previous studies used less standardized criteria for the categorization of patients. Indeed, while our study used the well-defined UHR criteria, previous investigations distinguished different subgroups of patients based merely on the severity of positive symptoms (where a subject was considered “at high risk of psychosis” when presenting a score higher than 3 in one of the 5 positive symptoms scales), without any consideration of the frequency and duration of symptoms (which are assessed in the UHR diagnosis). However, especially in the context of a longitudinal study, the inclusion of temporal aspects of the symptomatology is of the essence, as an extended presence of abnormal behavior is more likely related to long-term neuroanatomical anomalies.

Surprisingly, when considering findings in high risk patients of the general population, our finding of increased FA in the FMAJ departs from the most consistent findings in non-deleted UHR patients. Indeed, in non-deleted UHR patients, most studies report reduced levels of FA in several long association tracts, the cingulum, the stria terminalis, the internal and capsules, the corona radiata and the corpus callosum (reviewed in Canu et al., 2015). However, at later stages of the disease, results are more heterogeneous, as reduced levels of FA have been extensively highlighted in patients with first episode psychosis and chronic schizophrenia, but multiple studies also reported increased FA in several white matter tracts, including interhemispheric tracts (Canu et al., 2015). Thus, it is possible that, due to the deletion, patients with 22q11.2DS fulfilling the UHR criteria show more pronounced alterations at early stages of the illness compared to patients of the general population. However, we cannot discard the possibility that pathways leading to psychosis follow distinct patterns in the general population and in 22q11.2DS.

Regarding AD, although this metric has rarely been studied in the UHR population or in chronic idiopathic schizophrenia, evidence suggests that both early and advanced stages of the illness are associated with increased values of AD in several tracts and regions, including clusters of adjacent to the middle temporal gyrus which could include the CAB (Bakker et al., 2016; Fitzsimmons et al., 2013). The present findings may provide a refinement of this picture, where neurodevelopmental anomalies of AD are localized to the cingulum and start to show increased values starting from late adolescence only.

Of note, after removing patients older than 28 years in the non-UHR group as these were considered possible outliers, differences remained significant for the FMAJ but not for the left CAB. As such, results regarding the cingulum should be considered with caution, as patients assessed after 28 years may have driven the observed group differences.

The association of UHR diagnosis and deviant development of the FMAJ, however, is a robust finding that may represent a valuable biomarker of early stages of psychosis.

Importantly, on a more global level, both risk factors (cognitive decline and UHR status) share a common involvement of the splenium of the corpus callosum. Deviant developmental trajectories in this tract thus represent strong candidate biomarkers for conversion to psychosis on a neuroanatomical level. Moreover, this finding provides further evidence for the neurodevelopmental nature of schizophrenia, and supports the disconnection hypothesis suggesting that the illness is related to aberrant connectivity of cortical areas.

4.2.4 Limitations

In this section, we discuss the main limitations of this study.

Firstly, despite the relatively high sample size, it included a limited number of subjects with more than two time points ($n = 20$) and did not capture early childhood (i.e., before 5 years old) and later stages of adulthood (i.e., after 35 years old). Indeed, while our results consistently indicate identical developmental curves both for 22q11.2DS and TD controls, this does not exclude the possibility that when considering even larger ranges of the life span, differential trajectories would emerge. For instance, extensive white matter maturational processes are known to occur during the first months and years after birth (Gao et al., 2009; Mukherjee et al., 2002; Schneider et al., 2004) and these early changes could potentially be the origin of the subsequent, relatively persistent alterations observed in 22q11.2DS. Similarly, during adulthood and aging, white matter is also known to undergo some specific structural modifications (Lebel et al., 2012). It is not impossible that individuals with 22q11.2DS show differential patterns of aging that we were unable to capture in the present study, especially given that some of the white matter tracts reach their maturation peak only around the mid-30s, which corresponds to the oldest subjects of our study. Future investigations should thus include a longitudinal follow-up of younger, as well as older participants, in order to better characterize the corresponding developmental events.

Moreover, sample sizes were reduced for the characterization of developmental trajectories associated with risk factors for psychosis ($N = 49$ for the cognitive decline analysis; $N = 80$ for the UHR analysis), and our sample comprised a relatively restricted number of patients qualifying for the UHR status ($N = 17$), which may have reduced statistical power for the corresponding statistical analyses. In addition, while UHR criteria are well standardized and widely used, the UHR population still represents a heterogeneous group in terms of outcome. Indeed, around 30-40% of individuals (with or without 22q11.2DS) meeting the UHR criteria convert to psychosis (Schneider et al., 2016; Schultze-Lutter et al., 2015), but around 50% of UHR patients will remit (Addington et al., 2011). In the current study for instance, individuals with 22q11.2DS presented various psychiatric outcomes, as 3 were initially non-UHR and converted to UHR at later time points, 5 were initially UHR but remitted at later time points, 2 remained UHR across all as-

assessments, and 2 converted to psychosis (among whom one being initially UHR, and the other one initially non-UHR). However, due to the small sizes of these subgroups, their neuroanatomical trajectories could not be investigated in the present study. Evidence from a study investigating non-deleted patients provided preliminary evidence suggesting that white matter followed distinct developmental pathways depending on the outcome (Carletti et al., 2012). Thus, it is important that future studies including larger samples are conducted in order to better characterize the developmental trajectories of UHR individuals with different outcomes. It is likely that the subgroup of subjects converting to psychosis will demonstrate a pattern of deviant white matter development, while patients who remain at high risk or remit will show milder forms, or even an absence of anomalies.

A next limitation arises from the fact that individuals with 22q11.2DS often show relatively high levels of anxiety (Gothelf et al., 2007), which implies that MRI acquisitions were sometimes impossible, or yielded images of poor quality due to agitation during the scan. As a result, a certain number of patients could not be included in this study, which reduced the statistical power and may potentially have affected our results.

Furthermore, potential confounds can arise from medication, given that a substantial amount of patients with 22q11.2DS received medication during the studied developmental period (see 2.1). Drug administration during variable periods of development may indeed affect neuroanatomical measures including DTI metrics.

Patients with 22q11.2DS are also characterized by high levels of comorbidity, with frequent co-occurrences of psychotic disorders, mood disorders and/or anxiety disorders (Schneider et al., 2014a). As these psychiatric disorders have been associated with white matter alterations (Ayling et al., 2012; Brühl et al., 2014; Eng et al., 2015; Olvet et al., 2016; Sarrazin et al., 2014), their presence may represent a confounding factor.

Several limitations arise from TRACULA, the method used for tracts reconstruction. Indeed, this tractography tool overcomes the drawbacks of most other available methods due to its adapted longitudinal pipeline, its ability to avoid tracts misalignments and its sensitivity to variable diffusion values within tracts of interest. However, as this is a ROI-based method, TRACULA merely provides the possibility to study a predefined set of regions of interest (i.e., tracts) and is blind to any diffusion metrics located outside these areas. For instance, in 22q11.2DS, a recent machine-learning study has revealed the involvement of the extreme capsule and the middle longitudinal fasciculus (Tylee et al., 2017), two long-range tracts that are not reconstructed by TRACULA and are, more generally, not considered in other hypothesis-based DTI analysis methods. Moreover, in idiopathic schizophrenia, several post-mortem and DTI studies indicate that the illness is associated with abnormalities in short-range U-shaped fibers connecting adjacent gyri and local intraregional fibers (Akbarian et al., 1993; Eastwood and Harrison, 2005; Joshi et al., 2012; Nazeri et al., 2013). As short-range fibers have, to our knowledge, never been studied in 22q11.2DS, it would be important to identify alterations in this component of white matter for this population, and to determine whether these structures are involved in the neuroanatomical pathophysiology of psychosis.

Another limitation related to TRACULA is that prior to tracts reconstruction, the

longitudinal pipeline involves a robust rigid within-subject registration of all time points of a given subject, in order to create the within-subject template. Although the use of such as template is generally valid and provides considerable improvements regarding the reliability and sensitivity to changes, the current registration methods used for its creation are suboptimal in cases where intracranial volume, and thus the shape of tracts undergo extensive changes during the studied developmental period (Yendiki et al., 2016).

A final limitation of TRACULA lies in the fact that the processing involves several iterations of visual inspections to verify the quality of tracts reconstruction, making the analysis time consuming and prone to subjective interferences.

This study is further limited by aspects inherent to DTI image resolution, as DTI images provide information at a mm scale, and therefore do not contain information at the axonal (i.e., cellular) level (Mori et al., 2009) or even molecular level. As such, DTI studies can only formulate hypotheses regarding pathological mechanisms underlying the observed alterations of diffusion properties, but cannot provide direct causal inferences. Nevertheless, DTI studies currently represent one of the most powerful tools to assess white matter microstructural properties in humans *in vivo*, and results produced using this technique may provide crucial insights that will guide the development of animal study designs aiming at the identification of causal mechanisms underlying white matter anomalies.

Regarding diffusion metrics, the difficult interpretation of FA also brings some limitations. Indeed, both increased and decreased levels of FA have been related to pathological mechanisms, making this measure particularly ambiguous (Scariati et al., 2016). Interpretations thus extend in many different directions, starting with the most common proposal that FA is indicative of white matter integrity, to the suggestion that increased levels of FA could reflect abnormal decreases in axonal branching (Arlinghaus et al., 2011; Hoeft et al., 2007), or even the hypothesis that increased FA is resulting from flattened axonal bundles (Bode et al., 2011) or fewer arched fibers (Cheng et al., 2011). It thus becomes evident that the interpretation of FA alone is relatively precarious, and cannot really inform about the underlying microstructural properties related to a given disease. However, in the context of our study, this limitation was addressed through the consideration of other diffusion measures, particularly RD and AD, which provided the possibility to develop a more accurate understanding of microstructural abnormalities present throughout the development of individuals with 22q11.2DS.

Finally, the current study employed a univariate approach to study developmental characteristics of white matter microstructure in 22q11.2DS, investigating diffusion properties independently in every single tract. However, multivariate approaches combining diffusion metrics and white matter tracts may provide better characterizations of subtle or complex patterns of alterations (Tylee et al., 2017). Recently, even wider, multimodal multivariate techniques, using not only structural but also functional data, have demonstrated an accurate identification of pathological processes associated with 22q11.2DS or with psychotic symptoms, specifically (Padula et al., 2017). Nevertheless, although in-

herently univariate, mixed models currently represent the most advanced and strongly recommended tool for the analysis of developmental trajectories (Krueger and Tian, 2004; Locascio and Atri, 2011; Mills and Tamnes, 2014), making it the best suited tool for the analysis of longitudinal data.

CHAPTER 5

CONCLUSION

In summary, this study provided strong evidence that 22q11.2DS is associated with widespread developmental alterations in most white matter tracts and diffusion metrics, suggesting global disruptions of long-range communication. The direction of alterations systematically followed a pattern of reduced AD, RD and MD combined with increased FA in all tracts for patients with 22q11.2DS. In addition, 22q11.2DS and TD controls were characterized by similar developmental curves, with non-linear age-related changes for most tracts and DTI metrics. The persistent developmental gap observed in 22q11.2DS is likely resulting from both early and ongoing pathological mechanisms.

Moreover, this study provided preliminary evidence for the presence of deviant white matter developmental trajectories in commissural and limbic tracts for patients with 22q11.2DS at high risk of psychosis. In particular, abnormal development of the splenium of the corpus callosum was visible both in patients at UHR and in patients experiencing a cognitive decline. Thus, aberrant development in this tract represents a strong candidate biomarker for the prediction of psychosis. This neurodevelopmental marker may serve for the identification of populations in need of early intervention, but also for the development of pharmaceutical treatment targets. These findings also support the neurodevelopmental and dysconnectivity hypotheses of schizophrenia, where prodromal stages of the disease are associated with early alterations of structural connectivity.

Thus, the characterization of white matter development in the 22q11.2DS population and in subgroups of patients with risk factors of psychosis has provided valuable insights regarding the general neurodevelopmental profile of the syndrome, and regarding the neurodevelopmental pathways associated with early stages of schizophrenia. Yet, the neurobiological mechanisms underlying the observed developmental anomalies of white matter microstructure are still largely unknown. Future studies using animal models and post-mortem data should focus on the elucidation of processes responsible for disruptive white matter maturation. Another future line of research involves extensive longitudinal studies of white matter development, including large samples of patients with 22q11.2DS qualifying for the UHR status. Such studies would provide the opportunity to obtain a fine-

grained characterization of white matter development according to each clinical outcome (i.e., persisting UHR, remittent, or conversion to psychosis), and could further investigate the involvement of the splenium of the corpus callosum in the etiology of schizophrenia.

A.1 Supplementary material for the preliminary study

A.1.1 Annual percent change in 22q11.2DS and TD controls

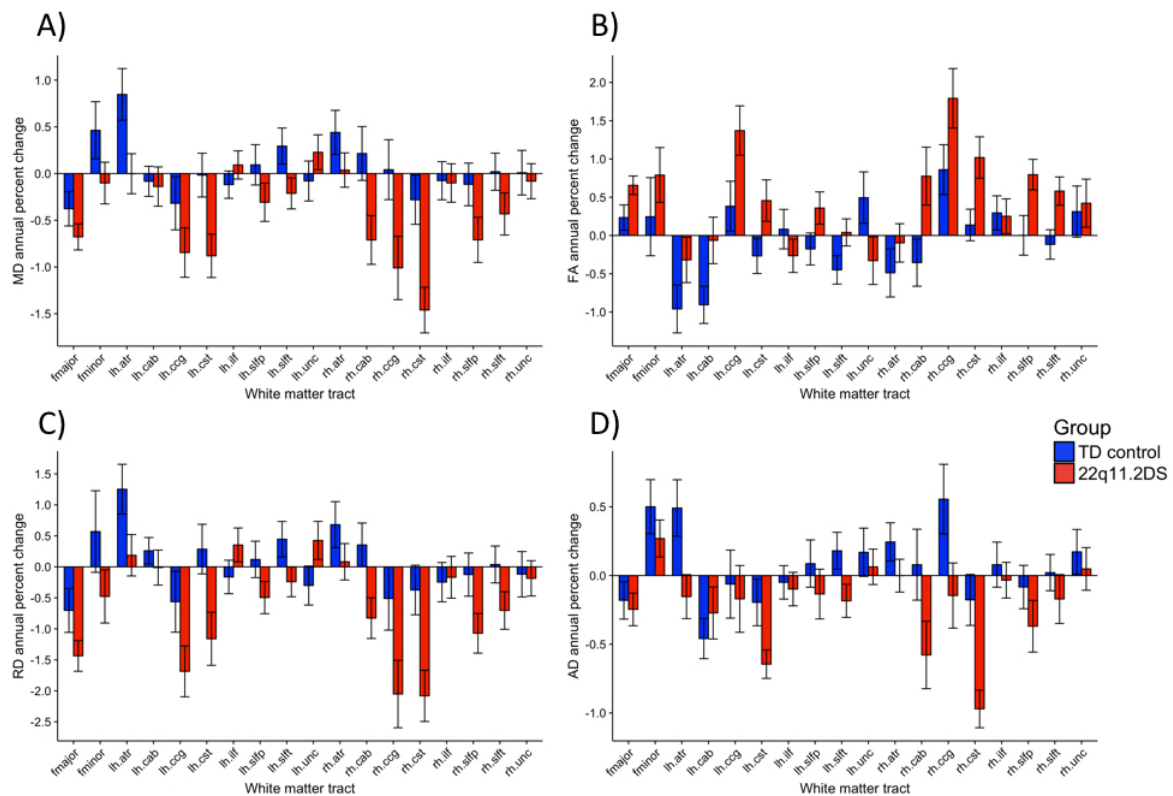


Figure A.1: Annual percent change (APC) is shown for MD (figure A), FA (figure B), RD (figure C) and AD (figure D), respectively. In each graph, the average APC is reported per group and for each white matter tract.

Legends: lh = left hemisphere; rh = right hemisphere; fmajor = forceps major; fminor = forceps minor; atr = anterior thalamic radiation; cab = cingulum, angular bundle; ccg = cingulum, cingulate bundle; cst = corticospinal tract; ilf = inferior longitudinal fasciculus; slfp = superior longitudinal fasciculus, parietal bundle; slft = superior longitudinal fasciculus, temporal bundle; unc = uncinatus fasciculus.

Tract type	Hem.	Tract	Mean Diffusivity		
			APC 22q11.2DS	APC TD controls	p- value
Projection	left	ATR	-0.002	0.847	0.124
	right	ATR	0.038	0.441	0.327
	left	CST	-0.881	-0.017	0.124
	right	CST	-1.461	-0.281	0.037
Commissural		FMAJ	-0.678	-0.377	0.356
		FMIN	-0.101	0.463	0.356
Association	left	CAB	-0.139	-0.083	0.356
	right	CAB	-0.711	0.215	0.124
	left	CCG	-0.846	-0.319	0.327
	right	CCG	-1.011	0.042	0.124
	left	ILF	0.092	-0.119	0.327
	right	ILF	-0.101	-0.076	0.882
	left	SLFP	-0.308	0.094	0.327
	right	SLFP	-0.71	-0.116	0.221
	left	SLFT	-0.213	0.295	0.124
	right	SLFT	-0.432	0.02	0.224
	left	UNC	0.228	-0.08	0.472
	right	UNC	-0.082	0.009	0.888

Table A.1: Mean annual percentage change (APC) of Mean Diffusivity in 22q11.2DS compared to TD controls. Significant group differences are indicated in bold. All p-values were corrected for multiple comparisons.

Tract type	Hem.	Tract	Axial Diffusivity		
			APC 22q11.2DS	APC TD controls	p- value
Projection	left	ATR	-0.154	0.491	0.184
	right	ATR	-0.001	0.245	0.542
	left	CST	-0.645	-0.196	0.187
	right	CST	-0.97	-0.177	0.011
Commissural		FMAJ	-0.247	-0.181	0.916
		FMIN	0.269	0.501	0.475
Association	left	CAB	-0.273	-0.459	0.807
	right	CAB	-0.578	0.079	0.187
	left	CCG	-0.17	-0.063	0.807
	right	CCG	-0.146	0.556	0.187
	left	ILF	-0.099	-0.05	0.763
	right	ILF	-0.034	0.079	0.834
	left	SLFP	-0.135	0.087	0.627
	right	SLFP	-0.369	-0.084	0.686
	left	SLFT	-0.184	0.18	0.227
	right	SLFT	-0.171	0.021	0.661
	left	UNC	0.063	0.169	0.763
	right	UNC	0.048	0.172	0.791

Table A.2: Mean annual percentage change (APC) of Axial Diffusivity in 22q11.2DS compared to TD controls. Significant group differences are indicated in bold. All p-values were corrected for multiple comparisons.

Tract type	Hem.	Tract	Radial Diffusivity			
			APC 22q11.2DS	APC controls	TD	p- value
Projection	left	ATR	0.187		1.253	0.17
	right	ATR	0.082		0.681	0.287
	left	CST	-1.16		0.286	0.112
	right	CST	-2.081		-0.374	0.069
Commissural		FMAJ	-1.437		-0.703	0.243
		FMIN	-0.478		0.57	0.287
Association	left	CAB	-0.012		0.261	0.261
	right	CAB	-0.827		0.354	0.123
	left	CCG	-1.686		-0.564	0.243
	right	CCG	-2.051		-0.511	0.184
	left	ILF	0.354		-0.163	0.261
	right	ILF	-0.169		-0.247	0.991
	left	SLFP	-0.495		0.12	0.243
	right	SLFP	-1.071		-0.125	0.17
	left	SLFT	-0.24		0.446	0.17
	right	SLFT	-0.704		0.039	0.17
	left	UNC	0.426		-0.301	0.264
	right	UNC	-0.185		-0.119	0.98

Table A.3: Mean annual percentage change (APC) of Radial Diffusivity in 22q11.2DS compared to TD controls. No significant group differences were evident in this measure. All p-values were corrected for multiple comparisons. All p-values were corrected for multiple comparisons.

Tract type	Hem.	Tract	Fractional Anisotropy			
			APC 22q11.2DS	APC controls	TD	p- value
Projection	left	ATR	-0.319		-0.959	0.215
	right	ATR	-0.097		-0.488	0.433
	left	CST	0.456		-0.267	0.151
	right	CST	1.019		0.138	0.081
Commissural		FMAJ	0.656		0.235	0.151
		FMIN	0.791		0.246	0.426
Association	left	CAB	-0.064		-0.906	0.151
	right	CAB	0.776		-0.355	0.125
	left	CCG	1.371		0.383	0.125
	right	CCG	1.793		0.86	0.199
	left	ILF	-0.265		0.083	0.464
	right	ILF	0.252		0.296	0.953
	left	SLFP	0.36		-0.176	0.167
	right	SLFP	0.796		0.002	0.111
	left	SLFT	0.041		-0.45	0.151
	right	SLFT	0.581		-0.117	0.081
	left	UNC	-0.329		0.495	0.151
	right	UNC	0.422		0.312	0.953

Table A.4: Mean annual percentage change (APC) of Fractional Anisotropy in 22q11.2DS compared to TD controls. No significant group differences were evident in this measure. All p-values were corrected for multiple comparisons.

A.1.2 Repeated measures ANOVA comparing 22q11.2DS and TD controls

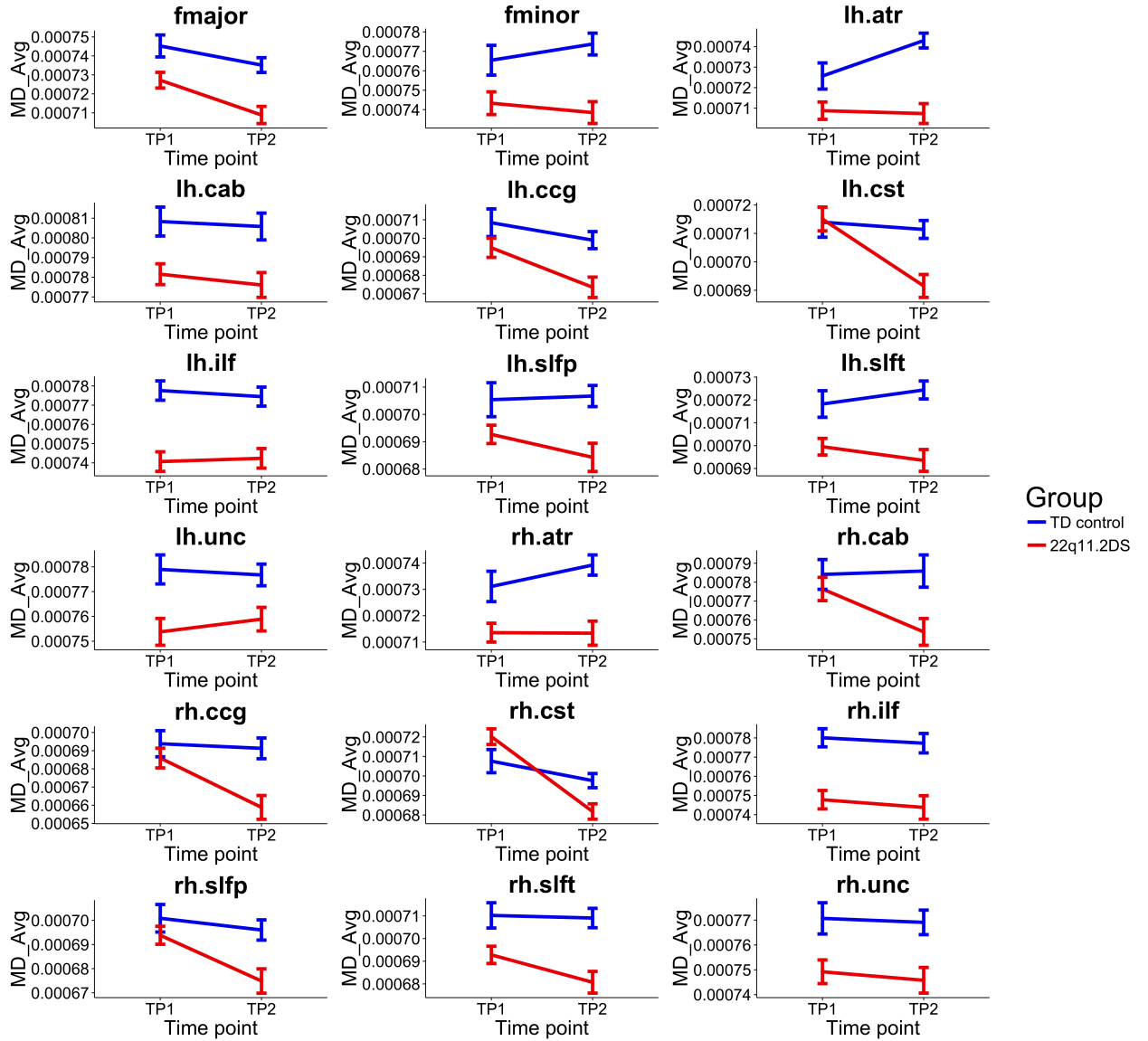


Figure A.2: Preliminary study ($N = 70$) - Repeated measures ANOVA results for Mean Diffusivity in each white matter tract.

Legends: lh = left hemisphere; rh = right hemisphere; fmajor = forceps major; fminor = forceps minor; atr = anterior thalamic radiation; cab = cingulum, angular bundle; ccg = cingulum, cingulate bundle; cst = corticospinal tract; ilf = inferior longitudinal fasciculus; slfp = superior longitudinal fasciculus, parietal bundle; slft = superior longitudinal fasciculus, temporal bundle; unc = uncinate fasciculus.

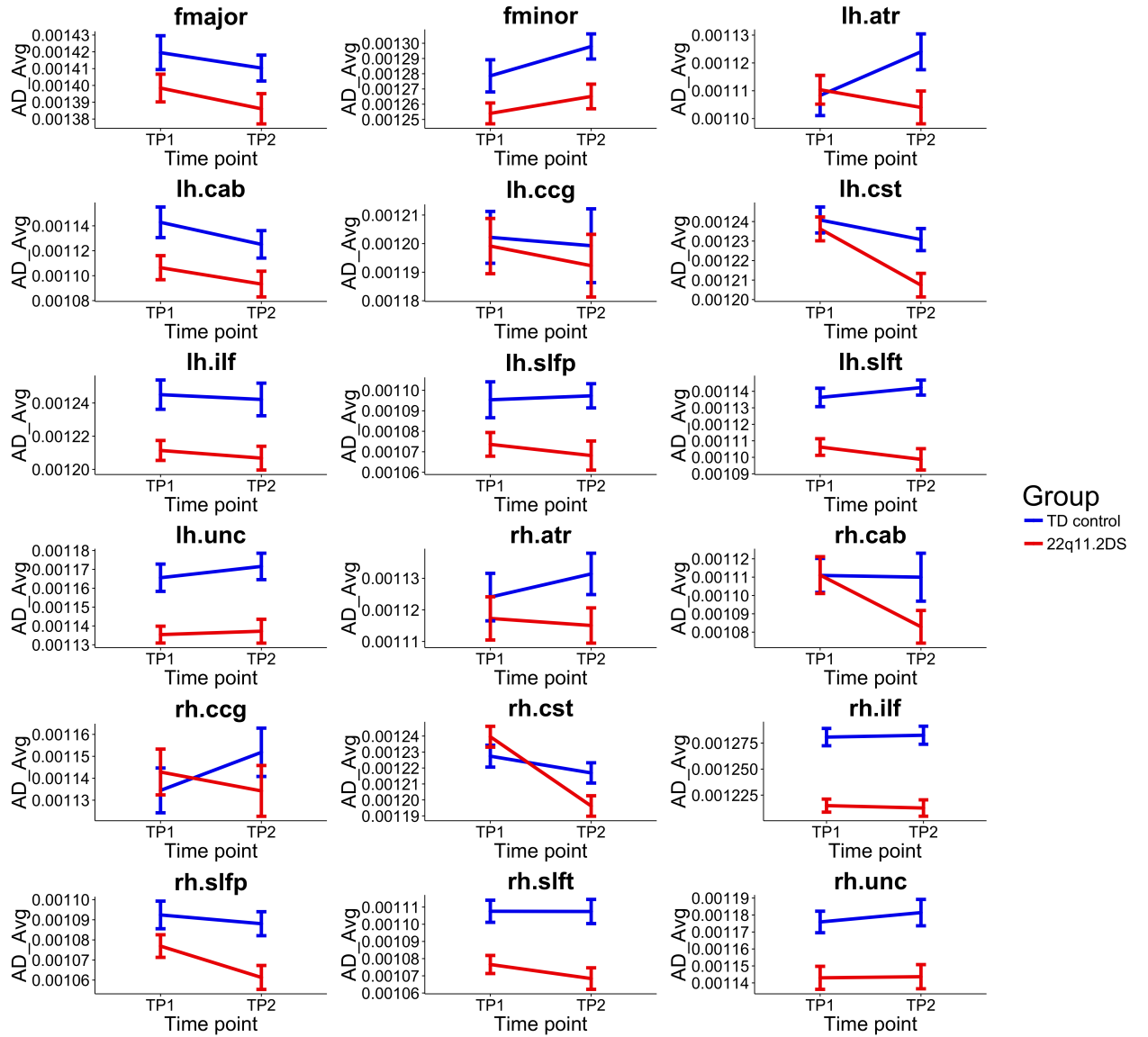


Figure A.3: Preliminary study ($N = 70$) - Repeated measures ANOVA results for Axial Diffusivity in each white matter tract.

Legends: lh = left hemisphere; rh = right hemisphere; fmajor = forceps major; fminor = forceps minor; atr = anterior thalamic radiation; cab = cingulum, angular bundle; ccg = cingulum, cingulate bundle; cst = corticospinal tract; ilf = inferior longitudinal fasciculus; slfp = superior longitudinal fasciculus, parietal bundle; slft = superior longitudinal fasciculus, temporal bundle; unc = uncinatus fasciculus.

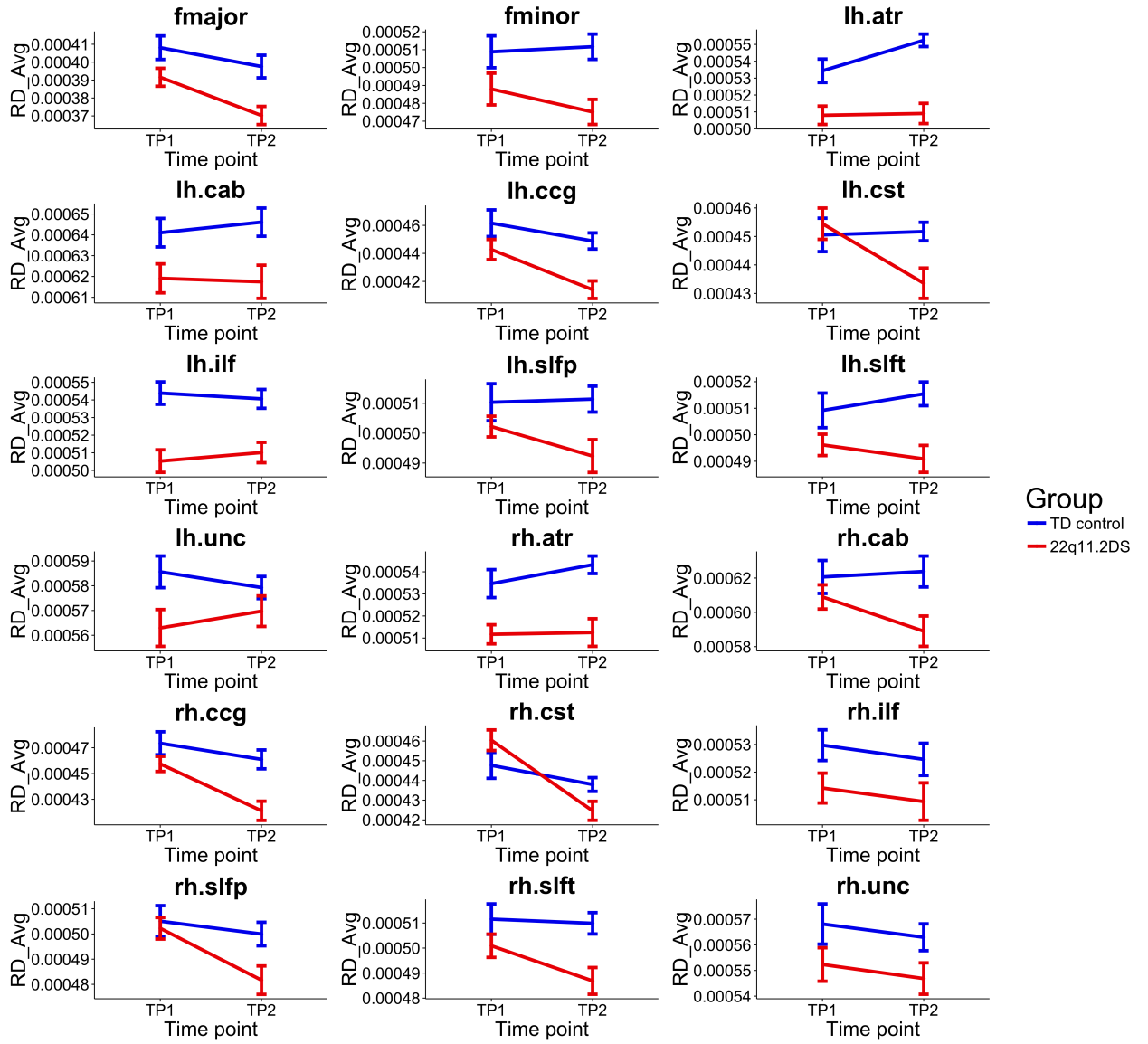


Figure A.4: Preliminary study ($N = 70$) - Repeated measures ANOVA results for Radial Diffusivity in each white matter tract.

Legends: lh = left hemisphere; rh = right hemisphere; fmajor = forceps major; fminor = forceps minor; atr = anterior thalamic radiation; cab = cingulum, angular bundle; ccg = cingulum, cingulate bundle; cst = corticospinal tract; ilf = inferior longitudinal fasciculus; slfp = superior longitudinal fasciculus, parietal bundle; slft = superior longitudinal fasciculus, temporal bundle; unc = uncinate fasciculus.

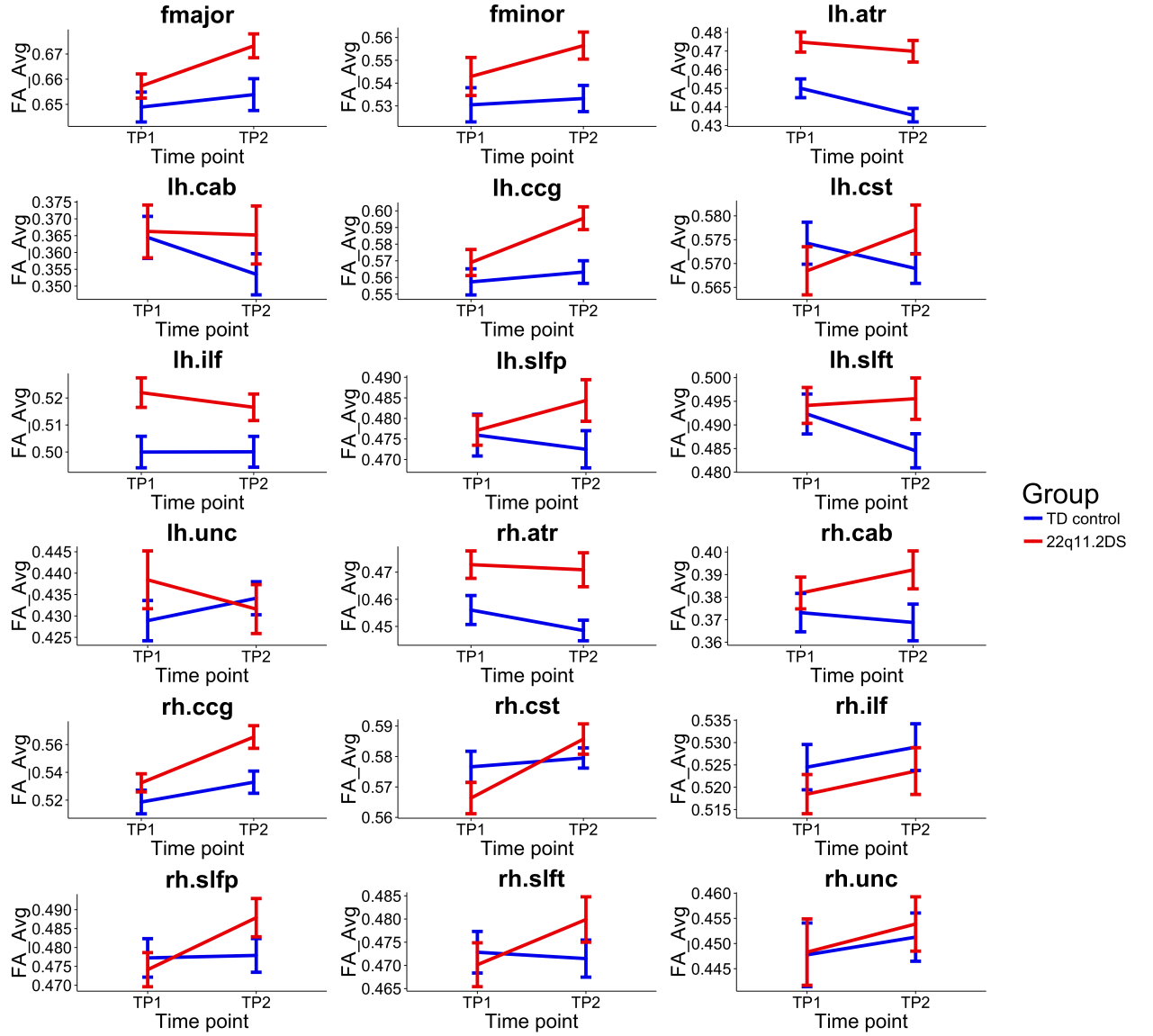


Figure A.5: Preliminary study ($N = 70$) - Repeated measures ANOVA results for Fractional Anisotropy in each white matter tract.

Legends: lh = left hemisphere; rh = right hemisphere; fmajor = forceps major; fminor = forceps minor; atr = anterior thalamic radiation; cab = cingulum, angular bundle; ccg = cingulum, cingulate bundle; cst = corticospinal tract; ilf = inferior longitudinal fasciculus; slfp = superior longitudinal fasciculus, parietal bundle; slft = superior longitudinal fasciculus, temporal bundle; unc = uncinatus fasciculus.

BIBLIOGRAPHY

- Aboitiz, F., Scheibel, A. B., Fisher, R. S., and Zaidel, E. (1992). Fiber composition of the human corpus callosum. *Brain Research*, 598(1):143–153.
- Addington, J., Cornblatt, B. A., Cadenhead, K. S., Cannon, T. D., McGlashan, T. H., Perkins, D. O., Seidman, L. J., Tsuang, M. T., Walker, E. F., Woods, S. W., and Heinssen, R. (2011). At Clinical High Risk for Psychosis: Outcome for Nonconverters. *American Journal of Psychiatry*, 168(8):800–805.
- Akbarian, S., Bunney, W. E., Potkin, S. G., Wigal, S. B., Hagman, J. O., Sandman, C. A., and Jones, E. G. (1993). Altered distribution of nicotinamide-adenine dinucleotide phosphate—diaphorase cells in frontal lobe of schizophrenics implies disturbances of cortical development. *Archives of general psychiatry*, 50(3):169–177.
- American Psychiatric Association (2013). *Diagnostic and statistical manual of mental disorders (DSM-5®)*. American Psychiatric Pub.
- Arciniegas, D. B. (2015). Psychosis. *Continuum : Lifelong Learning in Neurology*, 21(3 Behavioral Neurology and Neuropsychiatry):715–736.
- Arinami, T., Ohtsuki, T., Takase, K., Shimizu, H., Yoshikawa, T., Horigome, H., Nakayama, J., and Toru, M. (2001). Screening for 22q11 deletions in a schizophrenia population. *Schizophrenia Research*, 52(3):167–170.
- Arlinghaus, L. R., Thornton-Wells, T. A., Dykens, E. M., and Anderson, A. W. (2011). Alterations in diffusion properties of white matter in Williams syndrome. *Magnetic Resonance Imaging*, 29(9):1165–1174.
- Ashburner, J. and Friston, K. J. (2000). Voxel-Based Morphometry—The Methods. *NeuroImage*, 11(6):805–821.
- Ashburner, J. and Friston, K. J. (2001). Why Voxel-Based Morphometry Should Be Used. *NeuroImage*, 14(6):1238–1243.
- Ayling, E., Aghajani, M., Fouche, J.-P., and Wee, N. v. d. (2012). Diffusion Tensor Imaging in Anxiety Disorders. *Current Psychiatry Reports*, 14(3):197–202.
- Azuma, R., Daly, E. M., Campbell, L. E., Stevens, A. F., Deeley, Q., Giampietro, V., Brammer, M. J., Glaser, B., Ambery, F. Z., Morris, R. G., Williams, S. C. R., Owen, M. J., Murphy, D. G. M., and Murphy, K. C. (2009). Visuospatial working memory in children and adolescents with 22q11.2 deletion syndrome; an fMRI study. *Journal of Neurodevelopmental Disorders*, 1(1):46.
- Bach, M., Laun, F. B., Leemans, A., Tax, C. M. W., Biessels, G. J., Stieltjes, B., and Maier-Hein, K. H. (2014). Methodological considerations on tract-based spatial statistics (TBSS). *NeuroImage*, 100:358–369.
- Baker, K., Chaddock, C. A., Baldeweg, T., and Skuse, D. (2011). Neuroanatomy in adolescents and young adults with 22q11 Deletion Syndrome: Comparison to an IQ-matched group. *NeuroImage*, 55(2):491–499.

- Bakker, G., Caan, M. W. A., Schluter, R. S., Bloemen, O. J. N., da Silva-Alves, F., de Koning, M. B., Boot, E., Vingerhoets, W. A. M., Nieman, D. H., de Haan, L., Booij, J., and van Amelsvoort, T. A. M. J. (2016). Distinct white-matter aberrations in 22q11.2 deletion syndrome and patients at ultra-high risk for psychosis. *Psychological Medicine*, 46(11):2299–2311.
- Barnea-Goraly, N., Menon, V., Krasnow, B., Ko, A., Reiss, A., and Eliez, S. (2003). Investigation of White Matter Structure in Velocardiofacial Syndrome: A Diffusion Tensor Imaging Study. *American Journal of Psychiatry*, 160(10):1863–1869.
- Basser, P. J., Mattiello, J., and LeBihan, D. (1994). MR diffusion tensor spectroscopy and imaging. *Biophysical Journal*, 66(1):259–267.
- Bassett, A. S. and Chow, E. W. C. (1999). 22q11 deletion syndrome: a genetic subtype of schizophrenia. *Biological Psychiatry*, 46(7):882–891.
- Bassett, A. S., McDonald-McGinn, D. M., Devriendt, K., Digilio, M. C., Goldenberg, P., Habel, A., Marino, B., Oskarsdottir, S., Philip, N., Sullivan, K., Swillen, A., and Vorstman, J. (2011). Practical Guidelines for Managing Patients with 22q11.2 Deletion Syndrome. *The Journal of Pediatrics*, 159(2):332–339.e1.
- Baumann, N. and Pham-Dinh, D. (2001). Biology of Oligodendrocyte and Myelin in the Mammalian Central Nervous System. *Physiological Reviews*, 81(2):871–927.
- Bava, S., Thayer, R., Jacobus, J., Ward, M., Jernigan, T. L., and Tapert, S. F. (2010). Longitudinal characterization of white matter maturation during adolescence. *Brain Research*, 1327:38–46.
- Behrens, T. E. J., Berg, H. J., Jbabdi, S., Rushworth, M. F. S., and Woolrich, M. W. (2007). Probabilistic diffusion tractography with multiple fibre orientations: What can we gain? *NeuroImage*, 34(1):144–155.
- Behrens, T. E. J., Woolrich, M. W., Jenkinson, M., Johansen-Berg, H., Nunes, R. G., Clare, S., Matthews, P. M., Brady, J. M., and Smith, S. M. (2003). Characterization and propagation of uncertainty in diffusion-weighted MR imaging. *Magnetic Resonance in Medicine*, 50(5):1077–1088.
- Bendlin, B. B., Fitzgerald, M. E., Ries, M. L., Xu, G., Kastman, E. K., Thiel, B. W., Rowley, H. A., Lazar, M., Alexander, A. L., and Johnson, S. C. (2010). White Matter in Aging and Cognition: A Cross-Sectional Study of Microstructure in Adults Aged Eighteen to Eighty-Three. *Developmental Neuropsychology*, 35(3):257–277.
- Benjamini, Y. and Hochberg, Y. (1995). Controlling the False Discovery Rate: A Practical and Powerful Approach to Multiple Testing. *Journal of the Royal Statistical Society. Series B (Methodological)*, 57(1):289–300.
- Biomarkers Definitions Working Group. (2001). Biomarkers and surrogate endpoints: preferred definitions and conceptual framework. *Clinical Pharmacology and Therapeutics*, 69(3):89–95.
- Blouin, J.-L., Dombroski, B. A., Nath, S. K., Lasseter, V. K., Wolyniec, P. S., Nestadt, G., Thornquist, M., Ullrich, G., McGrath, J., Kasch, L., Lamacz, M., Thomas, M. G., Gehrig, C., Radhakrishna, U., Snyder, S. E., Balk, K. G., Neufeld, K., Swartz, K. L., DeMarchi, N., Papadimitriou, G. N., Dikeos, D. G., Stefanis, C. N., Chakravarti, A., Childs, B., Housman, D. E., Kazazian, H. H., Antonarakis, S. E., and Pulver, A. E. (1998). Schizophrenia susceptibility loci on chromosomes 13q32 and 8p21. *Nature Genetics*, 20(1):70–73.
- Bode, M. K., Mattila, M.-L., Kiviniemi, V., Rahko, J., Moilanen, I., Ebeling, H., Tervonen, O., and Nikkinen, J. (2011). White matter in autism spectrum disorders – evidence of impaired fiber formation. *Acta Radiologica*, 52(10):1169–1174.
- Bookstein, F. L. (2001). “Voxel-Based Morphometry” Should Not Be Used with Imperfectly Registered Images. *NeuroImage*, 14(6):1454–1462.
- Bostelmann, M., Schneider, M., Padula, M. C., Maeder, J., Schaer, M., Scariati, E., Deb-

- bané, M., Glaser, B., Menghetti, S., and Eliez, S. (2016). Visual memory profile in 22q11.2 microdeletion syndrome: are there differences in performance and neurobiological substrates between tasks linked to ventral and dorsal visual brain structures? A cross-sectional and longitudinal study. *Journal of Neurodevelopmental Disorders*, 8:41.
- Brouwer, R. M., Mandl, R. C. W., Schnack, H. G., Soelen, I. L. C. v., Baal, G. C. v., Peper, J. S., Kahn, R. S., Boomsma, D. I., and Pol, H. E. H. (2012). White Matter Development in Early Puberty: A Longitudinal Volumetric and Diffusion Tensor Imaging Twin Study. *PLOS ONE*, 7(4):e32316.
- Brühl, A. B., Delsignore, A., Komossa, K., and Weidt, S. (2014). Neuroimaging in social anxiety disorder—A meta-analytic review resulting in a new neurofunctional model. *Neuroscience & Biobehavioral Reviews*, 47:260–280.
- Budde, M. D., Xie, M., Cross, A. H., and Song, S.-K. (2009). Axial Diffusivity Is the Primary Correlate of Axonal Injury in the Experimental Autoimmune Encephalomyelitis Spinal Cord: A Quantitative Pixelwise Analysis. *Journal of Neuroscience*, 29(9):2805–2813.
- Budel, S., Padukkavidana, T., Liu, B. P., Feng, Z., Hu, F., Johnson, S., Lauren, J., Park, J. H., McGee, A. W., Liao, J., Stillman, A., Kim, J.-E., Yang, B.-Z., Sodi, S., Gelernter, J., Zhao, H., Hisama, F., Arnsten, A. F. T., and Strittmatter, S. M. (2008). Genetic Variants of Nogo-66 Receptor with Possible Association to Schizophrenia Block Myelin Inhibition of Axon Growth. *Journal of Neuroscience*, 28(49):13161–13172.
- Burdach, K. F. (1819). 1826. *Vom Baue und Leben des Gehirns. Leipzig (Germany): Dyk.*
- Campbell, L. E., Azuma, R., Ambery, F., Stevens, A., Smith, A., Morris, R. G., Murphy, D. G., and Murphy, K. C. (2010). Executive Functions and Memory Abilities in Children With 22q11.2 Deletion Syndrome. *Australian & New Zealand Journal of Psychiatry*, 44(4):364–371.
- Canu, E., Agosta, F., and Filippi, M. (2015). A selective review of structural connectivity abnormalities of schizophrenic patients at different stages of the disease. *Schizophrenia Research*, 161(1):19–28.
- Carletti, F., Woolley, J. B., Bhattacharyya, S., Perez-Iglesias, R., Poli, P. F., Valmaggia, L., Broome, M. R., Bramon, E., Johns, L., Giampietro, V., and others (2012). Alterations in white matter evident before the onset of psychosis. *Schizophrenia bulletin*, 38(6):1170–1179.
- Caruana, E. J., Roman, M., Hernández-Sánchez, J., and Solli, P. (2015). Longitudinal studies. *Journal of Thoracic Disease*, 7(11):E537–E540.
- Cayler, G. G. (1969). Cardiofacial syndrome. Congenital heart disease and facial weakness, a hitherto unrecognized association. *Archives of Disease in Childhood*, 44(233):69–75.
- Cheng, Y., Chou, K.-H., Fan, Y.-T., and Lin, C.-P. (2011). ANS: Aberrant Neurodevelopment of the Social Cognition Network in Adolescents with Autism Spectrum Disorders. *PLoS ONE*, 6(4):e18905.
- da Silva Alves, F., Schmitz, N., Bloemen, O., van der Meer, J., Meijer, J., Boot, E., Nederveen, A., de Haan, L., Linszen, D., and van Amelsvoort, T. (2011). White matter abnormalities in adults with 22q11 deletion syndrome with and without schizophrenia. *Schizophrenia Research*, 132(1):75–83.
- Davatzikos, C. (2004). Why voxel-based morphometric analysis should be used with great caution when characterizing group differences. *NeuroImage*, 23(1):17–20.
- de Schotten, M. T. d., ffytche, D. H., Bizzi, A., Dell’Acqua, F., Allin, M., Walshe, M., Murray, R., Williams, S. C., Murphy, D. G. M., and Catani, M. (2011). Atlasing location, asymmetry and inter-subject variability of white matter tracts in the human brain with MR diffusion tractography. *NeuroImage*, 54(1):49–59.
- Dejerine, J. and Dejerine-Klumpke, A. (1895). *Anatomie des centres nerveux*, volume 1. Rueff.

- Deng, Y., Goodrich-Hunsaker, N. J., Cabaral, M., Amaral, D. G., Buonocore, M. H., Harvey, D., Kalish, K., Carmichael, O. T., Schumann, C. M., Lee, A., Dougherty, R. F., Perry, L. M., Wandell, B. A., and Simon, T. J. (2015). Disrupted fornix integrity in children with chromosome 22q11.2 deletion syndrome. *Psychiatry Research: Neuroimaging*, 232(1):106–114.
- Di George, A. M. (1965). Discussion on: A new concept of the cellular basis of immunity by Cooper M.D, Peterson R.D. and Good, R.A. *Cas. Lek. Cesk.*, 67(5):907–908.
- Driscoll, D. A., Budarf, M. L., and Emanuel, B. S. (1992). A genetic etiology for DiGeorge syndrome: consistent deletions and microdeletions of 22q11. *American journal of human genetics*, 50(5):924.
- Dyrby, T. B., Sogaard, L. V., Parker, G. J., Alexander, D. C., Lind, N. M., Baaré, W. F. C., Hay-Schmidt, A., Eriksen, N., Pakkenberg, B., Paulson, O. B., and Jelsing, J. (2007). Validation of in vitro probabilistic tractography. *NeuroImage*, 37(4):1267–1277.
- Eastwood, S. L. and Harrison, P. J. (2005). Interstitial white matter neuron density in the dorsolateral prefrontal cortex and parahippocampal gyrus in schizophrenia. *Schizophrenia Research*, 79(2):181–188.
- Eliez, S., Schmitt, J. E., White, C. D., and Reiss, A. L. (2000). Children and adolescents with velocardiofacial syndrome: a volumetric MRI study. *American Journal of Psychiatry*, 157(3):409–415.
- Eng, G. K., Sim, K., and Chen, S.-H. A. (2015). Meta-analytic investigations of structural grey matter, executive domain-related functional activations, and white matter diffusivity in obsessive compulsive disorder: An integrative review. *Neuroscience & Biobehavioral Reviews*, 52:233–257.
- First, M. (1996). *Structured clinical interview for the DSM-IV-TR axis I disorders (SCID-I)*. Biometrics Research, New York State Psychiatric Institute, New York.
- Fitzmaurice, G., Davidian, M., Verbeke, G., and Molenberghs, G. (2008). *Longitudinal Data Analysis*. CRC Press. Google-Books-ID: zVBjCvQCoGQC.
- Fitzsimmons, J., Kubicki, M., and Shenton, M. E. (2013). Review of functional and anatomical brain connectivity findings in schizophrenia:. *Current Opinion in Psychiatry*, 26(2):172–187.
- Fornito, A., Zalesky, A., Pantelis, C., and Bullmore, E. T. (2012). Schizophrenia, neuroimaging and connectomics. *NeuroImage*, 62(4):2296–2314.
- Fournier, A. E., GrandPre, T., and Strittmatter, S. M. (2001). Identification of a receptor mediating Nogo-66 inhibition of axonal regeneration. *Nature*, 409(6818):341–346.
- Fusar-Poli, P., Bonoldi, I., Yung, A. R., Borgwardt, S., Kempton, M. J., Valmaggia, L., Barale, F., Caverzasi, E., and McGuire, P. (2012). Predicting Psychosis: Meta-analysis of Transition Outcomes in Individuals at High Clinical Risk. *Archives of General Psychiatry*, 69(3):220–229.
- Fusar-Poli, P., Borgwardt, S., Bechdolf, A., Addington, J., Riecher-Rössler, A., Schultze-Lutter, F., Keshavan, M., Wood, S., Ruhrmann, S., Seidman, L. J., Valmaggia, L., Cannon, T., Velthorst, E., Haan, L. D., Cornblatt, B., Bonoldi, I., Birchwood, M., McGlashan, T., Carpenter, W., McGorry, P., Klosterkötter, J., McGuire, P., and Yung, A. (2013). The Psychosis High-Risk State: A Comprehensive State-of-the-Art Review. *JAMA Psychiatry*, 70(1):107–120.
- Gao, W., Lin, W., Chen, Y., Gerig, G., Smith, J., Jewells, V., and Gilmore, J. (2009). Temporal and Spatial Development of Axonal Maturation and Myelination of White Matter in the Developing Brain. *American Journal of Neuroradiology*, 30(2):290–296.
- Gothelf, D., Eliez, S., Thompson, T., Hinard, C., Penniman, L., Feinstein, C., Kwon, H., Jin, S., Jo, B., and Antonarakis, S. E. (2005). COMT genotype predicts longitudinal cognitive decline and psychosis in 22q11. 2 deletion syndrome. *Nature neuroscience*, 8(11):1500.

- Gothelf, D., Hoefft, F., Ueno, T., Sugiura, L., Lee, A. D., Thompson, P., and Reiss, A. L. (2011). Developmental changes in multivariate neuroanatomical patterns that predict risk for psychosis in 22q11.2 deletion syndrome. *Journal of Psychiatric Research*, 45(3):322–331.
- Gothelf, D., Penniman, L., Gu, E., Eliez, S., and Reiss, A. (2007). Developmental trajectories of brain structure in adolescents with 22q11.2 deletion syndrome: A longitudinal study. *Schizophrenia Research*, 96(1-3):72–81.
- Gothelf, D., Schaer, M., and Eliez, S. (2008). Genes, brain development and psychiatric phenotypes in velo-cardio-facial syndrome. *Developmental Disabilities Research Reviews*, 14(1):59–68.
- Gothelf, D., Schneider, M., Green, T., Debbané, M., Frisch, A., Glaser, B., Zilkha, H., Schaer, M., Weizman, A., and Eliez, S. (2013). Risk Factors and the Evolution of Psychosis in 22q11.2 Deletion Syndrome: A Longitudinal 2-Site Study. *Journal of the American Academy of Child & Adolescent Psychiatry*, 52(11):1192–1203.e3.
- Green, T., Gothelf, D., Glaser, B., Debbane, M., Frisch, A., Kotler, M., Weizman, A., and Eliez, S. (2009). Psychiatric Disorders and Intellectual Functioning Throughout Development in Velocardiofacial (22q11.2 Deletion) Syndrome. *Journal of the American Academy of Child & Adolescent Psychiatry*, 48(11):1060–1068.
- Hagmann, P., Jonasson, L., Maeder, P., Thiran, J.-P., Wedeen, V. J., and Meuli, R. (2006). Understanding Diffusion MR Imaging Techniques: From Scalar Diffusion-weighted Imaging to Diffusion Tensor Imaging and Beyond. *RadioGraphics*, 26(suppl_1):S205–S223.
- Harsan, L. A., Poulet, P., Guignard, B., Steibel, J., Parizel, N., Sousa, P. L. d., Boehm, N., Grucker, D., and Ghandour, M. S. (2006). Brain dysmyelination and recovery assessment by noninvasive in vivo diffusion tensor magnetic resonance imaging. *Journal of Neuroscience Research*, 83(3):392–402.
- Hecke, W. V., Leemans, A., Backer, S. D., Jeurissen, B., Parizel, P. M., and Sijbers, J. (2010). Comparing isotropic and anisotropic smoothing for voxel-based DTI analyses: A simulation study. *Human Brain Mapping*, 31(1):98–114.
- Heuvel, M. P. v. d. and Fornito, A. (2014). Brain Networks in Schizophrenia. *Neuropsychology Review*, 24(1):32–48.
- Hoefft, F., Barnea-Goraly, N., Haas, B. W., Golarai, G., Ng, D., Mills, D., Korenberg, J., Bellugi, U., Galaburda, A., and Reiss, A. L. (2007). More Is Not Always Better: Increased Fractional Anisotropy of Superior Longitudinal Fasciculus Associated with Poor Visuospatial Abilities in Williams Syndrome. *Journal of Neuroscience*, 27(44):11960–11965.
- Hofer, S. and Frahm, J. (2006). Topography of the human corpus callosum revisited—Comprehensive fiber tractography using diffusion tensor magnetic resonance imaging. *NeuroImage*, 32(3):989–994.
- Insel, T. R. (2010). Rethinking schizophrenia. *Nature*, 468(7321):187–193.
- Jalbrzikowski, M., Villalon-Reina, J. E., Karlsgodt, K. H., Senturk, D., Chow, C., Thompson, P. M., and Bearden, C. E. (2014). Altered white matter microstructure is associated with social cognition and psychotic symptoms in 22q11.2 microdeletion syndrome. *Frontiers in Behavioral Neuroscience*, 8.
- Jones, D. K., Symms, M. R., Cercignani, M., and Howard, R. J. (2005). The effect of filter size on VBM analyses of DT-MRI data. *NeuroImage*, 26(2):546–554.
- Joshi, D., Fung, S. J., Rothwell, A., and Weickert, C. S. (2012). Higher Gamma-Aminobutyric Acid Neuron Density in the White Matter of Orbital Frontal Cortex in Schizophrenia. *Biological Psychiatry*, 72(9):725–733.
- Kahn, R. S. and Keefe, R. S. E. (2013). Schizophrenia Is a Cognitive Illness: Time for a Change in Focus. *JAMA Psychiatry*, 70(10):1107–1112.

- Karayiorgou, M. and Gogos, J. A. (2004). The molecular genetics of the 22q11-associated schizophrenia. *Molecular Brain Research*, 132(2):95–104.
- Karayiorgou, M., Morris, M. A., Morrow, B., Shprintzen, R. J., Goldberg, R., Borrow, J., Gos, A., Nestadt, G., Wolynec, P. S., and Lasseter, V. K. (1995). Schizophrenia susceptibility associated with interstitial deletions of chromosome 22q11. *Proceedings of the National Academy of Sciences*, 92(17):7612–7616.
- Karayiorgou, M., Simon, T. J., and Gogos, J. A. (2010). 22q11.2 microdeletions: linking DNA structural variation to brain dysfunction and schizophrenia. *Nature Reviews Neuroscience*, 11(6):402–416.
- Karlsgodt, K. H., Niendam, T. A., Bearden, C. E., and Cannon, T. D. (2009). White Matter Integrity and Prediction of Social and Role Functioning in Subjects at Ultra-High Risk for Psychosis. *Biological Psychiatry*, 66(6):562–569.
- Kates, W. R., Burnette, C. P., Jabs, E. W., Rutberg, J., Murphy, A. M., Grados, M., Geraghty, M., Kaufmann, W. E., and Pearlson, G. D. (2001). Regional cortical white matter reductions in velocardiofacial syndrome: a volumetric MRI analysis. *Biological Psychiatry*, 49(8):677–684.
- Kates, W. R., Olszewski, A. K., Gnirke, M. H., Kikinis, Z., Nelson, J., Antshel, K. M., Fremont, W., Radoeva, P. D., Middleton, F. A., Shenton, M. E., and Coman, I. L. (2015). White matter microstructural abnormalities of the cingulum bundle in youths with 22q11.2 deletion syndrome: Associations with medication, neuropsychological function, and prodromal symptoms of psychosis. *Schizophrenia Research*, 161(1):76–84.
- Kaufman, J., Birmaher, B., Brent, D., Rao, U., Flynn, C., Moreci, P., Williamson, D., and Ryan, N. (1997). Schedule for affective disorders and schizophrenia for school-age children-present and lifetime version (k-sads-pl): initial reliability and validity data. *Journal of the American Academy of Child & Adolescent Psychiatry*, 36(7):980–988.
- Keihaninejad, S., Ryan, N. S., Malone, I. B., Modat, M., Cash, D., Ridgway, G. R., Zhang, H., Fox, N. C., and Ourselin, S. (2012). The Importance of Group-Wise Registration in Tract Based Spatial Statistics Study of Neurodegeneration: A Simulation Study in Alzheimer’s Disease. *PLOS ONE*, 7(11):e45996.
- Kiehl, T. R., Chow, E. W. C., Mikulis, D. J., George, S. R., and Bassett, A. S. (2009). Neuropathologic Features in Adults with 22q11.2 Deletion Syndrome. *Cerebral Cortex*, 19(1):153–164.
- Kikinis, Z., Asami, T., Bouix, S., Finn, C. T., Ballinger, T., Tworog-Dube, E., Kucherlapati, R., Kikinis, R., Shenton, M. E., and Kubicki, M. (2012). Reduced fractional anisotropy and axial diffusivity in white matter in 22q11.2 deletion syndrome: A pilot study. *Schizophrenia Research*, 141(1):35–39.
- Kikinis, Z., Cho, K. I. K., Coman, I. L., Radoeva, P. D., Bouix, S., Tang, Y., Eckbo, R., Makris, N., Kwon, J. S., Kubicki, M., Antshel, K. M., Fremont, W., Shenton, M. E., and Kates, W. R. (2017). Abnormalities in brain white matter in adolescents with 22q11.2 deletion syndrome and psychotic symptoms. *Brain Imaging and Behavior*, 11(5):1353–1364.
- Kikinis, Z., Makris, N., Finn, C. T., Bouix, S., Lucia, D., Coleman, M. J., Tworog-Dube, E., Kikinis, R., Kucherlapati, R., Shenton, M. E., and Kubicki, M. (2013). Genetic contributions to changes of fiber tracts of ventral visual stream in 22q11.2 deletion syndrome. *Brain Imaging and Behavior*, 7(3):316–325.
- Klauser, P., Baker, S. T., Cropley, V. L., Bousman, C., Fornito, A., Cocchi, L., Fullerton, J. M., Rasser, P., Schall, U., Henskens, F., Michie, P. T., Loughland, C., Catts, S. V., Mowry, B., Weickert, T. W., Shannon Weickert, C., Carr, V., Lenroot, R., Pantelis, C., and Zalesky, A. (2017). White Matter Disruptions in Schizophrenia Are Spatially Widespread and Topologically Converge on Brain Network Hubs. *Schizophrenia Bulletin*, 43(2):425–435.

- Kobrynski, L. J. and Sullivan, K. E. (2007). Velocardiofacial syndrome, DiGeorge syndrome: the chromosome 22q11.2 deletion syndromes. *The Lancet*, 370(9596):1443–1452.
- Kraemer, H. C., Yesavage, J. A., Taylor, J. L., and Kupfer, D. (2000). How Can We Learn About Developmental Processes From Cross-Sectional Studies, or Can We? *American Journal of Psychiatry*, 157(2):163–171.
- Krueger, C. and Tian, L. (2004). A comparison of the general linear mixed model and repeated measures ANOVA using a dataset with multiple missing data points. *Biological Research for Nursing*, pages 151–157.
- Kufert, Y. M., Nachmani, A., Nativ, E., Weizman, A., and Gothelf, D. (2016). Association between prematurity and the evolution of psychotic disorders in 22q11.2 deletion syndrome. *Journal of Neural Transmission*, 123(12):1491–1497.
- Kumar, R., Nguyen, H. D., Macey, P. M., Woo, M. A., and Harper, R. M. (2012). Regional brain axial and radial diffusivity changes during development. *Journal of Neuroscience Research*, 90(2):346–355.
- Lawes, I. N. C., Barrick, T. R., Murugam, V., Spierings, N., Evans, D. R., Song, M., and Clark, C. A. (2008). Atlas-based segmentation of white matter tracts of the human brain using diffusion tensor tractography and comparison with classical dissection. *Neuroimage*, 39(1):62–79.
- Lebel, C. and Beaulieu, C. (2011). Longitudinal Development of Human Brain Wiring Continues from Childhood into Adulthood. *The Journal of Neuroscience*, 31(30):10937–10947.
- Lebel, C., Gee, M., Camicioli, R., Wieler, M., Martin, W., and Beaulieu, C. (2012). Diffusion tensor imaging of white matter tract evolution over the lifespan. *NeuroImage*, 60(1):340–352.
- Linderkamp, O., Janus, L., Linder, R., and Skoruppa, D. B. (2009). Time table of normal foetal brain development. *International Journal of Prenatal and Perinatal Psychology and Medicine*, 21(1/2):4–16.
- Locascio, J. J. and Atri, A. (2011). An Overview of Longitudinal Data Analysis Methods for Neurological Research. *Dementia and Geriatric Cognitive Disorders EXTRA*, 1(1):330–357.
- López-Bendito, G., Cautinat, A., Sánchez, J. A., Bielle, F., Flames, N., Garratt, A. N., Talmage, D. A., Role, L. W., Charnay, P., Marín, O., and Garel, S. (2006). Tangential Neuronal Migration Controls Axon Guidance: A Role for Neuregulin-1 in Thalamocortical Axon Navigation. *Cell*, 125(1):127–142.
- Madhyastha, T., Mérillat, S., Hirsiger, S., Bezzola, L., Liem, F., Grabowski, T., and Jäncke, L. (2014). Longitudinal reliability of tract-based spatial statistics in diffusion tensor imaging: Longitudinal DTI Reliability. *Human Brain Mapping*, 35(9):4544–4555.
- Maeder, J., Schneider, M., Bostelmann, M., Debbané, M., Glaser, B., Menghetti, S., Schaer, M., and Eliez, S. (2016). Developmental trajectories of executive functions in 22q11.2 deletion syndrome. *Journal of Neurodevelopmental Disorders*, 8:10.
- McCabe, K. L., Atkinson, R. J., Cooper, G., Melville, J. L., Harris, J., Schall, U., Loughland, C. M., Thienel, R., and Campbell, L. E. (2014). Pre-pulse inhibition and antisaccade performance indicate impaired attention modulation of cognitive inhibition in 22q11.2 deletion syndrome (22q11ds). *Journal of Neurodevelopmental Disorders*, 6:38.
- McCabe, K. L., Marlin, S., Cooper, G., Morris, R., Schall, U., Murphy, D. G., Murphy, K. C., and Campbell, L. E. (2016). Visual perception and processing in children with 22q11.2 deletion syndrome: associations with social cognition measures of face identity and emotion recognition. *Journal of Neurodevelopmental Disorders*, 8:30.
- McDonald-McGinn, D. M. and Sullivan, K. E. (2011). Chromosome 22q11.2 Deletion Syndrome (DiGeorge Syndrome/Velocardiofacial Syndrome):. *Medicine*, 90(1):1–18.
- McDonald-McGinn, D. M., Sullivan, K. E., Marino, B., Philip, N., Swillen, A., Vorstman,

- J. A. S., Zackai, E. H., Emanuel, B. S., Vermeesch, J. R., Morrow, B. E., Scambler, P. J., and Bassett, A. S. (2015). 22q11.2 deletion syndrome. *Nature reviews. Disease primers*, 1:15071.
- McGrath, J., Saha, S., Chant, D., and Welham, J. (2008). Schizophrenia: A Concise Overview of Incidence, Prevalence, and Mortality. *Epidemiologic Reviews*, 30(1):67–76.
- McGuffin, P., Owen, M., and Farmer, A. (1995). Genetic basis of schizophrenia. *The Lancet*, 346(8976):678–682.
- Meechan, D. W., Tucker, E. S., Maynard, T. M., and LaMantia, A.-S. (2009). Diminished dosage of 22q11 genes disrupts neurogenesis and cortical development in a mouse model of 22q11 deletion/DiGeorge syndrome. *Proceedings of the National Academy of Sciences*, 106(38):16434–16445.
- Meier, M. H., Caspi, A., Reichenberg, A., Keefe, R. S., Fisher, H. L., Harrington, H., Houts, R., Poulton, R., and Moffitt, T. E. (2014). Neuropsychological Decline in Schizophrenia From the Premorbid to the Postonset Period: Evidence From a Population-Representative Longitudinal Study. *American Journal of Psychiatry*, 171(1):91–101.
- Miller, T. J., McGlashan, T. H., Rosen, J. L., Somjee, L., Markovich, P. J., Stein, K., and Woods, S. W. (2002). Prospective diagnosis of the initial prodrome for schizophrenia based on the structured interview for prodromal syndromes: preliminary evidence of interrater reliability and predictive validity. *American Journal of Psychiatry*, 159(5):863–865.
- Mills, K. L. and Tamnes, C. K. (2014). Methods and considerations for longitudinal structural brain imaging analysis across development. *Developmental Cognitive Neuroscience*, 9:172–190.
- Mori, S., Oishi, K., and Faria, A. V. (2009). White matter atlases based on diffusion tensor imaging. *Current Opinion in Neurology*, 22(4):362–369.
- Mori, S., Wakana, S., Zijl, P. C. M. v., and Nagae-Poetscher, L. M. (2005). *MRI Atlas of Human White Matter*. Elsevier. Google-Books-ID: ltwRYlvFNLIC.
- Mukherjee, P., Miller, J. H., Shimony, J. S., Philip, J. V., Nehra, D., Snyder, A. Z., Conturo, T. E., Neil, J. J., and McKinstry, R. C. (2002). Diffusion-Tensor MR Imaging of Gray and White Matter Development during Normal Human Brain Maturation. *American Journal of Neuroradiology*, 23(9):1445–1456.
- Mutlu, A. K., Schneider, M., Debbané, M., Badoud, D., Eliez, S., and Schaer, M. (2013). Sex differences in thickness, and folding developments throughout the cortex. *NeuroImage*, 82:200–207.
- Nave, K.-A. (2010). Myelination and support of axonal integrity by glia. *Nature*, 468(7321):244–252.
- Nazeri, A., Chakravarty, M. M., Felsky, D., Lobaugh, N. J., Rajji, T. K., Mulsant, B. H., and Voineskos, A. N. (2013). Alterations of Superficial White Matter in Schizophrenia and Relationship to Cognitive Performance. *Neuropsychopharmacology*, 38(10):1954–1962.
- Nuninga, J. O., Bohlken, M. M., Koops, S., Fiksinski, A. M., Mandl, R. C. W., Breetvelt, E. J., Duijff, S. N., Kahn, R. S., Sommer, I. E. C., and Vorstman, J. A. S. (2017). White matter abnormalities in 22q11.2 deletion syndrome patients showing cognitive decline. *Psychological Medicine*, pages 1–9.
- Olszewski, A. K., Kikinis, Z., Gonzalez, C. S., Coman, I. L., Makris, N., Gong, X., Rath, Y., Zhu, A., Antshel, K. M., Fremont, W., Kubicki, M. R., Bouix, S., Shenton, M. E., and Kates, W. R. (2017). The social brain network in 22q11.2 deletion syndrome: a diffusion tensor imaging study. *Behavioral and Brain Functions*, 13(1).
- Olvet, D. M., Delaparte, L., Yeh, F.-C., DeLorenzo, C., McGrath, P. J., Weissman, M. M., Adams, P., Fava, M., Deckersbach, T., McInnis, M. G., et al. (2016). A comprehensive

- examination of white matter tracts and connectometry in major depressive disorder. *Depression and anxiety*, 33(1):56–65.
- Oskarsdóttir, S., Vujic, M., and Fasth, A. (2004). Incidence and prevalence of the 22q11 deletion syndrome: a population-based study in Western Sweden. *Archives of Disease in Childhood*, 89(2):148–151.
- Ottet, M.-C. (2013). *Analyzing quantitatively and topologically the white matter organization in 22Q11. 2 deletion syndrome*. PhD Thesis, University of Geneva.
- Ottet, M.-C., Schaer, M., Cammoun, L., Schneider, M., Debbané, M., Thiran, J.-P., and Eliez, S. (2013). Reduced Fronto-Temporal and Limbic Connectivity in the 22q11.2 Deletion Syndrome: Vulnerability Markers for Developing Schizophrenia? *PLoS ONE*, 8(3):e58429.
- Padula, M. C., Scariati, E., Schaer, M., Sandini, C., Ottet, M. C., Schneider, M., Van De Ville, D., and Eliez, S. (2017). Altered structural network architecture is predictive of the presence of psychotic symptoms in patients with 22q11.2 deletion syndrome. *NeuroImage: Clinical*, 16:142–150.
- Padula, M. C., Schaer, M., Armando, M., Sandini, C., Zöller, D., Scariati, E., Schneider, M., and Eliez, S. (2018). Cortical morphology development in patients with 22q11.2 deletion syndrome at ultra-high risk of psychosis. *Psychological Medicine*, pages 1–9.
- Padula, M. C., Schaer, M., Scariati, E., Schneider, M., Van De Ville, D., Debbané, M., and Eliez, S. (2015). Structural and functional connectivity in the default mode network in 22q11.2 deletion syndrome. *Journal of Neurodevelopmental Disorders*, 7:23.
- Peng, H. and Lu, Y. (2012). Model selection in linear mixed effect models. *Journal of Multivariate Analysis*, 109:109–129.
- Perlstein, M. D., Chohan, M. R., Coman, I. L., Antshel, K. M., Fremont, W. P., Gnirke, M. H., Kikinis, Z., Middleton, F. A., Radoeva, P. D., Shenton, M. E., and Kates, W. R. (2014). White matter abnormalities in 22q11.2 deletion syndrome: Preliminary associations with the Nogo-66 receptor gene and symptoms of psychosis. *Schizophrenia Research*, 152(1):117–123.
- Peters, B. D., Haan, L. d., Dekker, N., Blaas, J., Becker, H. E., Dingemans, P. M., Akkerman, E. M., Majoie, C. B., Amelsvoort, T. v., Heeten, G. J. d., and Linszen, D. H. (2008). White Matter Fibertracking in First-Episode Schizophrenia, Schizoaffective Patients and Subjects at Ultra-High Risk of Psychosis. *Neuropsychobiology*, 58(1):19–28.
- Pettersson-Yeo, W., Allen, P., Benetti, S., McGuire, P., and Mechelli, A. (2011). Dysconnectivity in schizophrenia: Where are we now? *Neuroscience & Biobehavioral Reviews*, 35(5):1110–1124.
- Rabinowitz, J., De Smedt, G., Harvey, P. D., and Davidson, M. (2002). Relationship Between Premorbid Functioning and Symptom Severity as Assessed at First Episode of Psychosis. *American Journal of Psychiatry*, 159(12):2021–2026.
- Radoeva, P. D., Coman, I. L., Antshel, K. M., Fremont, W., McCarthy, C. S., Kotkar, A., Wang, D., Shprintzen, R. J., and Kates, W. R. (2012). Atlas-based white matter analysis in individuals with velo-cardio-facial syndrome (22q11.2 deletion syndrome) and unaffected siblings. *Behavioral and Brain Functions*, 8:38.
- Rapoport, J. L., Giedd, J. N., and Gogtay, N. (2012). Neurodevelopmental model of schizophrenia: update 2012. *Molecular Psychiatry*, 17(12):1228–1238.
- Reich, W. (2000). Diagnostic interview for children and adolescents (dica). *Journal of the American Academy of Child & Adolescent Psychiatry*, 39(1):59–66.
- Reichenberg, A., Weiser, M., Rapp, M. A., Rabinowitz, J., Caspi, A., Schmeidler, J., Knobler, H. Y., Lubin, G., Nahon, D., Harvey, P. D., and Davidson, M. (2005). Elaboration on Premorbid Intellectual Performance in Schizophrenia: Premorbid Intellectual Decline and Risk for Schizophrenia. *Archives of General Psychiatry*, 62(12):1297–1304.

- Reuter, M. and Fischl, B. (2011). Avoiding asymmetry-induced bias in longitudinal image processing. *NeuroImage*, 57(1):19–21.
- Reuter, M., Schmansky, N. J., Rosas, H. D., and Fischl, B. (2012). Within-subject template estimation for unbiased longitudinal image analysis. *NeuroImage*, 61(4):1402–1418.
- Rinholm Johanne E, Vervaeke Koen, Tadross Michael R, Tkachuk Ariana N, Kopek Benjamin G, Brown Timothy A, Bergersen Linda H, and Clayton David A (2016). Movement and structure of mitochondria in oligodendrocytes and their myelin sheaths. *Glia*, 64(5):810–825.
- Roalf, D. R., Schmitt, J. E., Vandekar, S. N., Satterthwaite, T. D., Shinohara, R. T., Ruparel, K., Elliott, M. A., Prabhakaran, K., McDonald-McGinn, D. M., Zackai, E. H., Gur, R. C., Emanuel, B. S., and Gur, R. E. (2017). White matter microstructural deficits in 22q11.2 deletion syndrome. *Psychiatry Research: Neuroimaging*, 268:35–44.
- Sarrazin, S., Poupon, C., Linke, J., Wessa, M., Phillips, M., Delavest, M., Versace, A., Almeida, J., Guevara, P., Duclap, D., Duchesnay, E., Mangin, J.-F., Dudal, K. L., Daban, C., Hamdani, N., D’Albis, M.-A., Leboyer, M., and Houenou, J. (2014). A Multicenter Tractography Study of Deep White Matter Tracts in Bipolar I Disorder: Psychotic Features and Interhemispheric Disconnectivity. *JAMA Psychiatry*, 71(4):388–396.
- Scambler, P. J. (2000). The 22q11 deletion syndromes. *Human molecular genetics*, 9(16):2421–2426.
- Scambler, P. J., Carey, A. H., Wyse, R. K. H., Roach, S., Dumanski, J. P., Nordenskjold, M., and Williamson, R. (1991). Microdeletions within 22q11 associated with sporadic and familial DiGeorge syndrome. *Genomics*, 10(1):201–206.
- Scariati, E., Padula, M. C., Schaer, M., and Eliez, S. (2016). Long-range dysconnectivity in frontal and midline structures is associated to psychosis in 22q11.2 deletion syndrome. *Journal of Neural Transmission*, 123(8):823–839.
- Schaer, M., Debbané, M., Bach Cuadra, M., Ottet, M.-C., Glaser, B., Thiran, J.-P., and Eliez, S. (2009). Deviant trajectories of cortical maturation in 22q11.2 deletion syndrome (22q11ds): A cross-sectional and longitudinal study. *Schizophrenia Research*, 115(2-3):182–190.
- Schmithorst, V. J. and Yuan, W. (2010). White matter development during adolescence as shown by diffusion MRI. *Brain and Cognition*, 72(1):16–25.
- Schneider, J. F. L., Il’yasov, K. A., Hennig, J., and Martin, E. (2004). Fast quantitative diffusion-tensor imaging of cerebral white matter from the neonatal period to adolescence. *Neuroradiology*, 46(4):258–266.
- Schneider, M., Armando, M., Pontillo, M., Vicari, S., Debbané, M., Schultze-Lutter, F., and Eliez, S. (2016). Ultra high risk status and transition to psychosis in 22q11.2 deletion syndrome. *World Psychiatry*, 15(3):259–265.
- Schneider, M., Debbané, M., Bassett, A. S., Chow, E. W., Fung, W. L. A., van den Bree, M. B., Owen, M., Murphy, K. C., Niarchou, M., Kates, W. R., Antshel, K. M., Fremont, W., McDonald-McGinn, D. M., Gur, R. E., Zackai, E. H., Vorstman, J., Duijff, S. N., Klaassen, P. W., Swillen, A., Gothelf, D., Green, T., Weizman, A., Van Amelsvoort, T., Evers, L., Boot, E., Shashi, V., Hooper, S. R., Bearden, C. E., Jalbrzikowski, M., Armando, M., Vicari, S., Murphy, D. G., Ousley, O., Campbell, L. E., Simon, T. J., and Eliez, S. (2014a). Psychiatric Disorders From Childhood to Adulthood in 22q11.2 Deletion Syndrome: Results From the International Consortium on Brain and Behavior in 22q11.2 Deletion Syndrome. *American Journal of Psychiatry*, 171(6):627–639.
- Schneider, M., Schaer, M., Mutlu, A. K., Menghetti, S., Glaser, B., Debbané, M., and Eliez, S. (2014b). Clinical and cognitive risk factors for psychotic symptoms in 22q11.2 deletion syndrome: a transversal and longitudinal approach. *European Child & Adolescent Psychiatry*, 23(6):425–436.

- Schultze-Lutter, F., Michel, C., Schmidt, S. J., Schimmelmann, B. G., Maric, N. P., Salokangas, R. K. R., Riecher-Rössler, A., Gaag, M. v. d., Nordentoft, M., Raballo, A., Meneghelli, A., Marshall, M., Morrison, A., Ruhrmann, S., and Klosterkötter, J. (2015). EPA guidance on the early detection of clinical high risk states of psychoses. *European Psychiatry*, 30(3):405–416.
- Schwartz, E. D., Cooper, E. T., Fan, Y., Jawad, A. F., Chin, C.-L., Nissarov, J., and Hackney, D. B. (2005). MRI diffusion coefficients in spinal cord correlate with axon morphometry. *Neuroreport*, 16(1):73–76.
- Sedlackova, E. (1955). Insufficiency of palatolaryngeal passage as a developmental disorder. *Casopis lekaru ceskych*, 94(47-48):1304–1307.
- Shaikh, T. H., O'Connor, R. J., Pierpont, M. E., McGrath, J., Hacker, A. M., Nimmakayalu, M., Geiger, E., Emanuel, B. S., and Saitta, S. C. (2007). Low copy repeats mediate distal chromosome 22q11.2 deletions: Sequence analysis predicts breakpoint mechanisms. *Genome Research*, 17(4):482–491.
- Shapiro, H. M., Wong, L. M., and Simon, T. J. (2013). A Cross-Sectional Analysis of the Development of Response Inhibition in Children with Chromosome 22q11.2 Deletion Syndrome. *Frontiers in Psychiatry*, 4.
- Shashi, V., Francis, A., Hooper, S. R., Kranz, P. G., Zapadka, M., Schoch, K., Ip, E., Tandon, N., Howard, T. D., and Keshavan, M. S. (2012). Increased corpus callosum volume in children with chromosome 22q11.2 deletion syndrome is associated with neurocognitive deficits and genetic polymorphisms. *European Journal of Human Genetics*, 20(10):1051–1057.
- Shaw, P., Greenstein, D., Lerch, J., Clasen, L., Lenroot, R., Gogtay, N., Evans, A., Rapoport, J., and Giedd, J. (2006). Intellectual ability and cortical development in children and adolescents. *Nature*, 440(7084):676–679.
- Shaw, S., Mary, K., B, S. A., Gail, S., J, H. P., Josephine, L., H, L. S., Antonio, V., Marc, D. H., R, C. L., J, C. T., Robin, S., and E, D. L. (1998). A genome-wide search for schizophrenia susceptibility genes. *American Journal of Medical Genetics*, 81(5):364–376.
- Shprintzen, R., Goldberg, R., Lewin, M., Sidoti, E., Berkman, M., Argamaso, R., and Young, D. (1978). A new syndrome involving cleft palate, cardiac anomalies, typical facies, and learning disabilities: velo-cardio-facial syndrome. *The Cleft palate journal*, 15(1):56–62.
- Shprintzen, R. J. (2005). Velo-cardio-facial syndrome. *Progress in Pediatric Cardiology*, 20(2):187–193.
- Shprintzen, R. J. (2008). Velo-cardio-facial syndrome: 30 Years of study. *Developmental Disabilities Research Reviews*, 14(1):3–10.
- Simon, T. J., Bearden, C. E., Mc-Ginn, D. M., and Zackai, E. (2005a). Visuospatial and Numerical Cognitive Deficits in Children with Chromosome 22q11.2 Deletion Syndrome. *Cortex*, 41(2):145–155.
- Simon, T. J., Ding, L., Bish, J. P., McDonald-McGinn, D. M., Zackai, E. H., and Gee, J. (2005b). Volumetric, connective, and morphologic changes in the brains of children with chromosome 22q11. 2 deletion syndrome: an integrative study. *Neuroimage*, 25(1):169–180.
- Simon, T. J., Wu, Z., Avants, B., Zhang, H., Gee, J. C., and Stebbins, G. T. (2008). Atypical cortical connectivity and visuospatial cognitive impairments are related in children with chromosome 22q11.2 deletion syndrome. *Behavioral and Brain Functions*, 4:25.
- Smith, S. M., Jenkinson, M., Johansen-Berg, H., Rueckert, D., Nichols, T. E., Mackay, C. E., Watkins, K. E., Ciccarelli, O., Cader, M. Z., Matthews, P. M., and Behrens, T. E. J. (2006). Tract-based spatial statistics: Voxelwise analysis of multi-subject diffusion data. *NeuroImage*, 31(4):1487–1505.

- Solot, C. B., Knightly, C., Handler, S. D., Gerdes, M., McDonald-McGinn, D. M., Moss, E., Wang, P., Cohen, M., Randall, P., Larossa, D., Driscoll, D. A., Emanuel, B. S., and Zackai, E. H. (2000). Communication disorders in the 22q11.2 microdeletion syndrome. *Journal of Communication Disorders*, 33(3):187–204.
- Song, J. W. and Chung, K. C. (2010). Observational Studies: Cohort and Case-Control Studies. *Plastic and reconstructive surgery*, 126(6):2234–2242.
- Song, S.-K., Sun, S.-W., Ju, W.-K., Lin, S.-J., Cross, A. H., and Neufeld, A. H. (2003). Diffusion tensor imaging detects and differentiates axon and myelin degeneration in mouse optic nerve after retinal ischemia. *NeuroImage*, 20(3):1714–1722.
- Song, S.-K., Sun, S.-W., Ramsbottom, M. J., Chang, C., Russell, J., and Cross, A. H. (2002). Dysmyelination Revealed through MRI as Increased Radial (but Unchanged Axial) Diffusion of Water. *NeuroImage*, 17(3):1429–1436.
- Squarcione, C., Torti, M. C., Di Fabio, F., and Biondi, M. (2013). 22q11 deletion syndrome: a review of the neuropsychiatric features and their neurobiological basis. *Neuropsychiatric Disease and Treatment*, 9:1873–1884.
- Steen, R. G., Hamer, R. M., and Lieberman, J. A. (2007). Measuring Brain Volume by MR Imaging: Impact of Measurement Precision and Natural Variation on Sample Size Requirements. *American Journal of Neuroradiology*, 28(6):1119–1125.
- Strong, W. B. (1968). Familial syndrome of right-sided aortic arch, mental deficiency, and facial dysmorphism. *The Journal of pediatrics*, 73(6):882–888.
- Sundram, F., Campbell, L. E., Azuma, R., Daly, E., Bloemen, O. J. N., Barker, G. J., Chitnis, X., Jones, D. K., Amelsvoort, T., Murphy, K. C., and Murphy, D. G. M. (2010). White matter microstructure in 22q11 deletion syndrome: a pilot diffusion tensor imaging and voxel-based morphometry study of children and adolescents. *Journal of Neurodevelopmental Disorders*, 2(2):77.
- Swillen, A. (2016). The importance of understanding cognitive trajectories: the case of 22q11.2 deletion syndrome. *Current opinion in psychiatry*, 29(2):133–137.
- Swillen, A. and McDonald-McGinn, D. (2015). Developmental trajectories in 22q11. 2 deletion syndrome. 169(2):172–181.
- Talairach, J. and Tournoux, P. (1988). Co-planar stereotaxic atlas of the human brain: 3-dimensional proportional system: an approach to cerebral imaging.
- Tang, K. L., Antshel, K. M., Fremont, W. P., and Kates, W. R. (2015). Behavioral and Psychiatric Phenotypes in 22q11.2 Deletion Syndrome. *Journal of developmental and behavioral pediatrics: JDBP*, 36(8):639–650.
- Thompson, W. K., Hallmayer, J., O’Hara, R., and Initiative, A. D. N. (2011). Design considerations for characterizing psychiatric trajectories across the lifespan: application to effects of apoe- ϵ 4 on cerebral cortical thickness in alzheimer’s disease. *American Journal of Psychiatry*, 168(9):894–903.
- Tylee, D. S., Kikinis, Z., Quinn, T. P., Antshel, K. M., Fremont, W., Tahir, M. A., Zhu, A., Gong, X., Glatt, S. J., Coman, I. L., Shenton, M. E., Kates, W. R., and Makris, N. (2017). Machine-learning classification of 22q11.2 deletion syndrome: A diffusion tensor imaging study. *NeuroImage: Clinical*, 15:832–842.
- Uhlhaas, P. J. and Singer, W. (2010). Abnormal neural oscillations and synchrony in schizophrenia. *Nature reviews neuroscience*, 11(2):100.
- Van, L., Butcher, N. J., Costain, G., Ogura, L., Chow, E. W. C., and Bassett, A. S. (2016). Fetal growth and gestational factors as predictors of schizophrenia in 22q11.2 deletion syndrome. *Genetics in Medicine*, 18(4):350–355.
- Van Amelsvoort, T., Daly, E., Robertson, D., Suckling, J., Ng, V., Critchley, H., Owen, M. J., Henry, J., Murphy, K. C., and Murphy, D. G. (2001). Structural brain abnormalities associated with deletion at chromosome 22q11: quantitative neuroimaging study of adults with velo-cardio-facial syndrome. *The British Journal of Psychiatry*,

- 178(5):412–419.
- Van Amelsvoort, T. v., Daly, E., Henry, J., Robertson, D., Ng, V., Owen, M., Murphy, K. C., and Murphy, D. G. M. (2004). Brain Anatomy in Adults With Velocardiofacial Syndrome With and Without Schizophrenia: Preliminary Results of a Structural Magnetic Resonance Imaging Study. *Archives of General Psychiatry*, 61(11):1085–1096.
- Villalon-Reina, J., Jahanshad, N., Beaton, E., Toga, A. W., Thompson, P. M., and Simon, T. J. (2013). White matter microstructural abnormalities in girls with chromosome 22q11.2 deletion syndrome, Fragile X or Turner syndrome as evidenced by diffusion tensor imaging. *NeuroImage*, 81:441–454.
- Vorstman, J. A. S., Breetvelt, E. J., Duijff, S. N., Eliez, S., Schneider, M., Jalbrzikowski, M., Armando, M., Vicari, S., Shashi, V., Hooper, S. R., Chow, E. W. C., Fung, W. L. A., Butcher, N. J., Young, D. A., McDonald-McGinn, D. M., Vogels, A., van Amelsvoort, T., Gothelf, D., Weinberger, R., Weizman, A., Klaassen, P. W. J., Koops, S., Kates, W. R., Antshel, K. M., Simon, T. J., Ousley, O. Y., Swillen, A., Gur, R. E., Bearden, C. E., Kahn, R. S., and Bassett, A. S. (2015). Cognitive Decline Preceding the Onset of Psychosis in Patients With 22q11.2 Deletion Syndrome. *JAMA Psychiatry*, 72(4):377.
- Wechsler, D. (1991). *The Wechsler intelligence scale for children—third edition: administration and scoring manual*. Psychological corporation, San Antonio.
- Wechsler, D. (1997). *Wechsler adult intelligence scale-III: administration and scoring manual*. Psychological Corporation, San Antonio.
- Wechsler, D. (2004). *WISC-IV: Wechsler Intelligence Scale for Children: Technical and Interpretive Manual*. Psychological Corporation.
- Wechsler, D. (2008). *Wechsler Adult Intelligence Scale—Fourth Edition (WAIS-IV)*. San Antonio, TX: The Psychological Corporation.
- Wheeler, A. L. and Voineskos, A. N. (2014). A review of structural neuroimaging in schizophrenia: from connectivity to connectomics. *Frontiers in Human Neuroscience*, 8.
- Woodberry, K. A., Giuliano, A. J., and Seidman, L. J. (2008). Premorbid IQ in Schizophrenia: A Meta-Analytic Review. *American Journal of Psychiatry*, 165(5):579–587.
- Woodin, M., Wang, P. P., Aleman, D., McDonald-McGinn, D., Zackai, E., and Moss, E. (2001). Neuropsychological profile of children and adolescents with the 22q11.2 microdeletion. *Genetics in Medicine*, 3(1):34–39.
- Wright, I. C., McGuire, P. K., Poline, J. B., Travers, J. M., Murray, R. M., Frith, C. D., Frackowiak, R. S. J., and Friston, K. J. (1995). A Voxel-Based Method for the Statistical Analysis of Gray and White Matter Density Applied to Schizophrenia. *NeuroImage*, 2(4):244–252.
- Yang, H.-J., Vainshtein, A., Maik-Rachline, G., and Peles, E. (2016). G protein-coupled receptor 37 is a negative regulator of oligodendrocyte differentiation and myelination. *Nature Communications*, 7:10884.
- Yendiki, A., Panneck, P., Srinivasan, P., Stevens, A., Zöllei, L., Augustinack, J., Wang, R., Salat, D., Ehrlich, S., Behrens, T., Jbabdi, S., Gollub, R., and Fischl, B. (2011). Automated Probabilistic Reconstruction of White-Matter Pathways in Health and Disease Using an Atlas of the Underlying Anatomy. *Frontiers in Neuroinformatics*, 5.
- Yendiki, A., Reuter, M., Wilkens, P., Rosas, H. D., and Fischl, B. (2016). Joint reconstruction of white-matter pathways from longitudinal diffusion MRI data with anatomical priors. *NeuroImage*, 127:277–286.